THE EFFECTS OF TRIFLUOPERAZINE ON CISPLATIN-INDUCED CELL
DEATH IN H460 CELLS AND THEIR BCL-2 OVEREXPRESSION
COUNTERPARTS

Miss Buntitabhon Sirichanchuen

A Dissertation Submitted in Partial Fulfillment of the Requirements
for the Degree of Doctor of Philosophy Program in Biopharmaceutical Sciences
Faculty of Pharmaceutical Sciences
Chulalongkorn University
Academic year 2010
Copyright of Chulalongkorn University

ผลของไตรฟลูออเพอราซินต่อการตายของเซลล์เมื่อเหนี่ยวนำด้วยซิสพลาทินในเซลล์เอช 460

และเซลล์เอช 460 ที่มีการแสดงออกของบีซีแอล-2 สูง

นางสาวบัณฑิตาภรณ์ ศิริจันทร์ชื่น

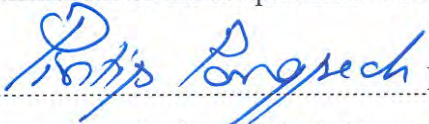|	
Thesis Title	THE EFFECTS OF TRIFLUOPERAZINE ON CISPLATIN-INDUCED CELL DEATH IN H460 CELLS AND THEIR BCL-2 OVEREXPRESSION COUNTERPARTS
By	Miss Buntitabhon Sirichanchuen
Field of Study	Biopharmaceutical Sciences
Thesis Advisor	Associate Professor Thitima Pengsuparp, Ph.D.
Thesis Co-Advisor	Assistant Professor Pithi Chanvorachote, Ph.D.

Accepted by the Faculty of Pharmaceutical Sciences, Chulalongkorn University in Partial Fulfillment of the Requirements for the Doctoral Degree

.... Dean of the Faculty of Pharmaceutical Sciences
(Associate Professor Pintip Pongpech, Ph.D.)

THESIS COMMITTEE

.... Chairman
(Associate Professor Nongluksna Sriubolmas, Ph.D.)

.... Thesis Advisor
(Associate Professor Thitima Pengsuparp, Ph.D.)

.... Thesis Co-Advisor
(Assistant Professor Pithi Chanvorachote, Ph.D.)

.... Examiner
(Associate Professor Duangdeun Meksuriyen, Ph.D.)

.... Examiner
(Assistant Professor Rataya Luechapudiporn, Ph.D.)

.... External Examiner
(Assistant Professor Wisit Tangkeangsirisin, Ph.D.)

บัณฑิตาภรณ์ ศิริจันทร์ชื่น : ผลของไตรฟลูออเพอราซินต่อการตายของเซลล์เมื่อเหนี่ยวนำด้วยซิสพลาทินในเซลล์เอช 460 และเซลล์เอช 460 ที่มีการแสดงออกของบีซีแอล-2 สูง (THE EFFECTS OF TRIFLUOPERAZINE ON CISPLATIN-INDUCED CELL DEATH IN H460 CELLS AND THEIR BCL-2 OVEREXPRESSION COUNTERPARTS) อ. ที่ปรึกษาวิทยานิพนธ์หลัก : รศ. ดร. ธิติมา เพ็งสุภาพ, อ.ที่ปรึกษาวิทยานิพนธ์ร่วม : ผศ. ดร.ปิติ จันทร์วรโชติ, 120 หน้า

วัตถุประสงค์ของการศึกษานี้ เพื่อศึกษาผลของไตรฟลูออเพอราซินต่อการตายของเซลล์เมื่อเหนี่ยวนำด้วยซิสพลาทินและรูปแบบการตายในเซลล์มะเร็งปอดเอช 460 และเซลล์ที่ดื้อต่อเคมีบำบัดซึ่งเกิดจากเซลล์เอช 460 ทั้งชนิดที่ถูกเหนี่ยวนำให้ดื้อยาด้วยซิสพลาทิน (เซลล์เอช 460/ซิส) และเซลล์เอช 460 ที่มีการแสดงออกของโปรตีนบีซีแอล-2 สูง (เซลล์อาร์เอแอลพี) อีกทั้งยังศึกษากลไกที่เป็นไปได้ของไตรฟลูออเพอราซินในปรับเปลี่ยนการตายของเซลล์เมื่อเหนี่ยวนำด้วยซิสพลาทิน เซลล์เอช 460/ซิสนั้นเกิดจากที่เซลล์เอช 460 ได้รับซิสพลาทินในขนาดที่เพิ่มขึ้นจนพบการดื้อยา ส่วนเซลล์อาร์เอแอลพีคือเซลล์เอช 460 ที่มีการถ่ายยีนเพื่อเพิ่มการแสดงออกของโปรตีนบีซีแอล-2 และเลือกโคลนที่ 1และ 6 ซึ่งมีการแสดงออกของโปรตีนบีซีแอล-2 ที่แตกต่างกัน พบว่าเซลล์เอช 460/ซิส เซลล์อาร์เอแอลพี 1 และเซลล์อาร์เอแอลพี 6 ดื้อต่อการตายเมื่อเหนี่ยวนำด้วยซิสพลาทินอย่างมีนัยสำคัญ จากนั้นเซลล์ทั้งหมดถูกนำไปทดสอบความเป็นพิษเมื่อได้รับซิสพลาทินที่ความเข้มข้น 20-50 µM หรือให้ซิสพลาทินในความเข้มข้นดังกล่าวร่วมกับไตรฟลูออเพอราซินในความเข้มข้นที่ไม่ก่อพิษที่ 1-5 µM พบว่าการให้ซิสพลาทินร่วมกับไตรฟลูออเพอราซิน สามารถเพิ่มการตายของเซลล์เอช 460/ซิส เซลล์อาร์เอแอลพี 1 และเซลล์อาร์เอแอลพี 6 ได้อย่างมีนัยสำคัญเมื่อเทียบกับการได้รับซิสพลาทินเพียงอย่างเดียว และยังพบว่าการตายที่เพิ่มขึ้นไม่เกี่ยวข้องกับกระบวนการอะพอพโตซิสหรือเนคโครซิสเมื่อตรวจสอบด้วยการย้อมสี Hoechst/PI และ comet assay ในขณะเดียวกันพบว่าปริมาณของออโตฟาโกโซมเพิ่มมากขึ้นหลังได้รับซิสพลาทินร่วมกับไตรฟลูออเพอราซินเมื่อตรวจสอบด้วยการย้อมสี acridine orange และพบการเพิ่มขึ้นของโปรตีน LC3-II เมื่อตรวจสอบด้วย Western blot อย่างไรก็ตามการเพิ่มความไวเซลล์มะเร็งต่อความเป็นพิษของซิสพลาทินนั้นเป็นไปอย่างจำเพาะ เนื่องจากไม่พบฤทธิ์ที่เพิ่มความเป็นพิษในเซลล์เอช 460 ซึ่งเป็นชนิดที่ไวต่อซิสพลาทินอยู่แล้ว และเมื่อให้ 3-เมธิลอะดีนีนซึ่งเป็นตัวยับยั้งกระบวนการออโตฟาจี ร่วมกับซิสพลาทินและไตรฟลูออเพอราซิน พบว่าปริมาณเซลล์ที่มีชีวิตเพิ่มขึ้นในปริมาณใกล้เคียงกับการให้ซิสพลาทินเพียงอย่างเดียว อีกทั้งยังพบว่าปริมาณของโปรตีนบีซีแอล-2 ลดลงในการให้ไตรฟลูออเพอราซินร่วมกับซิสพลาทิน จากผลการทดลองที่กล่าวมาทำให้ทราบว่ากลไกของไตรฟลูออเพอราซินในการปรับเปลี่ยนการตายของเซลล์เมื่อเหนี่ยวนำด้วยซิสพลาทินเกิดจากกระบวนการออโตฟาจีและการลดปริมาณโปรตีนบีซีแอล-2 จากการศึกษานี้สรุปได้ว่าการกระตุ้นให้เกิดกระบวนการออโตฟาจีด้วยไตรฟลูออเพอราซินสามารถเพิ่มความไวของเซลล์มะเร็งปอดที่ดื้อยาทั้งชนิดที่เหนี่ยวนำด้วยซิสพลาทินหรือชนิดที่มีการแสดงออกของโปรตีนบีซีแอล-2 สูงต่อการเหนี่ยวนำให้ตายด้วยซิสพลาทินได้ ซึ่งอาจเป็นประโยชน์ต่อการรักษามะเร็งปอดสำหรับชนิดที่มีการดื้อต่อเคมีบำบัดต่อไปได้

สาขาวิชา ....เภสัชศาสตร์ชีวภาพ........   ลายมือชื่อนิสิต ....บัณฑิตากากรณ์ ศิริจันทร์ชื่น.......

ปีการศึกษา ....2553.......   ลายมือชื่ออ.ที่ปรึกษาวิทยานิพนธ์หลัก.......................

ลายมือชื่ออ.ที่ปรึกษาวิทยานิพนธ์ร่วม.......................

4976955933   : MAJOR BIOPHARMACEUTICAL SCIENCES

KEYWORDS: TRIFLUOPERAZINE / CISPLATIN / BCL-2 / AUTOPHAGY

BUNTITABHON SIRICHANCHUEN: THE EFFECTS OF TRIFLUOPERAZINE ON CISPLATIN-INDUCED CELL DEATH IN H460 CELLS AND THEIR BCL-2 OVEREXPRESSION COUNTERPARTS. THESIS ADVISOR: ASSOC.PROF. THITIMA PENGSUPARP, Ph.D., THESIS CO-ADVISOR: ASSIST.PROF. PITHI CHANVORACHOTE, Ph.D., 120 pp.

The purposes of this study were to examine the effects of trifluoperazine on cisplatin-induced cell death and types of cell death in H460 (human non-small cell lung cancer) cells and their resistant counterparts; cisplatin-induced resistant H460/cis cells and Bcl-2 transfected RALP cells. Moreover, the possible mechanisms of trifluoperazine in modulating cisplatin-induced cell death were evaluated. The cisplatin-induced resistant clone (H460/cis) of lung carcinoma H460 cells was established by exposing the cells with gradually increasing concentrations of cisplatin until chemoresistance acquisition, measured by MTT assay. The apoptotic defect clone (RALP) was generated by transfecting H460 cells with Bcl-2 enforced-expression plasmids. The selected RALP clone no.1 and 6 showed the different level of Bcl-2 protein expression determined by Western blot analysis. H460/cis, RALP1and RALP6 cells showed significantly resistance to cisplatin-induced cytotoxicity. Then, all cells were co-treated with sub-toxic concentrations of trifluoperazine (1–5 µM) and toxic concentrations of cisplatin (20-50 µM). The results indicated that treatment with trifluoperazine could significantly sensitize H460/cis, RALP1 and RALP6 cells to cisplatin-induced cell death. This sensitization did not affect apoptosis or necrosis induction, determined by cell counter-staining with Hoechst/PI and comet assay. Interestingly, it was well correlated with the increasing incidence of autophagy formation detected by acridine orange staining and the induction of an autophagy marker quantitated by Western blot analysis. Nonetheless, this resistance reversal effect showed the selectivity due to not cause more toxicity in sensitive H460 cells. The mechanisms of trifluoperazine in potentiating the effect of cisplatin were partially through the induction of autophagy, since 3-methyladenine, a specific autophagy inhibitor of class III phosphatidylinositol 3 kinase, could reverse its effects. Furthermore, the level of Bcl-2 protein was diminished in cisplatin-trifluoperazine co-treatment. These suggested that trifluoperazine could sensitize the chemoresistance of non-small cell lung cancers, both acquired resistance and Bcl-2 overexpression through the induction of autophagic cell death and lowering the level of Bcl-2 proteins. In conclusion, this study provided the novel sensitizing effects of trifluoperazine in cisplatin-induced cell death in cisplatin-induced acquired resistance and Bcl-2-mediated apoptosis resistance, which might facilitate the development of new strategy to overcome the chemotherapeutic resistance cancers.

Field of study Biopharmaceutical Sciences   Student's signature.Buntitabhon Sirichanchuen

Academic year 2010   Advisor's signature.T. Pengsuparp

Co-Advisor's signature. Pithi Chant

ACKNOWLEDGEMENTS

I would like to express my deep appreciate to my advisor, Associate Professor Dr. Thitima Pengsuparp and co-advisor, Assistant Professor Dr. Pithi Chanvorachote for their invaluable advice, supervision and encouragement throughout this study.

I am very much indebted to Varisa Pongrakasnanon, from Pharmaceutical Technology program, Faculty of Pharmaceutical Sciences, Chulalongkorn University, for providing RALP cells for this research.

I would like to thank Professor Kiat Ruxrungtham, Head of Allergy and Clinical Immunology Division, Department of Medicine, Faculty of Medicine and Department of Immunology, Faculty of Dentistry, Chulalongkorn University for providing flow cytometry and Ms. Supranee Buranapraditkun for her excellent technical assistance in flow cytometric techniques.

Also, I would like to thank Pharmaceutical Research Instrument Center, Department of Biochemistry and Microbiology, Department of Pharmacology and Physiology, Faculty of Pharmaceutical Sciences, Chulalongkorn University for providing laboratory equipments and analytical instruments and Chulalongkorn University Drugs & Health Product Innovation Promotion Center for providing the inverted-fluorescence microscope.

I am very much obliged and honored to the members of the dissertation committee for their supportive attitude, constructive criticisms and for their invaluable discussions over my dissertation.

It would not be completed without expressing my heartfelt gratitude to my family and to my colleges for their love, understanding, moral support and tremendous encouragements throughout my life.

CONTENTS

LIST OF TABLES

LIST OF FIGURES

Figure   **Page**

Figure   **Page**

LIST OF ABBREVIATIONS

%	Percentage
°C	Degree Celsius (centigrade)
µg	Microgram (s)
µl	Microliter
3-MA	3-methyladenine
Akt/PKB	Serine/threonine protein kinase B
ANOVA	Analysis of variance
AO	Acridine orange
ATCC	American type culture collection, Maryland, USA
Atg	Autophagy-related
Bad	Bcl-2-associated death promoter protein
Bak	Bcl-2 homologous antagonist/killer
Bax	Bcl-2-associated X protein
Bcl-2	B-cell lymphoma-2
Bcl-X_L	B-cell lymphoma-extra large
BER	Base-excision repair
BID	BH3 interacting domain death agonist
CO_2	Carbon dioxide
Ctr1	Copper transporter-1
Cyt c	Cytochrome c
DDW	Double distilled water
DMSO	Dimethylsulfoxide
DNA	Deoxyribonucleic acid
EDTA	Ethylene diamine tetraacetic acid
et al.	*et alii*, and others
FACS	Fluorescent Activated Cell Sorter
FDA	Food and Drug Administration
g	Gram (s)
GSH	Glutathione

GST	Glutathione-S-transferase
h	Hour
H460/cis	Cisplatin-induced resistant H460 cells
IC_{50}	50% inhibitory concentration
Ig	Immunoglobulin
LC3	Microtubule-associated proteins 1 light chain 3
LC3 II/I	The conversion of LC3 type I to II
LC3-I	Microtubule-associated proteins 1 light chain 3 type I
LC3-II	Microtubule-associated proteins 1 light chain 3 type II
MAP1 LC3	Microtubule-associated proteins 1 light chain 3
mg	Milligram (s)
min	Minute (s)
ml	Milliliter (s)
mM	Millimolar
mm	Millimeter (s)
MMR	Mismatch repair
mTOR	Mammalian target of rapamycin
MTT	3-(4,5-dimethythiazol-2-yl)-2,5-diphenyltetrazolium bromide
NaCl	Sodium chloride
NaF	Sodium fluoride
NER	Nucleotide-excision repair
NSCLC	Non-small cell lung cancer
OD	Optical density
PBS	Phosphate-buffered saline
PE	Phosphatidylethanolamine
pH	The negative logarithm of hydrogen ion concentration
PI	Propidium iodide
PI3K	Phosphatidylinositol 3-kinase
PVDF	Polyvinylidene fluoride
qs.	Make to volume
RALP	Bcl-2-overexpressed H460 cells

RALP1   Clone no.1 of Bcl-2-overexpressed H460 cells

RALP6   Clone no.6 of Bcl-2-overexpressed H460 cells

RPMI   Roswell Park Memorial Institute's medium

SCGE   Single-cell microgel electrophoresis

SDS-PAGE   Sodium dedocyl sulfate polyacrylamide gel electrophoresis

SEM   Standard error of mean

SPSS   Statistical package for social sciences

TBST   Tris-buffered saline, 0.05 % Tween 20

TFP   Trifluoperazine

TGN   Trans-Golgi network

UV   Ultraviolet

V   Volt

CHAPTER I

INTRODUCTION

Lung cancer is considered as the most common cancers which is a leading cause of cancer-related death worldwide [Deesomchok, Dechayonbancha and Thongprasert, 2005; Chang, 2011]. Among two main types of lung cancer; small cell lung cancer (SCLC) and non-small cell lung cancer (NSCLC), NSCLC has garnered most attention. Not only does this type of lung cancer account for more than 80 % of all diagnosed lung cancer patients, but also 5-year survival rate of the patients is only approximately 15% [Stoppler, 2005; Chang, 2011]. Although chemotherapy has been shown to be an effective treatment for various types of cancer, NSCLC is often resistant to chemotherapy and the benefits for individual patients are unpredictable [Chang, 2011]. Thus, the novel strategy for NSCLC treatment emerges and becomes a research of interest.

In the treatment of lung cancer, cisplatin, a platinum-containing agent (*cis*-diammine-dichloroplatinum(II)), has been recommended as a first-line drug [Siddik, 2003; Wang and Lippard, 2005; Kelland, 2007; Rabik and Dolan, 2007; Azzoli, Giaccone and Temin, 2010]. Cisplatin exerts its antineoplastic effect through a direct binding to DNA resulting in a cross-linking and ultimately apoptotic cell death [Fisher, 1994; Siddik, 2003; Rabik *et al.*, 2007]. Cisplatin-based therapy is superior in response rate, and marginally superior in overall-survival, compared to non-platinum based therapy [Azzoli *et al.*, 2010].

According to the effectiveness of regimens and patients' performance status in cisplatin-based therapy in a number of clinical trials, the standard protocol for NSCLC has been set. Approximately 2-4 cycles of cisplatin are given over a month-long period [Le Chevalier *et al.*, 2001; Pisters *et al.*, 2007; Azzoli *et al.*, 2010]. Exposure to the cisplatin for long period has given an opportunity for cancer cells to adapt themselves and finally become acquired-drug resistant clones. A number of drug resistance-related mechanisms developing during chemotherapy have been proposed for example; decreasing in intracellular drug accumulation, activation of detoxifying system, and increasing in DNA repair machinery [Siddik, 2003; Wang *et al.*, 2005; Rabik *et al.*, 2007; Stewart, 2007; Chang, 2011]. However, the most

prevalent resistance mechanism was the result of disturbing cellular apoptosis process [Mese *et al.*, 1998; Yoon *et al.*, 2001; Siddik, 2003; Hövelmann, Beckers and Schmidt, 2004; Cho *et al.*, 2006; Martínez-Lacacia *et al.*, 2007; Rabik *et al.*, 2007; Stewart, 2007; de Bruin and Medema, 2008].

Several lines of evidence have shown that upregulation of anti-apoptotic Bcl-2 protein is a key mechanism in inhibition of apoptosis induced by chemotherapeutic drugs [Waggoner *et al.*, 1998; Sartorius and Krammer, 2002; Douarre *et al.*, 2005; Cho *et al.*, 2006; Wesarg *et al.*, 2007; Coates *et al.*, 2009]. Recently, there is an increasing evidence supported that Bcl-2 protein also plays an important role in cell death blockage, not only apoptosis, but also autophagic cell death or type II programmed-cell death [Saeki *et al.*, 2000; Pattingre and Levine, 2006]. In addition, cancers expressing high level of Bcl-2 protein are often found to be resistant to chemotherapy [Waggoner *et al.*, 1998; Sartorius *et al.*, 2002; Douarre *et al.*, 2005; Cho *et al.*, 2006].

As Bcl-2 protein has been of great interest in cancer-therapy development, several types of inhibitors targeting Bcl-2 protein were emerged. Those are small non-peptidic molecules targeting BH3 binding site of Bcl-2 (BH-3-mimetic) and Bcl-2 antisense. To date, only one Bcl-2 antisense and three small molecules, Bcl-2 protein inhibitors, are being tested in clinical trials. Most of novel agents were likely effective in hematological malignancies, rather than in solid tumors, especially, lung cancer [Azmi and Mohammad, 2009]. The preclinical studies seem promising, especially in combination with additional chemotherapeutic agents. Nonetheless, some Bcl-2 inhibitors in the phase II investigations failed to confirm this benefit [Kang and Reynolds, 2009; Patel *et al.*, 2009]. Moreover, some Bcl-2 antagonists also showed neurologic-related toxicity, including ataxia, mood alterations, somnolence, and cognitive dysfunction [Paik *et al.*, 2010].

While apoptosis modulation by Bcl-2 antagonists could not give the good result as expect, an alternative pathway like autophagic cell death should be employed. Recently, advance information in cancer research suggested that autophagy plays an important part in controlling cell survival and death. Autophagy is indicated by the increasing of autophagosome formation [Wang and Klionsky, 2003; Yang *et al.*, 2005; Kondo and Kondo, 2006; Levine, 2007]. The process involves the formation of autophagosomes in which subcellular membranes sequester intracellular proteins or organelles, then, deliver to lysosomes for lysosomal degradation [Wang *et*

al., 2003; Yang *et al.*, 2005; Kondo *et al.*, 2006; Levine, 2007]. The autophagic responses are not only the removal of non-necessary or long-lived proteins and faulty organelles, but also the cause of autophagic cell death, recognized as type II programmed-cell death. It has been shown to regulate normal physiology and pathology such as carcinogenesis and chemotherapeutic susceptibility. However, that information is still controversial [Edinger and Thompson, 2003; Gozuacik and Kimchi, 2004; Levine and Klionsky, 2004].

There were some data supporting that autophagy induction could gain benefit for cancer treatment [Ito *et al.*, 2006; Kondo *et al.*, 2006; Pattingre *et al.*, 2006; Lefranc, Facchini and Kiss, 2007; Moretti *et al.*, 2007], for example, resveratrol can induce autophagy and resulted in tumor growth arrest in ovarian cancer [Opipari *et al.*, 2004]. Moreover, autophagy paves the way to sensitize to several anticancer agents, such as tamoxifen [Kondo *et al.*, 2005] and camptothecin [Lamparska-Przybysz, Gajkowska and Motyl, 2004] in breast cancer and also the specific inhibitor of DNA-dependent protein kinase (DNA-PK) in malignant glioma cell lines [Daido *et al.*, 2005]. Besides that, autophagy induction by overexpression of Beclin-1, one of human homologues of autophagy-related genes, in human gastric cancer cells augmented cisplatin-induced cell death [Furuya *et al.*, 2005]. However, there was conflict evidence indicated that autophagy could promotes tumor cell survival [Degenhardt *et al.*, 2006] and also acts as a cytoprotective mechanism protecting DNA damaging effects of temozolomide and etoposide in several malignant glioma cell lines [Katayama *et al.*, 2007]. Thus, autophagic process affects cells differently depending on cell types and particular agents [Kondo *et al.*, 2005]. Autophagy could be observed in non-small cell lung cancer [Karpathiou *et al.*; Kim *et al.*, 2008; Liu *et al.*, 2008]. However, the effects of autophagy in sensitizing chemotherapeutic agents in non-small cell lung cancer are far from understood.

Hence, autophagy inducer is in the point of consideration. Among a number of autophagic inducers, trifluoperazine (TFP) [Zhang *et al.*, 2007], a FDA-approved anti-psychotic and anti-emetic drug, has a most potential to be used as chemotherapy sensitizer. Sub-toxic concentrations of TFP was able to retard cancer cell growth in U87MG glioma cells [Shin *et al.*, 2004], inhibited DNA repair and sensitized U1810 cells in bleomycin-induced cell death [Polischouk *et al.*, 2007]. Moreover, the combination of trifluoperazine and bleomycin is now under clinical trial phase I and II for non–Hodgkin's lymphoma and glioblastoma multiforme, respectively [Polischouk

et al., 2007]. Trifluoperazine is also able to overcome adriamycin-resistant L1210 mouse leukemia cells by suppression of P-glycoprotein expression [Shina *et al.*, 2006]. In addition, trifluoperazine could sensitize ionizing radiation-induced cell killing through inhibition of DNA repair [Gangopadhyay *et al.*, 2007]. This information suggested that TFP might be able to sensitize cisplatin-induced cytotoxicity in cancer, even resistance cancer. Moreover, the other benefits gaining from TFP are the reduction of nausea-vomiting symptoms and it may improve quality of life of patients as an anti-depression and anti-anxiety.

In the case of cisplatin-induced resistant NSCLC cells, it is interesting to know whether autophagy induction could modulate these cells to be more susceptible to cisplatin-induced cell death. This study thus focuses on the effect of autophagy inducer, TFP, on cisplatin-mediated cytotoxicity in NSCLC H460 cells. Furthermore, to gain more understanding on resistant cancers, long-term cisplatin exposure-mediated- and Bcl-2-overexpressed-mediated-resistant H460 cells were also used as a model.

Objectives

1. To examine the effect of TFP on cisplatin-induced cytotoxicity and types of cell death in H460 (human non-small cell lung cancer) cells and their resistant counterparts, both cisplatin-induced acquired resistance (H460/cis cells) and Bcl-2 overexpression (RALP cells).
2. To investigate the possible mechanisms of TFP in modulating cisplatin sensitivity.

```
┌─────────────────────────────────────────────┐
│        Human non-small cell lung cancer       │
└─────────────────────────────────────────────┘
```

| H460 | H460/cis (Cisplatin-induced resistant H460 cells) | RALP (Bcl-2-overexpressed H460 cells) |

Cisplatin/ Cisplatin and TFP co-treatment

Cell viability assay (MTT assay)

| Apoptotic cell death | Necrotic cell death | Autophagic cell death |

- Hoechst/PI staining
- Comet assay

- Hoechst/PI staining

- AO staining
- Western blot of LC3 II
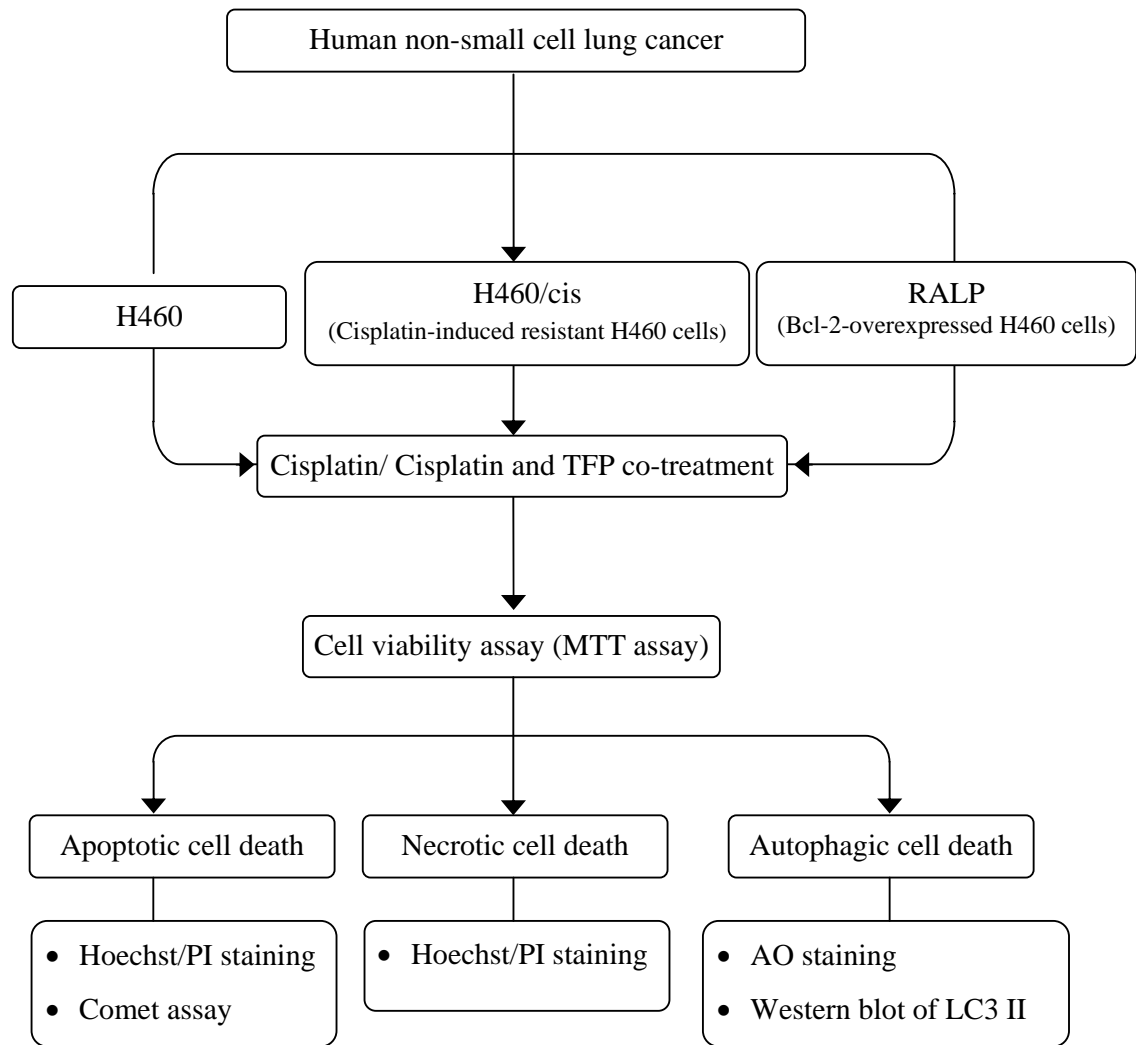
Figure 1 The conceptual framework of this study

Scope of study

The present study covered the *in vitro* assay of the effect of TFP on cisplatin-induced cytotoxicity in non-small cell lung carcinomas which are cisplatin-sensitive H460 cells and cisplatin-resistant H460/cis cells and RALP cells. The methods were designed as the followings. Establishment of resistant H460/cis cells by exposuring cells to gradually increasing concentrations of cisplatin and resistant RALP cells by transfecting with plasmids containing Bcl-2 gene. Then, all cells were treated with either cisplatin or the combination of cisplatin and TFP. The cytotoxic effects to those treatments were accessed using cell viability assay and types of cell death were evaluated. For apoptosis and necrosis determination, cell death was detected by Hoechst 33342/propidium iodide staining and single-cell microgel electrophoresis (comet assay). For autophagic cell death, the degree of autophagosome formation was determined by acridine orange staining, detected under inverted-fluorescence microscope for qualitative results and by flow cytometer for quantitative results. Protein analysis for microtubule-associated protein 1 light chain 3 (MAP1-LC3) or LC3, the marker of autophagy, was done by Western blotting.

To elucidate the effects of TFP, it was co-treated with cisplatin and types of cell death were differentiated, using the assay described previously. To confirm whether the effect of TFP in modulating cisplatin-induced toxicity was the result of autophagy, 3-methayadenine, an autophagy inhibitor, was accessed and all parameters described above were determined.

Contribution of the study

1. The information about the effect of TFP on cisplatin-induced cytotoxicity may be useful as supporting data for developing new strategy of using TFP as a chemotherapeutic sensitizer in NSCLC treatment.
2. Knowing the possible mechanisms of TFP in modulating cisplatin-induced cell death.

CHAPTER II
LITERATURE REVIEWS

Lung cancer

Lung cancer is a common cancer of the respiratory system, which is the leading cause of cancer-related death in both women and men worldwide. In Thailand, the incidence of lung cancer is the second most common cancer in males after liver cancer and the fourth in females after breast, cervix and liver cancer [Deesomchok, Dechayonbancha and Thongprasert, 2005]. Diagnosing lung cancer in its earliest stage provides the best hope for successful treatment and a cure. However, patients with lung cancer are commonly found to be aged more than 50 years and present in the advanced stage (metastasis and locally advanced). For example, the 5-year survival rate for stage 1 non-small cell lung cancer is 60% to 80%, whereas the 5-year survival rate for stage 4 (metastatic) non-small cell lung cancer is approximately 15% [Chang, 2011].

There are two main types of lung cancer; small cell lung cancer (SCLC) and non-small cell lung cancer (NSCLC). Among the two types, NSCLC is the predominant form with more than 80% of lung cancer cases [Pisters *et al.*, 2007; Chang, 2011]. This dissertation will focus only on this type of lung cancer. There are three sub-types of NSCLC. It is categorized according to size, shape, and chemical properties.

- **Squamous cell carcinoma:** About 25% to 30% of all lung cancers are this kind. They are linked to smoking and mostly found in the middle of the lungs, near a bronchus.

- **Adenocarcinoma:** This type accounts for about 40% of lung cancers. It is usually found in the outer part of the lung.

- **Large-cell (undifferentiated) carcinoma:** About 10% to 15% of lung cancers are this type. It can start in any part of the lung. It can grow and spread quickly, which makes it difficult to treat.

However, the cancer that occurs in other organs, such as the breast, pancreas, kidney or skin and metastasizes to the lungs, is not recognized as lung cancer.

The management of NSCLC requires a multidisciplinary approach. Patients generally require a combination of surgery, radiotherapy and/or chemotherapy, depending on their stage, resectability and overall performance status. Chemotherapy is recognized as an important component of therapy for all stages, even in patients with completely resected or early disease stage.

Platinum-based therapy is the first line of chemotherapy for NSCLC which cisplatin is used as the main agent. It is usually given in combination with one or two other drugs, like tubulin binding agents including the taxanes, Vinca alkaloids, a camptothecin analog, gemcitabine, or pemetrexed.

Table 1 Summary of recommendations for cisplatin-based chemotherapy for stages I-IIIA resectable non–small-cell lung cancer from the Cancer Care Ontario and American society of clinical oncology [Pisters *et al.*, 2007] and for stage IV non–small-cell lung cancer from American Society of clinical oncology [Azzoli, Giaccone and Temin, 2010].

Stage	Summary of recommendations for cisplatin-based chemotherapy
IA	Adjuvant cisplatin-based chemotherapy is not recommended.
IB	Adjuvant cisplatin-based chemotherapy is not recommended for routine use.
IIA	Adjuvant cisplatin-based chemotherapy is recommended.
IIB	Adjuvant cisplatin-based chemotherapy is recommended.
IIIA	Adjuvant cisplatin-based chemotherapy is recommended.
IV	Cisplatin-based chemotherapy is recommended.
General	The use of adjuvant cisplatin-based chemotherapy regimens that include alkylating agents is not recommended as these agents have been found to be detrimental to survival.

According to American Society of Clinical Oncology Clinical Practice guideline update on chemotherapy for stage IV NSCLC [Azzoli *et al.*, 2010], cisplatin is also the first line therapy in the combination with second- and third-generation antineoplastic drug. Regarding of many clinical trials, platinum-based therapy is

superior in response rate, and marginally superior in overall survival than that in non-platinum therapy combinations. Cisplatin is slightly more effective than carboplatin, the second-generation of platinum-based agent, with a higher response rate but more adverse effect. Therefore, either drug is acceptable depending on the individual acceptability. Cisplatin combination with the third-generation cytotoxic drugs such as docetaxel, gemcitabine, irinotecan, paclitaxel, pemetrexed or vinorelbine may improve survival.

Nonetheless, the chemotherapy should be stopped at disease progression or after four cycles in patients whose disease is not responding to treatment. Moreover, the cytotoxic combinations should not be administered for more than six cycles. For patients who have stable disease or who respond to first-line therapy, evidence does not support the continuation of cytotoxic chemotherapy until disease progression or the initiation of a different chemotherapy before disease progression [Azzoli *et al.*, 2010; Chang, 2011].

Cisplatin

Cisplatin or cis-diammine-dichloroplatinum(II) is a commonly used chemotherapeutic agent which was accidental discovered in 1948. Its clinical introduction in the 1970's represented a major landmark of anti-cancer drugs [Rabik and Dolan, 2007]. The clinical benefits of cisplatin as an anti-cancer agent have been recognized for over 30 years [Kelland, 2007]. Cisplatin is used as the first line and effective drug for many types of cancer, including ovarian, cervical, head and neck, non-small cell lung and lymphoma [Siddik, 2003; Wang and Lippard, 2005; Kelland, 2007; Rabik *et al.*, 2007].
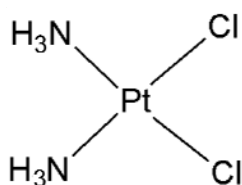
Figure 2 The structure of cisplatin

The mechanisms of cellular uptake and efflux of cisplatin are still not fully understood. In addition to passive diffusion, it was found that Ctr1, a high-affinity copper transporter-1, also play an important role in cisplatin influx into the cells [Wang *et al.*, 2005; Kelland, 2007].
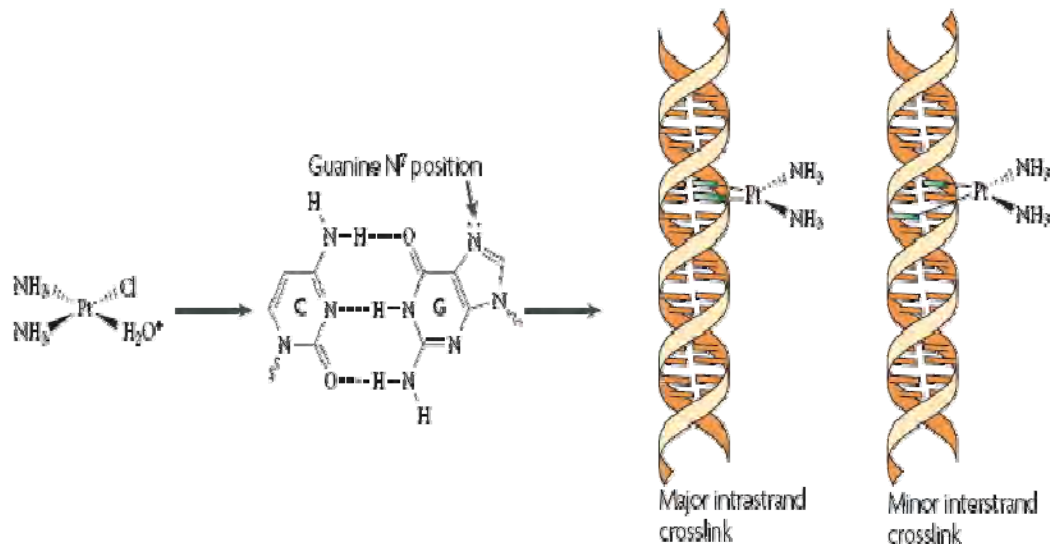
Figure 3 The mechanism of cisplatin adducts [Kelland, 2007]

Once cisplatin entering cells, it becomes aquated, losing chloride and forms $[Pt(NH_3)_2Cl(OH_2)]f^+$ and $[Pt(NH_3)_2(OH2)_2]^{2+}$ which are more reactive to the cellular target. The platinum atom of cisplatin interacts with nucleophilic molecules within the cell, including DNA, RNA, and proteins. However, DNA is the primary biological target [Wang *et al.*, 2005]. It binds covalently to the N7 position of purines to generate several forms of DNA lesions: mono-adducts, 1,2- or 1,3-intrastrand crosslink, and inter-strand crosslink (Figure 3). That cisplatin-DNA adducts result in transduction various DNA-damage signals through Akt, c-ABL, p53, MAPK, JNK and ERK pathways. As shown in Figure 4, these lead to transcription inhibition, cell-cycle arrest and initiate DNA-repair system which finally turn to activate apoptosis or necrosis [Siddik, 2003; Wang *et al.*, 2005; Rabik *et al.*, 2007].
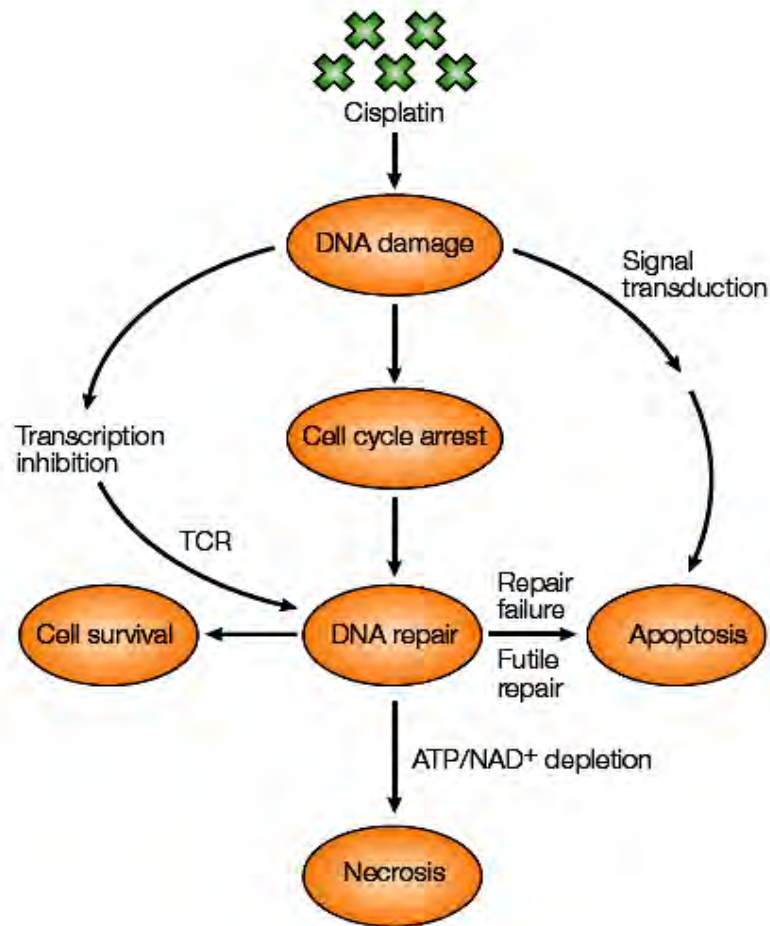
Figure 4 The effects of cisplatin-DNA adducts [Wang *et al.*, 2005].

(TCR; transcription-coupled repair)

Cisplatin resistance

Regardless of a high potency of cisplatin, it also faces with cancer resistant problem. The mechanisms of cisplatin resistance are classified into four major pathways [Siddik, 2003; Wang *et al.*, 2005; Rabik *et al.*, 2007; Stewart, 2007]. As shown in Figure 5, those are decreasing drug accumulation, activation of detoxifying system, activation of DNA repair and blocked apoptosis [Waggoner *et al.*, 1998; Sartorius and Krammer, 2002; Douarre *et al.*, 2005; Cho *et al.*, 2006; Wesarg *et al.*, 2007; Coates *et al.*, 2009].

1. Decreasing intracellular cisplatin accumulation

The mutation or deletion of the copper transporter CTR1 gene encoding for Ctr1, a high-affinity copper transporter which can also transports cisplatin, resulted in decrease amount of drug entering cells [Wang *et al.*, 2005]. Besides that, ATP-binding cassette sub-family C 2 (ABCC2), also known as MRP2 or cMOAT, has a role in cisplatin resistance by promoting drug efflux [Rabik *et al.*, 2007; Stewart, 2007].

2. Activation of detoxifying system

Although cisplatin can enter into cancer cells, its toxicity can be reduced by many cytosolic molecules and enzymes. Glutathione, glutathione-S-transferase (GST) and metallothionein are key cytosolic components which reduced cisplatin efficiency [Stewart, 2007].

3. Increasing in DNA repair machinery

Activation of DNA repair is also one of the processes that can reduce cytotoxic effect of cisplatin. Four major DNA-repair pathways are nucleotide-excision repair (NER), base-excision repair (BER), mismatch repair (MMR) and double-strand-break repair. NER is the major pathway known to remove cisplatin lesions from DNA [Kelland, 2007], however, other DNA-repair pathways may be involved with cisplatin resistance.

4. Blockage of apoptosis induction

Several genes regulating DNA damage, apoptosis and survival signaling may contribute to resistance. There are many anti-apoptotic proteins upregulated in cisplatin-resistance cells; for example, p53 and Bcl-2 family, which are suggested to be responsible for cisplatin resistance [Kelland, 2007; Rabik *et al.*, 2007; Stewart, 2007].
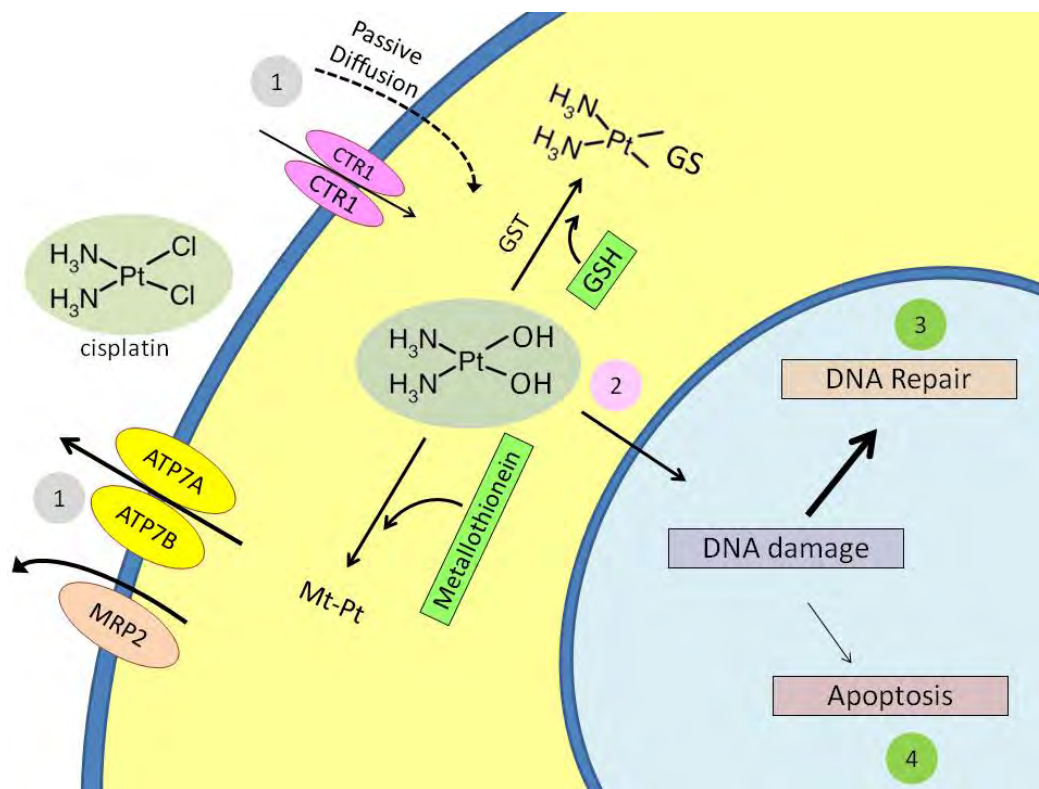
Figure 5 The possible mechanisms of cisplatin resistance: (1) Decreasing of drug accumulation, (2) Activation of detoxifying system, (3) Activation of DNA repair and (4) Blockage of apoptosis.

Apoptosis

Apoptosis (self-killing) is recognized as type I programmed-cell death, which involves the activation of catabolic enzymes in signaling cascades and result in cell morphologic alteration. The unique characteristics of apoptosis are cellular shrinkage with nuclear chromatin condensation (pyknosis) and nuclear fragmentation (karyorrhexis). Apoptosis can be initiated by two different types of signals and generates two different pathways as shown in Figure 6. The intracellular stress signals result in the change of mitochondrial membrane permeability. This type of apoptosis is called intrinsic or mitochondrial pathway involving with anti-apoptotic Bcl-2 family proteins such as, Bcl-2, Bcl-X$_L$ and Mcl-2 and pro-apoptotic Bcl-2 family proteins such as Bax, Bad or Bak. Anti-apoptotic Bcl-2 proteins inhibit cytochrome c (Cyt c) release as the consequence of pore formation of pro-apoptotic proteins. Cyt c signals in a cascade and results in activating caspase 9. For extracellular signaling,

this pathway involves the death receptors and ligands such as FasL or TRAIL. This type is called extrinsic or death receptor pathway. In this pathway, caspase 8 is activated. Finally, the execution molecule of both pathways is caspase 3 and then initiates apoptosis.

An anti-apoptotic protein, Bcl-2 protein, plays an important role in intrinsic pathway in preventing Cyt c release.
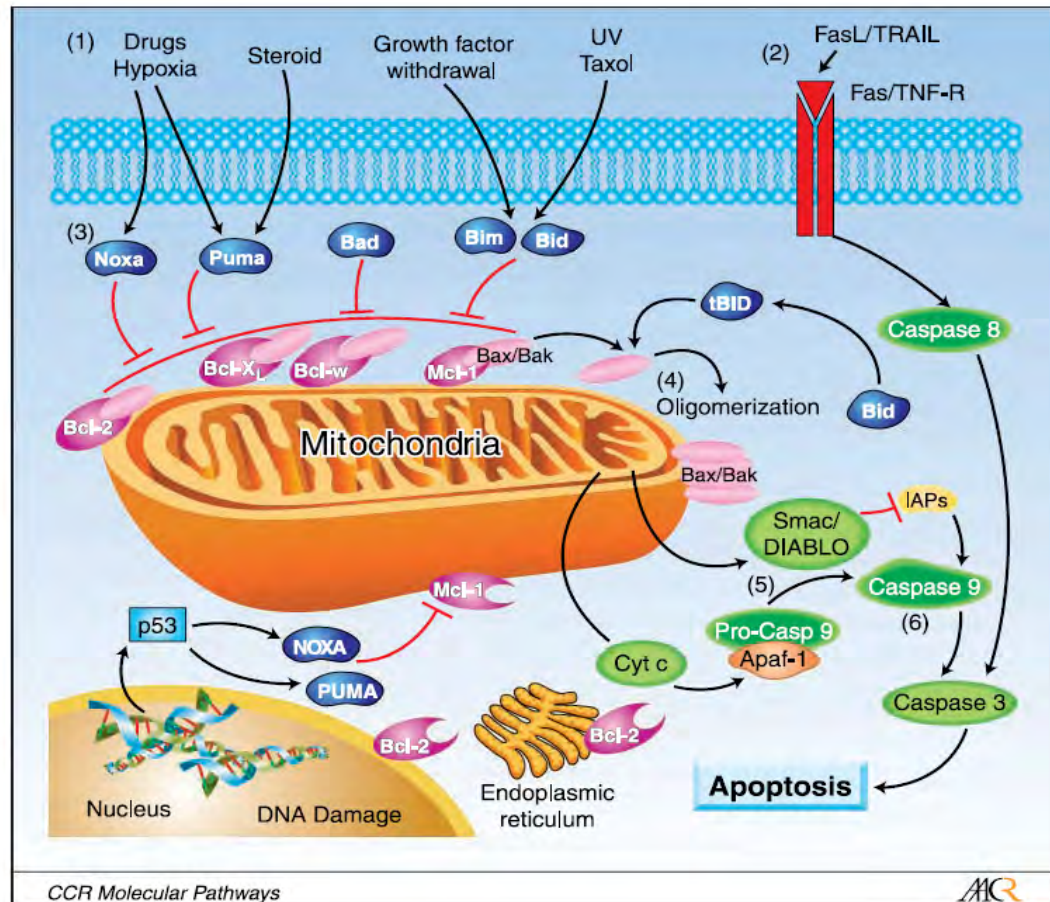
Figure 6 Apoptosis pathways [Kang and Reynolds, 2009]

Bcl-2 protein and apoptosis

Bcl-2 protein is the prototype for its family which is the product of human proto-oncogene. They govern mitochondrial outer membrane permeabilization (MOMP) and can be either pro-apoptotic proteins (Bax, Bak or Bad) or anti-apoptotic proteins (Bcl-2, Bcl-X_L or Bcl-w). There are 25 genes in the Bcl-2 family known to date. Bcl-2 derives its name from B-cell lymphoma 2, as it is the second member of a

range of proteins initially described as a reciprocal gene translocation in chromosomes 14 and 18 in follicular lymphomas.

Bcl-2 protein has shown an important role in cancer treatment failure. There were many evidences confirmed that overexpression of Bcl-2 resulted in decreasing chemotherapy sensitivity and failure to apoptosis induction [Waggoner *et al.*, 1998; Sartorius *et al.*, 2002; Kuwana and Newmeyer, 2003; Douarre *et al.*, 2005; Cho *et al.*, 2006; Wesarg *et al.*, 2007; Coates *et al.*, 2009]. Consistently, siRNA of Bcl-2 could reverse those resistances [Cho *et al.*, 2006]. Therefore, Bcl-2-overexpressed cells could be used as representative chemotherapy-resistant cells, due to their apoptosis defect.

Autophagy

Autophagy is a dynamic process involving proteins degradation in which occurring in living eukaryotic cells, conserved from yeast to mammals. In this process, subcellular membranes undergo morphological changes to sequester intracellular proteins or organelles and subsequently delivered to lysosomes and digested by lysosomal enzymes [Klionsky, 2007; Mizushima, 2007]. Autophagy functions as a homeostasis maintaining process in which eliminates excessive, faulty or injured proteins and organelles. It can be induced by both intracellular and extracellular stimuli, for example, stress; starvation from amino acid or growth factor; or invasion of microorganisms; to protect cells against mutation or injury and also to recycle cellular products to provide materials for protein synthesis or energy for themselves [Katayama *et al.*, 2007; Periyasamy-Thandavan *et al.*, 2008]. In addition to its role in proteins and organelles degradation, autophagy also causes cell death, known as type II programmed cell death [Yang *et al.*, 2005; Kondo *et al.*, 2008].

Classification of autophagy

Autophagy is a multi-step process and different types of autophagy show the distinguished process. It is classified into 3 groups (Figure 8). Those are microautophagy, macroautophagy and chaperon-mediated autophagy [Mizushima, 2007].

1. Microautophagy

It is the direct invagination of lysosomal membrane to engulf cytosolic material and transfer to lysosomal lumen. This process is not involved with autophagosomes trafficking [Wang and Klionsky, 2003].

2. Macroautophagy

It is the most prevalent form of autophagy found in cells [Yang *et al.*, 2005]. The word "autophagy" is referred to macroautophagy and all autophagy that is mentioned later means this type of autophagy. Autophagy consists of multi-steps (Figure 7). At the beginning, portions of intracellular membrane which is not known the exact origin are isolated, called isolated membrane. After that isolated membrane elongates both sides, simultaneously engulf of cytoplasmic material and then both ends join together to form autophagosome. Next, autophagosome is trafficking to lysosome and then fuse to form autolysosome. Finally, sequestered contents are degraded by lysosomal hydrolases and are recycled [Wang *et al.*, 2003; Mizushima, 2007; Ravikumar *et al.*, 2009].
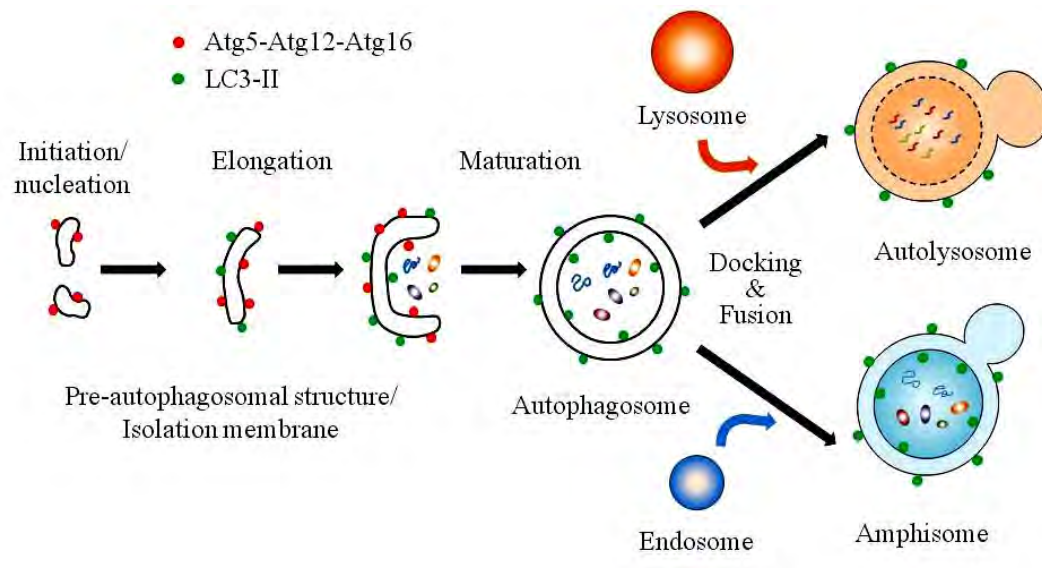
Figure 7 The steps of autophagy (Adapted from Ravikumar *et al.,* 2009*)*

Both microautophagy and autophagy are non-specific degradation. However, autophagy can select its target in case of harmful or injured proteins or organelles; for example, damaged mitochondria or endoplasmic reticulum [Yang *et al.*, 2005].

3. Chaperon-mediated autophagy (CMA)

Chaperon-mediated autophagy (CMA) is the specific degradation with help of cytosolic chaperone complex. The targets of CMA are cytosolic peptides. When target peptides are recognized by chaperone complex, the peptide-chaperone complex is trafficking to lysosome and binds to receptors on lysosomal membrane, LAMP-2A. By then, peptides are transferred to lysosomal lumen for degradation [Yang *et al.*, 2005].
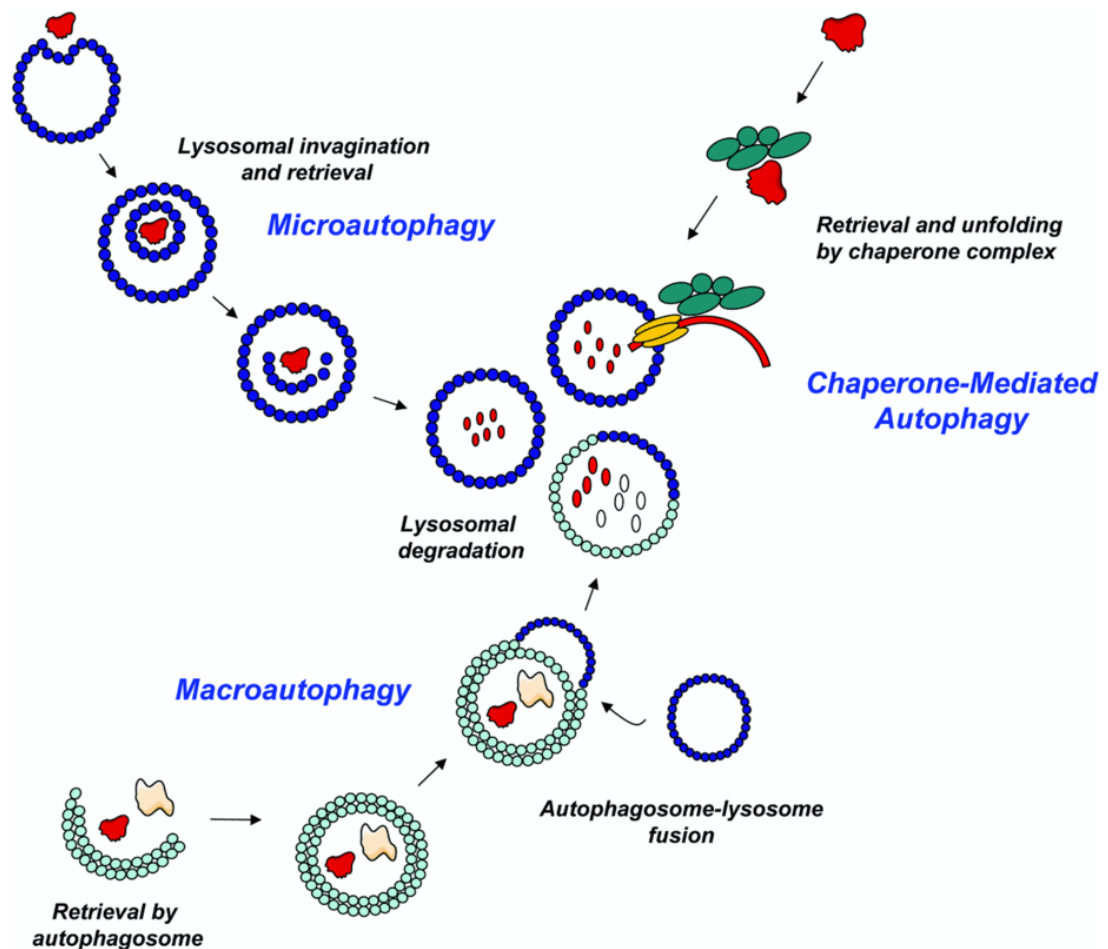
Figure 8 Classification of autophagy [Martinet *et al.*, 2009]

Molecular mechanism of autophagy

Various signaling pathways have been identified to play part in autophagy (Figure 9). Molecular information about the regulation of autophagy in both normal and cancer cells is still fragmented, and far from complete [Kondo *et al.*, 2005].

There are a large number of evidences indicated that the phosphatidylinositol 3-kinase (PI3K) is important in autophagy [Brown *et al.*, 1995; Yang *et al.*, 2005; Kroemer, 2008]. PI3K Class I and III regulate autophagy differently [Kondo *et al.*, 2005].

The class I PI3K-Akt-mTOR signaling pathway which is activated in diverse types of cancer through the growth factor receptor inhibits autophagy. This autophagy suppression results from activation of the kinase mTOR which is located downstream of Akt, a serine-threonine kinase. Akt is also located downstream of class I PI3K as seen in Figure 9 [Gozuacik and Kimchi, 2004; Kondo *et al.*, 2005]. This finding was confirmed with rapamycin, an inhibitor of mTOR. It induced autophagy in metastatic renal cancer, breast cancer and also several other types [de Bruin and Medema, 2008; Thorburn, 2008; Morselli *et al.*, 2009]. However, there are some miscellaneous molecules involving this negative regulation such as oncogenic forms of Ras that are also implicated in several tumors [Kroemer and Jäättelä, 2005; Morselli *et al.*, 2009]. The phosphatase and tensin homologue (PTEN), a tumor-suppressor gene, also regulate in this class I PI3K-Akt-mTOR signaling pathway. PTEN dephosphorylates class I PI3K resulting in Akt activity suppression and allow autophagy to be initiated [Kroemer *et al.*, 2005]. Nevertheless, PTEN is often deleted or mutated in various cancers such as malignant gliomas, prostate, breast and endometrial cancers [Kondo *et al.*, 2005]. Deletion or mutation in PTEN results in constitutive activation of the Akt pathway and therefore inhibit autophagy. However, the class I PI3K-Akt-mTOR signaling pathway is not an only pathway controlling autophagy.

The class III PI3K-beclin1 signaling pathway can promote the sequestration of cytoplasmic material during autophagy [Wang *et al.*, 2003; Yang *et al.*, 2005; Thorburn, 2008; Zhang *et al.*, 2009]. The binding of Beclin 1 to class III PI3K at trans-Golgi-network (TGN) might relate to the autophagosome trafficking because class III PI3K promotes the trafficking of lysosomal enzymes from the TGN to the lysosome [Brown *et al.*, 1995; Kihara *et al.*, 2001]. Beclin-1 was also the first molecule demonstrating a direct link between tumorigenesis and autophagy activation

[Liang *et al.*, 1999]. It was confirmed with exogenous expression of beclin-1 in MCF7 cells resulting autophagy induction and proliferation suppression and tumorigenesis inhibition [Liang *et al.*, 1999].   Another study showed that ceramide-mediated autophagy in colon cancer cells inhibits Akt and upregulates beclin1 [Scarlatti *et al.*, 2004]. Consistently, 3-methyaldenine (3-MA), an inhibitor of class III PI3K, inhibits autophagy in Hela cells [Zhang *et al.*, 2009].
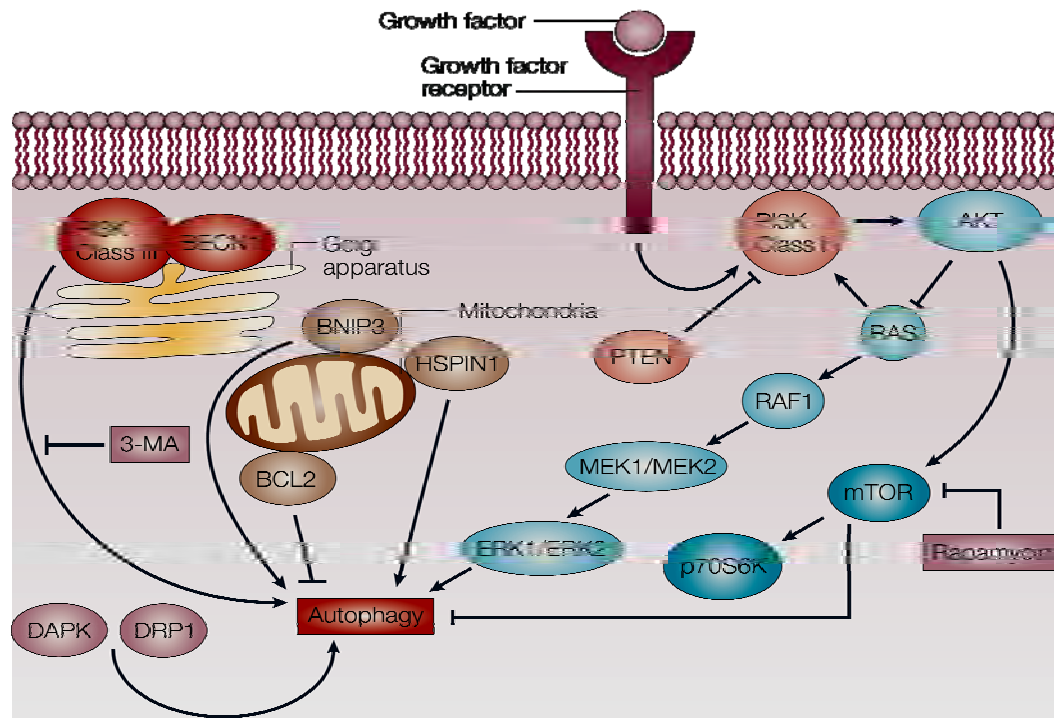
Figure 9 The molecular regulation of autophagy [Kondo *et al.*, 2005].

There are also other molecules which can regulate autophagy; for example death-associated protein kinase (DAPK) and death-associated related protein kinase 1 (DRP1) [Inbal *et al.*, 2002], Bcl-2 [Pattingre *et al.*, 2005; Levine, Sinha and Kroemer, 2008; Coates *et al.*, 2009] and its family members (HSPIN1, Bax and Bak) [Lu, 2008; Thorburn, 2008] and mitogen-activated kinases [Ogier-Denis *et al.*, 2000].

DAPK and DRP1 proteins are calcium-calmudulin regulated serine-threonine kinase that are identified as positive mediators for regulation various forms of programmed cell death, including apoptosis, autophagic cell death and programmed necrosis. It was also indicted that DAPK and DRP 1 induced autophagy in MCF7 cells and Hela cells [Inbal *et al.*, 2002].

The mitogen-activated protein kinases belong to family of serine-threonine kinases that are involved in a wide range of cellular responses. Inhibition of mitogen-activated protein kinase (MAPK)/extracellular signal-regulated protein kinase kinase (ERK) reduced autophagic vacuoles content, mitochondrial degradation and cell death in 1-methyl-4-phenylpyridinium-treated cells [Zhu *et al.*, 2007]. Consistently, the ERK1 and ERK 2, stimulated by the Ras-RAF1- mitogen activated protein kinase kinase (MEK) signaling pathway, have been shown to induce autophagy in HT-29 colon cancer cells [Ogier-Denis *et al.*, 2000].

Detection of Autophagy

In autophagic process, the induction of autophagosome formation is the critical step. To date, microtubule-associated protein 1 light chain (MAP1 LC3 or LC3), a mammalian homolog of Atg8, is the only reliable protein used as a marker of autophagosome formation [Klionsky *et al.*, 2008; Mizushima, Yoshimori and Levine, 2010]. The increasing number of autophagosome formation corresponds to cellular autophagic activity. In normal physiology, LC3 proteins are in cytosol in the form of LC3 type I (LC3-I). Immediately after autophagy activation, LC3-I is subsequently conjugated with phosphatidylethanolamine (PE) to become LC3 type II (LC3-II or LC3-PE) by an ubiquitination-like enzymatic reaction. In contrast to the cytoplasmic localization of LC3-I, LC3-II associates with both the outer and inner membranes of the autophagosome. Therefore, the increasing of LC3-II level or of the conversion of LC3-I to LC3-II is an indicator of autophagic activity [Klionsky *et al.*, 2008]. The level of LC3 proteins can be determined by using immunoblotting with antibodies against LC3 proteins or using LC3 tagging with green fluorescence protein (GFP) [Mizushima *et al.*, 2010] as shown in Figure 10.

Since mammalian LC3 and other autophagy-related (Atg) genes may be transcriptionally upregulated in response to autophagic stimuli such as stress conditions, there is no clear evidence supporting the transcriptional upregulation in autophagic induction. Moreover, Atg proteins are constitutively expressed in sufficient amounts. Thus, the induction of autophagy is due to Atg proteins post-translational modifications and/or associations with other members of the autophagic machinery, rather than the regulation of their expression levels [Mizushima *et al.*, 2010]. Therefore, Atg mRNA or protein expression levels are not considered as appropriate indicators for monitoring autophagy. However, the conversion of LC3-II

is still considered as the reliable marker to detect autophagic activity [Klionsky *et al.*, 2008].

(A) **Number of LC3 or GFP-LC3 punctae per cell**   (B) LC3-II amount (LC3-conversion)

LC3-I

LC3-II
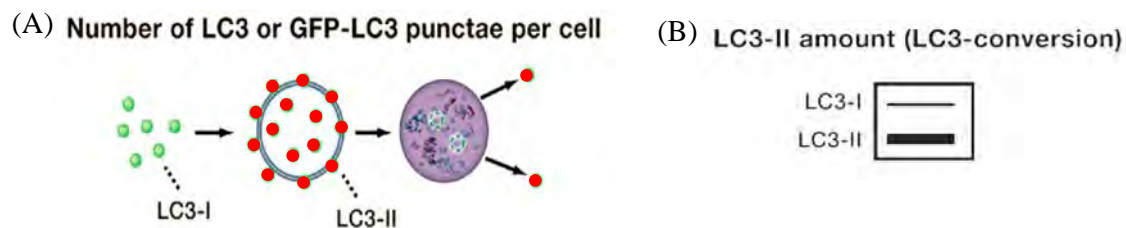
Figure 10   The conversion of LC3 protein. (A) LC3 protein detected by tagging with green fluorescence protein (B) LC3 protein detected by using Western blotting [Mizushima *et al.*, 2010].

Bcl-2 protein and autophagy

Bcl-2 protein not only involves in apoptosis inhibition, but also plays an important role in autophagy process. The downregulation of Bcl-2 protein and its subfamily members, using antisense, triggers autophagy but not apoptosis in HL60 cells [Saeki *et al.*, 2000]. The relation of Bcl-2 with autophagy is linked with the inhibitory interaction with Beclin 1 in HEK29 [Pattingre *et al.*, 2005; Levine *et al.*, 2008]. Bcl-2 binds with BH-3 domain of Beclin 1 resulting in blocking autophagy induction. Moreover, BH3-only subfamily of Bcl-2 family such as BNIP3 and HSPIN1 participated in the induction of autophagy in MCF7 and HeLa cells [Kondo *et al.*, 2005] as they competitively bind with Bcl-2 and then Beclin 1 is released and functions. Furthermore, murine embryonic fibroblasts (MEFs) deficient in Bax and Bak are resistant to apoptosis but undergo autophagy after etoposide treatment or growth factor withdrawal [Kondo *et al.*, 2005]. Altogether, the information about Bcl-2 protein and its family member indicated that Bcl-2 family not only regulate apoptosis, but also control autophagic pathway. However, Bcl-2 with autophagy regulation is believed to locate in ER membrane, not in mitochondria [Saeki *et al.*, 2000; Shimizu *et al.*, 2004; Pattingre *et al.*, 2005; Pattingre and Levine, 2006; Kessel and Reiners Jr, 2007; Swerdlow *et al.*, 2008].

The differences between types of cell death

As there are distinguished characteristics and molecular signalings in different types of cell death, the determination of types of cell death is relied on the different morphological and biochemical features as summarized in Table 2. Apoptotic cell death shows the blebbing of cell membrane with chromatin condensation, DNA laddering and nuclear fragmentation, the hallmark of apoptosis, as the result of caspase activation [de Bruin *et al.*, 2008]. These unique characters of apoptotic nuclei can be detected by Hoechst nuclear staining and DNA ladder as the DNA fragmentation produces a ladder pattern in agarose gel electrophoresis. Even though, this technique is used as a standard indication of apoptosis, this technique will misinterpret in heterogeneous cell population and results cannot be quantified [Chakraborty *et al.*, 2006]. The detection of apoptosis of individual cells using single-cell microgel electrophoresis (SCGE) or comet assay showed high degree of correlation with the formation of apoptotic bodies, flow cytometric analysis, activation of caspases and expressions of apoptosis related genes such as Bcl-2 and Bax [Chakraborty *et al.*, 2006]. Moreover, comet assay also allows the determination of apoptotic cells in quantitative manner [Singh, 2000; Chakraborty *et al.*, 2006].

In autophagic cell death, unlike apoptotic cell death, neither caspase enzymes are activated nor DNA fragmentations are present. Instead, autophagic cell death is characterized by degradation of intracellular compartments such as golgi apparatus, polyribosomes and endoplasmic reticulum before nuclear destruction [Kondo *et al.*, 2005]. The autophagic morphology with numerous autophagic vesicle or autophagosomes can be detected under electron microscope. To date, there are no other precise methods determining the amount of exact autophagic cell death. However, the increasing of autophagosome with the reduction of cell viability can be used as the indicator of autophagic cell death. The induction of autophagosome formation can be determined by using the conversion of LC3-II proteins or the autophagosome staining. [Mizushima *et al.*, 2010]. Although tumor cells have been observed to undergo both apoptosis and autophagic cell death in response to therapy, little is known about the connection between these two processes. Apoptosis and autophagy do not always separate [Wang *et al.*, 2007]. In many cases, inhibition of apoptosis causes autophagy, and inhibition of autophagy triggers apoptosis.

Unlike apoptotic and autophagic cell death, necrotic cell death is an unorganized cell-death pathway. The pattern of necrosis cannot be exactly concluded. However, the hallmark morphology of necrotic cell death is swelling or rupture of cell membranes. Propidium iodide nuclear can be used to detect of necrotic cell death [Okada and Mak, 2004].

Table 2 Comparison of different types of cell death (Modification from Okada and Mark, 2004; Kondo *et al*., 2005)

Characteristic	Apoptosis (Type I Programmed cell death)	Autophagic cell death (Type II Programmed cell death)	Necrosis
Morphological changes			
Cell membrane	Blebbing	Blebbing	Swelling or rupture
Nucleus	Chromatin condensation, DNA laddering, Nuclear fragmentation	Partial chromatin condensation, No DNA laddering	
Cytoplasm	Formation of apoptotic bodies, Preservation of organelles	Increase autophagic vesicles, Degradation of Golgi apparatus, polyribosomes, and endoplasmic reticulum	Increased vacuolation, Organelle degeneration, Mitochondrial swelling
Biochemical features			
Cell-death pathway	Caspase-dependent	Caspase-independent, Increase lysosomal activity	-
Detection methods			
Ultrastructure	Electron microscopy	Electron microscopy	Electron microscopy
Cell biological assays	TUNEL staining, Annexin V staining Caspase-activity assays, Hoechst nuclear staining DNA fragmentation assay, Sub G1 population Detection of changes in mitochondrial membrane potential, Single-cell microgel electrophoresis (Comet Assay)	Protein-degradation assay MDC or Acridine orange staining Assays for marker-protein translocation to autophagic membranes Conversion of LC3 type I to type II	Propidium iodide nuclear staining Detection of inflammation and damage in surrounding tissues

LC3: microtubule-associated protein 1 light chain 3, TUNEL: terminal deoxynucleotidyl transferasemediated dUTP nick-end labeling, MDC: monodansylcadaverine

Crosstalk between apoptosis and autophagy

There are numerous evidences supporting the crosstalk between apoptosis and autophagy [Maiuri *et al.*, 2007; Eisenberg-Lerner *et al.*, 2009; Maiuri, Criollo and Kroemer, 2010]. Apoptosis is well programmed for cell death, but autophagy is programmed to protect cell, favoring stress adaptation and avoids cell death by suppressing apoptosis. In some conditions, autophagy contributes to autophagic cell death. However, there are no definite conclusions for the connections between apoptosis and autophagy.

Apoptosis and autophagy can be triggered by common stimuli or signals. Sometimes, the results are the combination of autophagic and apoptotic response as shown in Figure 11. As the stressors initiate the signals, the decision is determined depending on the context and their different sensitivity-thresholds. They can mutually inhibit each other. Mostly, adaptation is the result of autophagy, but numerous of autophagosome formation can cause cell death. These mean that there are common pathways shared in apoptotic and autophagic response machineries.
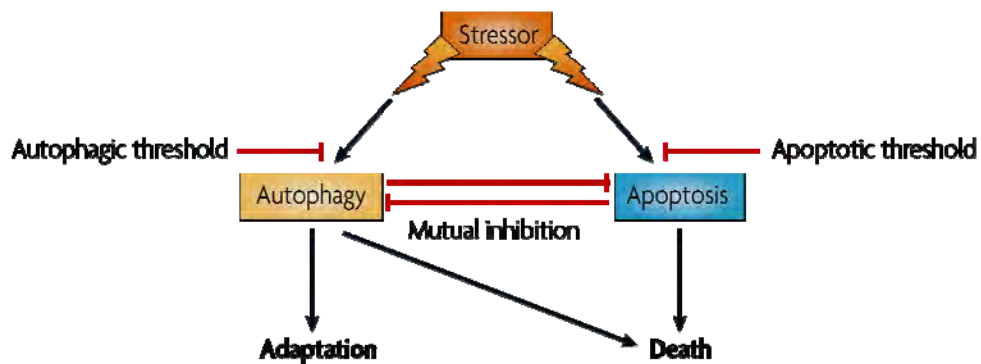
Figure 11 Crosstalk between apoptosis and autophagy [Maiuri *et al.*, 2007]

In perturbation of apoptosis by removal or functional inhibition of essential proteins from apoptotic machinery, such as knockout of Bax and Bak gene or caspase inhibitor (Z-VAD-FMK), could activate autophagy and sometimes results in autophagic cell death [Shimizu *et al.*, 2004; Yu *et al.*, 2004]. In absence of nutrients, autophagy is rapidly induced. In this condition, if autophagy is inhibited either at the early or late stages of the processes, the death cells show characteristics of apoptosis, instance, chromatic condensation, mitochondrial outer membrane permeability (MOMP) and caspase activations [Boya *et al.*, 2005].

The connection of apoptosis and autophagy is polarized processes. The types of initiating stimuli might determine which process will dominate. Several molecules account for this destiny. Among those molecules, the involvement of a functional and physical Beclin 1 and Bcl-2 protein interaction is suggested [Levine and Klionsky, 2004; Shimizu *et al.*, 2004; Pattingre *et al.*, 2005; Pattingre *et al.*, 2006; Maiuri *et al.*, 2007]. Beclin 1 (the mammalian ortholog of yeast Atg6) was originally discovered as a Bcl-2-interacting protein. Beclin1, containing BH3 (Bcl-2 homolog-3) domain, participates in phosphatidylinositol 3 kinase (PI3K), Vps34 complexes containing hVps34 and hVps15. In addition, Beclin 1 also interacts with UVRAG, Ambra1 and Bif-1 as shown in Figure 12. The interaction of Beclin 1 with Vps34, UVRAG, Ambra1 and Bif-1 turns autophagy to active, in contrast, the interaction of Beclin1 with Bcl-2 and Bcl-X_L acts as inhibitors of autophagy. Even though, Beclin is a BH-3 only protein, it cannot neutralize the effect of anti-apoptosis function of Bcl-2, which is exerted at the mitochondria membranes. In contrast, anti-autophagic functions of Bcl-2 or Bcl-X_L are in the area of ER only [Maiuri *et al.*, 2010]. When autophagic inductive stimuli initiate signals, Bcl-2 is phosphorylated near the site of Beclin 1-binding site. It leads to the disassociation of Beclin 1 and then autophagy can be induced. Moreover, other BH3-only protein can displace Beclin 1 and let it function as seen in Figure 12.
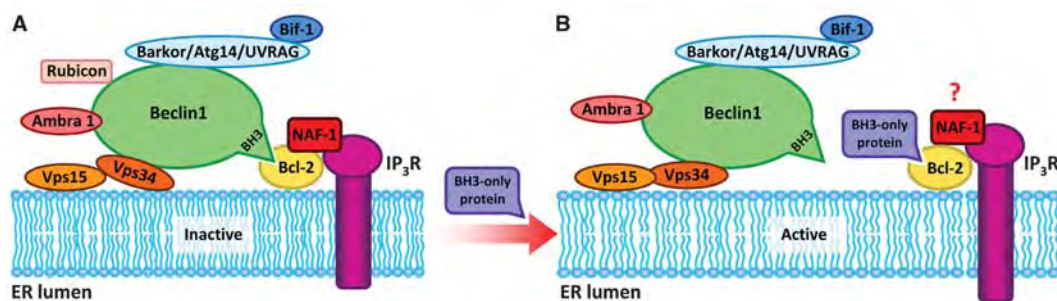
Figure 12 Model of the Beclin 1 and Bcl-2 interaction and autophagy regulation at the ER. (A) inactive autophagy induction and (B) active autophagy induction [Maiuri *et al.*, 2010].

Trifluoperazine

Trifluoperazine (TFP) is a FDA-approved antipsychotic drug belonging to phenothiazine group. It is used as antipsychotic agent for schizophrenia, depression and anxiety and as anti-emetic agent. The mechanisms of action of TFP are believed to block postsynaptic mesolimbic dopaminergic D1 and D2 receptors in the brain, depress the release of hypothalamic and hypophyseal hormones and depress the reticular activating system thus affecting basal metabolism, body temperature, wakefulness, vasomotor tone, and emesis.
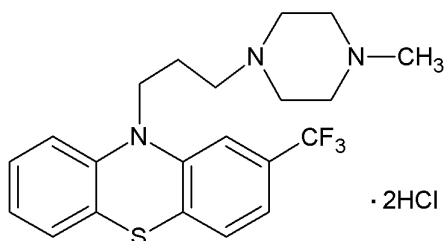
Figure 13 The structure of trifluoperazine

Interestingly, TFP has been found to be an effective autophagic inducer since it could induce the accumulation of autophagosomes and promote long-lived protein degradation in human glioblastoma H4 cell line [Zhang *et al.*, 2007]. The exact mechanism of TFP in autophagy induction is not yet elucidated. However, TFP has a potential to be used as chemotherapy sensitizer because TFP with sub-toxic dose was able to retard cancer cell growth in U87MG glioma cells [Shin *et al.*, 2004], inhibited DNA repair and sensitized U1810 cells in bleomycin-induced cell death [Polischouk *et al.*, 2007]. The combination of TFP and bleomycin is now under clinical trial phase I and II for non–Hodgkin's lymphoma and glioblastoma multiforme, respectively [Polischouk *et al.*, 2007]. TFP is also able to overcome adriamycin-resistant L1210 mouse leukemia cells by suppression of P-glycoprotein expression [Shina *et al.*, 2006]. Besides that, TFP can also sensitize ionizing radiation-induced cell killing through inhibition of DNA repair [Gangopadhyay *et al.*, 2007].

CHAPTER III

MATERIALS AND METHODS

1. Materials

The human non-small cell lung cancer NCI-H460 cells (H460 cells) were obtained from the American Type Culture Collection (ATCC; Manassas, VA, USA). Bcl-2 overexpression H460 (RALP) cells were kindly provided by Varisa Pongrakhananon (Pharmaceutical Technology program, Faculty of Pharmaceutical Sciences, Chulalongkorn University, Thailand). RPMI 1640 medium and Penicillin-streptomycin were purchased from Gibco (Carlsbad, CA, USA). Fetal Bovine Serum was purchased from Hyclone (Cramlington, UK). Acridine orange, cisplatin, MTT (3-(4,5-dimethythiazol-2-yl)-2,5-diphenyltetrazolium bromide), neomycin, propidium iodide, Hoechst 33342, trifluoperazine and 3-methyladenine were purchased from Sigma Chemical Inc. (St. Louis, MO, USA). Polyvinylidene difluoride (PVDF) membrane, sodium dodecyl sulfate (SDS), ammonium persulfate (APS) and skimmed milk were purchased from Bio-Rad Laboratories (Hercules, CA, USA). Protease inhibitors mixture was purchased from GE Healthcare Biosciences (Pittsburgh, PA, USA). Prestain protein ladder was purchased from Fermentus (Hanover, MD, USA). Pefabloc FC was purchased from Roche (Penzberg, Germany). Rabbit polyclonal Bcl-2 antibody, rabbit polyclonal Beclin1 antibody, rabbit polyclonal LC3 antibody, rabbit polyclonal β-Actin antibody and HRP-conjugated rabbit IgG secondary antibody were purchased from Abcam (Cambridge, MA, USA). The enhance chemiluminescence Western blotting detection reagent was purchased from Thermo Scientific Pierce Protein Research Products (Rockford, IL, USA). All other chemicals used were commercially available reagents or analytical reagent quality.

2. Cell culture

2.1. Cell Maintenance

Human non-small cell lung carcinomas H460 (NCI-H460) cells, Bcl-2-overexpressed H460 (RALP) cells and cisplatin-induced resistant H460 (H460/cis) cells were maintained in Roswell Park Memorial Institute (RPMI) 1640 medium supplemented with 10% fetal bovine serum and 1% antibiotics (100 U/ml penicillin and 100 µg/ml streptomycin) in a humid atmosphere of 5% CO_2 at 37°C. The medium for H460/cis cells were also supplemented with 1.44 µg/ml of cisplatin.

2.2 Establishment and characterization of cisplatin-resistant cells: H460/cis cells and RALP cells

H460 cells were grown and cisplatin was then added to the medium at gradually increasing concentrations starting from 0.33 µM (0.1 µg/ml) until the concentration reach 4.67 µM (1.4 µg/ml). During continuous exposure to cisplatin, culture medium was replaced with freshly prepared medium containing cisplatin at indicated concentration every three days and maintained in that concentration for at least two passages [Mese *et al.*, 1998; Yoon *et al.*, 2001]. Cell population survived when concentration reach 4.67 µM was named "H460/cis" cells.

For Bcl-2-mediated resistance, H460 cells were transfected with Bcl-2-expressed plasmids generously provided by Varisa Pongrakhananon (Pharmaceutical Technology program, Faculty of Pharmaceutical Sciences, Chulalongkorn University [Pongrakhananon *et al.*, 2010]. Briefly, Bcl-2 plasmids at the concentration of 1 µg and 2 µl of Promofectin solution were mixed and incubated at room temperature for 30 min and then added to the cells in the absence of serum. After 24 h, the medium was replaced with RPMI 1640 medium supplemented with 10% FBS. For stable transfection, Bcl-2-transfected H460 cells were maintained in medium containing with 400 µg/ml of G418 (geneticin) antibiotic for at least 2 weeks [McCoy *et al.*, 2010]. As Bcl-2 plasmids was contained sequences for neomycin resistance gene, cells without incorporation of Bcl-2 plasmids into DNA which were not able to live for long in G418 containing media were death. Viable cells were collected and named "RALP" cells. RALP cells were now heterogeneous cells since the level of Bcl-2 expression among them was inhomogeneous. In order to get the homogenous clone

with different Bcl-2 expression levels, Western blot analysis was assessed as described below.

RALP cells (25 cells) were seeded into each well of 96-well cell culture plate. The 96-well cell culture plates were incubated until cell colonies were clearly observed. The cells from a single colony growing from one progenitor cell were picked up and further cultured until amount of cells were greater than $5x10^5$ cells. Then, cells were harvested and rinsed twice with PBS. Cells extract was prepared using ice-cold lysis buffer (50 mM Tris pH 7.4, 100 mM NaCl, 2mM EDTA, 1% sodium deoxycholate, 0.1% SDS, 1% Triton X-100, 2mM Na_3VO_4 and protease inhibitors mix) for 30 min followed by centrifugation at 15,000 rpm for 15 min at 4^oC and supernatants were collected. Protein concentration was determined using Bradford assay. Samples containing 30 µg of proteins were loaded and separated on 12 % sodium dodecyl sulphate polyacrylaminde gel electrophoresis (SDS-PAGE) with a constant 90 V for about 1.5 h. Protein bands were then transferred to PVDF membranes with a constant 45 V for 2 h and blocked for 1 h at room temperature with 5% skimmed milk in TBST buffer (10 mM Tris-base; pH 7.5, 100 mM NaCl, 0.05% tween20). The membranes were immunoblotted with rabbit polyclonal Bcl-2 antibody (1:1,000) and simultaneously incubated with rabbit polyclonal β-actin antibody (1:3,000) overnight at $4\,^oC$ or 1.5 h at room temperature. Membranes were washed for 10 min, three times with TBST, then, incubated with HRP-conjugated rabbit IgG secondary antibody for 1 h at room temperature and washed extensively before detection. Protein bands were visualized using an enhanced chemiluminescence Western blot analysis system and exposed to film.

The protein band intensities were determined using ImageJ 1.43 software (NIH, USA). Finally, cells with the first and second highest expression of Bcl-2 were selected and further used in other experiments.

3. The cytotoxic effects of cisplatin and trifluoperazine

Before evaluating the effect of trifluoperazine (TFP) in modulating cisplatin-induced cytotoxicity, cisplatin-sensitive H460 cells and cisplatin-resistant H460/cis and RALP cells were treated with either cisplatin or TFP at various concentrations. Then, the inhibitory concentration at fifty percentage (IC_{50}) of cisplatin was evaluated. The IC_{50} value of cisplatin in H460 cells and the non-toxic concentration of TFP were used in further study.

3.1 Cell viability assay (MTT assay)

To determine the cytotoxic effect of cisplatin and TFP in H460, H460/cis and RALP cells, MTT assay was used. H460 cells, H460/cis cells and RALP cells were harvested with trypsin and resuspended to a final concentration of 5×10^4 cells/ml. Cell suspension (200 µl) were distributed evenly into 96-well cell culture plate. After 24 h of incubation, cisplatin at various concentrations from 0.1 µM to 1,000 µM and TFP at various concentrations from 0.625 to 10 µM were added to cells and cells were further incubated for 24 h. After incubation period, cell viability was determined using MTT assay. As viable cells can convert yellow MTT to purple formazan by mitochondria reductase, the absorbance of crystal formazan is referred to amount of living cells [Mosmann, 1983; Carmichael *et al.*, 1987].

Yellow MTT (a tetrazole)   Purple formazan
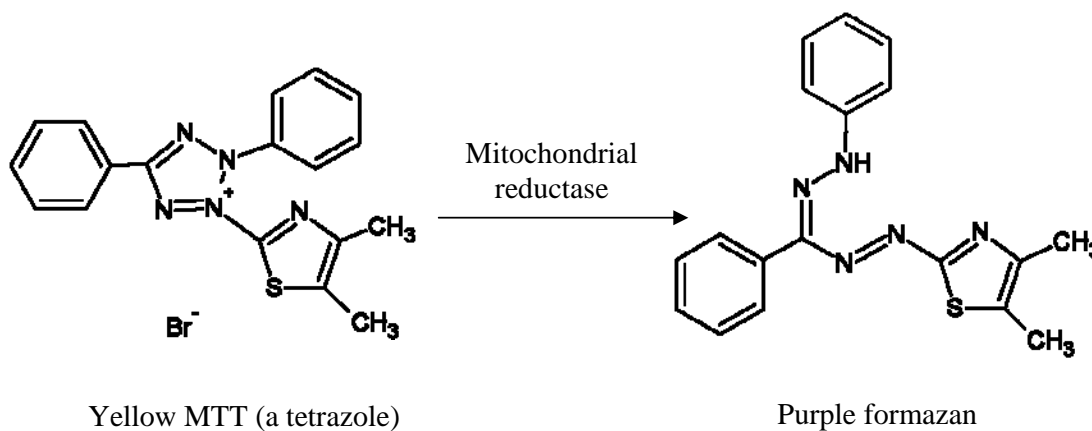
Figure 14 The conversion of yellow MTT to purple formazan

MTT assay can be described briefly as follow, 100 µl of 0.4 mg/ml MTT is added into each well, incubated for 4 h and then formazan crystals were dissolved in 100 µl of DMSO. The absorbance of formazan solution is quantified by Microplate reader at 570 nm.

Cell viability is calculated as follow:

$$\% \text{ Cell viability} = \frac{A_{570} \text{ (Treatment – Blank)}}{A_{570} \text{ (Without treatment – Blank)}} \times 100$$

Where A_{570} = Absorbance at 570 nm

Dose-response curve was plotted between % cell viability and concentrations used in log scale. The IC_{50} value of cisplatin was calculated using CurveExpert 1.4.

4. Evaluation of the effects of trifluoperazine on types of cisplatin-induced cell death

The effects of TFP on types of cisplatin-induced cell death were determined by co-treating cells with TFP at non-toxic concentration and cisplatin at the IC_{50} value detected in H460 cells. The differentiation between cell apoptosis, necrosis and autophagy was performed.

4.1 Determination of apoptotic and necrotic cell death

To determine apoptotic cell death, cell viability assay (MTT assay), cell counter-staining with Hoechst 33342 and propidium iodide (PI), and single-cell microgel electrophoresis (Comet Assay) were accessed.

4.1.1 Cell viability assay (MTT assay)

All cells (1×10^4 cells) were seeded in each well in 96-well plates. After 24 h of incubation, cisplatin at the concentration of IC_{50} value detected in H460 cells and TFP at non-toxic concentrations were added to cells. Cells were further incubated for 24 h. Then, cell viability was determined by MTT assay, as described in 3.1.

4.1.2 Cell staining with Hoechst 33342 and propidium iodide

Cell counter-staining with Hoechst 33342 and PI was used to determined nuclear morphology, in order to differentiated apoptotic cell death from necrotic cell death.

Hoechst 33342 is a popular cell-permeable nuclear counter-stain that emits blue fluorescence when bound to dsDNA. This dye is often used to differentiate apoptosis or necrosis in muti-color stain. Cells that displayed intensely condensed and/or fragment nuclei stained by Hoechst 33342 are considered as apoptotic cells.

PI is also a fluorescent nucleic acid-binding dye which binds only to double-stranded nucleic acids. It is membrane impermeable and generally excluded from viable cells. It is commonly used for identifying dead cells in a counter-stain in multicolor fluorescent techniques as Hoechst 33342. Cells stained with PI only are considered as necrotic cells.

Treated cells were washed with PBS. New medium 100 µl containing 10 µg/ml of Hoechst 33342 and 5 µg/ml of PI was distributed to the cells and immediately examined.

For Hoechst 33342 and PI staining, they were analyzed under an inverted fluorescence microscope (IX51 Olympus, Japan) using blue filter for Hoechst 33342 and red filter for PI and photographs were obtained. In each culture, four microscopic fields were counted. To determine the proportion of viable, apoptotic or necrotic cells, at least 200 cells were counted per culture. Numbers of cells in different stages were presented as the percentage of total cell count.

Hoechst 33342   Propidium iodide
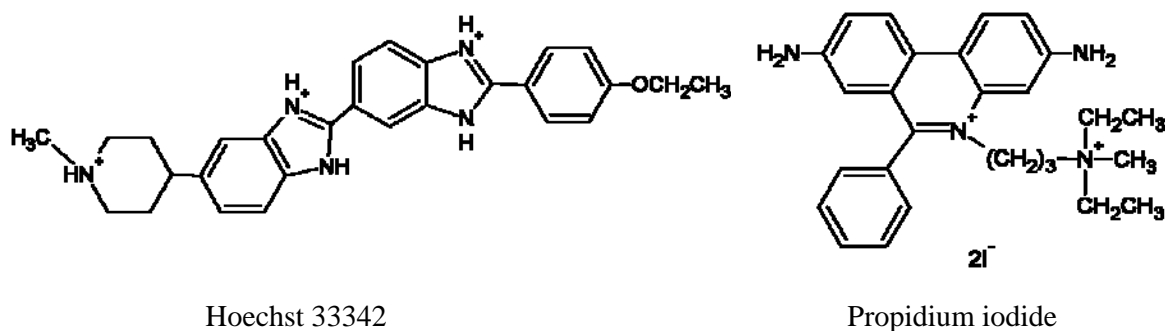
Figure 15 Structure of fluorescent dye

To simplify the types of cell death classification by using DNA staining fluorescence dye (Hoechst 33342 and PI), the criteria for distinguishing are described below in Table 3.

Table 3   The criteria for the simultaneous assessment of apoptotic and necrotic cell death by two-color fluorescence DNA staining (The images were adapted from Goodlett *et al*., 2005).

Cell subpopulation	*Hoechst 33342 (Blue)*	*Propidium iodide (Red)*
Viable cell	Intermediate intensity	Negative
Early apoptosis	Increased intensity Condense or fragmented nuclei	negative
Late apoptosis	Decreased intensity Condense or fragmented nuclei	Positive Condense or fragmented nuclei
Dead or necrosis	Much decreased	Highly positive

4.1.3 Single-cell microgel electrophoresis (Comet assay)

According to the concept of comet assay, it is used to quantify a variety of DNA lesions, including single-strand breaks, double strand breaks, inter-strand cross-links, and damage to the DNA bases. Apoptotic cell death can be easily identified since highly fragmented DNA in apoptotic cells migrates efficiently.

The widely comet assay is performed under alkaline conditions according to the procedure of Singh with minor modifications [Singh *et al.*, 1988; Olive *et al.*, 2001]. Quantification of DNA damage was determined in three different parameters; tail length, tail intensity and tail moment (TM) [Moretti *et al.*, 1999].
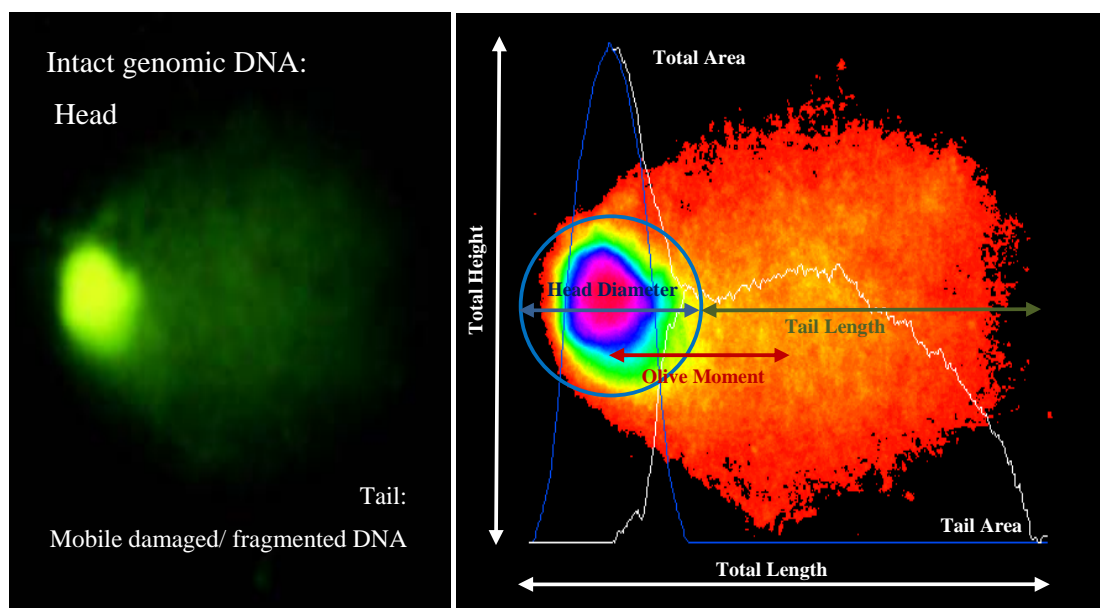
Figure 16 Morphology of comet cell
(The images were converted using CometScore V1.5)

Tail length considers DNA migration by measurement of the length of the comet, % DNA in tail is the nuclear material migrated out from the comet head into the comet tail and tail moment considers both the tail length and the fraction of DNA in the comet, calculated according to the following formula:

$$\text{Tail Moment (TM)} = \left[\frac{\text{Tail intensity}}{\text{Total comet intensity}} \right] \times \text{Tail center of gravity-head center}$$

Where the tail intensity/total comet intensity is the percentage of DNA in tail.

Cells treated with cisplatin alone and the combination of cisplatin and TFP were harvested, 50 µl of cell suspension was embedded in 50 µl of 1% low melting temperature agarose and spread on a microscope slide, which was pre-coated with 0.8% normal melting agarose to promote attachment. After letting the low melting agarose dry, slides were placed in a lysis solution (2.5 M NaCl, 0.1 M EDTA, 10 mM Tris-base pH 10, 1% triton X-100 and 10% DMSO) for 60 min at 4 ^{O}C in the dark. Then, slides were equilibrated in electrophoresis buffer (0.3 M NaOH, 1 mM EDTA, pH 13), ran in a horizontal electrophoresis chamber at 700 mA 25 V for 5 min. Slides were gently washed with 0.4 M Tris buffer pH 7.5, to neutralize the excess alkali and remove detergents. Then, slides were fixed with absolute MeOH for 5 min. Finally, slides were stained with SYBRgreen, fluorescent DNA binding dye and detected under fluorescence microscope. The rate of DNA damage was evaluated for 150 randomly selected cells in each experiment (50 cells from each of three replicate slides). The results were analyzed by CometScore v1.5 for tail length, % DNA in tail, tail moment and olive moment parameters.

4.2 Determination of autophagic cell death

To elucidate whether cells treated with cisplatin alone and the combination of cisplatin and TFP resulting in autophagic cell death, the degree of autophagosome formation was determined by acridine orange (AO) staining detected under inverted-fluorescence microscope for qualitative results and by flow cytometer for quantitative results. Protein analysis for microtubule-associated protein 1 light chain 3 (MAP-LC3) or LC3, the marker of autophagy, was done by Western blot analysis.

4.2.1 Cell staining with acridine orange

Acridine orange (AO) is a cell-permeable fluorescent cationic dye. It interacts with nucleic acid and also enters acidic compartments such as lysosomes. It has been accepted as a marker of autophagy [Paglin *et al.*, 2001; Arthur *et al.*, 2007]. To classified autophagic cell death, counter-stain of Hoechst 33342 and AO was used.

Treated cells were harvested and stained with 1 µM of AO and 10 µg/ml of Hoechst 33342 for 17 min [Paglin *et al.*, 2001; Kanzawa *et al.*, 2003]. Autophagosome formation was qualitatively detected by fluorescence inverted-microscope. Moreover, AO fluorescence intensity was also measured by flow cytometer (BD FACSCalibur, CA, USA) when excitation and emission wavelengths

is 488/530 nm [Wang *et al.*, 2009]. The cells for flow cytometry assay were washed and then trypsinized. All cells were resuspended in 300 µl of PBS containing 1 µM of AO. After incubating for 17 min, at least 10,000 cells were analyzed for AO intensity. Results were compared with untreated cells.
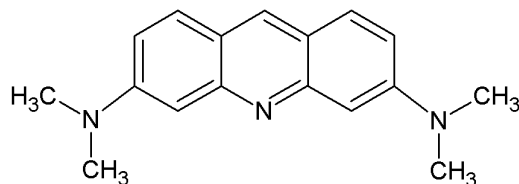
Figure 17 Structure of acridine orange

4.2.2 Level of LC3 protein expression

As microtubule-associated protein 1 light chain 3 (MAP1-LC3) or LC3 is recognized as the marker of autophagy which the conversion of LC3 type I to type II is the proportion of the activity of autophagic process. In order to confirm whether treated cells undergo autophagy, Western blot analysis for LC3 type I and II was assessed.

After treatment, cells (2.5 x 10^5 cells) were harvested and rinsed twice with PBS. Cells extract is prepared used ice-cold lysis buffer (50 mM Tris pH 7.4, 100 mM NaCl, 2 mM EDTA, 1% sodium deoxycholate, 0.1% SDS, 1% Triton X-100, 2 mM Na_3VO_4 and protease inhibitors mix) for 30 min followed by centrifugation at 15,000 rpm for 15 min at 4^oC and supernatants were collected. Protein concentration was determined using Bradford assay. Samples containing 30 µg of proteins were loaded and separated on 12 % sodium dodecyl sulphate polyacrylaminde gel electrophoresis (SDS-PAGE) with a constant 90 V for about 1.5 h. Protein bands were then transferred to PVDF membranes with a constant 45 V for 2 h and blocked for 1 h at room temperature with 5% skimmed milk in TBST buffer (10 mM Tris-base; pH 7.5, 100 mM NaCl, 0.05% tween20). The membranes were immunoblotted with rabbit polyclonal LC3B antibody (1:500) and simultaneously incubated with rabbit polyclonal β-actin antibody (1:3,000) overnight at 4 ^{o}C or 1.5 h at room temperature. Membranes were washed for 10 min, three times with TBST, then, incubated with HRP-conjugated rabbit IgG secondary antibody for 1 h at room temperature and washed extensively before detection. Protein bands were visualized using an

enhanced chemiluminescence Western blot analysis system and exposed to film. The protein band intensities were determined using ImageJ 1.43 software (NIH, USA).

5. Evaluation of the effects of trifluoperazine on types of cisplatin-induced cell death

5.1 Determination of autophagic cell death

Since, there are no reliable methods to detect autophagic cell death available, the cell death excluding from apoptosis and necrosis with the incidence of autophagy induction was assumed as the autophagic cell death. Due to that concept, the amount of autophagic cell death could be calculated as the following formula. % Cell viability was obtained from MTT assay. % Cell apoptosis and necrosis was obtained from cell counter-stained with Hoechst/PI when the results were calculated as the percentage of either apoptosis or necrosis compared to total cells. Then, % autophagic cell death can be calculated as following formula:

% Cell death　　　　　　 =　　Total cells (100%) - % Cell viability

% Autophagic cell death =　　%Cell death – (% apoptosis + % necrosis)

5.2 Determination of cytotoxic effect of 3-methyladenine

As we focused on autophagic cell death, the specific inhibitor of class III PI3K-Beclin1 signaling pathway, 3-methyladenine (3-MA), was used. 3-MA specifically inhibits the formation of autophagosomes via the inhibition of class III PI3K-Beclin1 signaling pathways [Seglen and Gordon, 1982; Stroikin *et al.*, 2004] which is one of the pathway regulating autophagy. To prevent misinterpreting the effect of the combination of cisplatin, TFP and 3-MA in H460, H460/cis and RALP, the cytotoxic effect of 3-MA was evaluated first. The concentration of 3-MA which exhibited no toxic effect was further used.

All cells (1×10^4 cells) were seeded in each well in 96-well plates. After 24 h of incubation, various concentrations of 3-MA ranging from 0.1 to 1,000 µM were added to cells and further incubated for 24 h. Then, cell viability was determined by MTT assay, as described above in 3.1.

5.3 Evaluation of the effects of cisplatin, trifluoperazine and 3-methyladenine combination

The combination of cisplatin at the concentration of IC_{50} value in H460 cells together with TFP and 3-MA at sub-toxic concentration were added to cells after 24 h of incubation. Then, cell viability was determined in time-dependent manner at 8, 12, 16 and 24 h. Moreover, after 8 h of incubation, the expression of LC-3 and Bcl-2 proteins were detected by Western blotting as described in 4.2.2 and after 24 h of incubation, the nucleus morphology was also determined using comet assay as described in 4.1.3.

6. Data summation and Statistical Analysis

All results were expressed as means ± SEM. The reproducibility of the results was confirmed in at least three independent sets of experiments. Data shown in figures were from a representative set of experiment. Statistical differences between two groups were determined by Student's t-test. For comparison of multiple groups, analysis of variance (ANOVA) with a post hoc test was conducted. $p < 0.05$ was selected to reflect significance.

CHAPTER IV

RESULTS

1. Establishment and characterization of cisplatin-resistant cells: H460/cis cells and RALP cells

To investigate the cisplatin-resistant mechanisms of H460 cells, cisplatin-resistant cells: H460/cis cells and RALP cells were established.

For H460/cis cells, H460 cells were exposure to stepwise increasing concentrations of cisplatin starting from 0.33 µM (0.1 µg/ml) until reach 4.67 µM (1.4 µg/ml) over a period of 12 months. and the duration of resistance induction was over a period of 12 months. The increasing concentration of cisplatin used in resistance induction more than 4.67 µM caused cell-cycle arrest and cells could not propagate farther. Thus, the concentration of cisplatin used to induce resistance was limited to 4.67 µM.

The cell shape detected under phase-contrast microscopy indicated that in normal culture condition, H460 cells showed almost round cell shape, in contrast with H460/cis cells that showed irregular shape and dramatic enlargement of cell. The size of H460/cis cells noticeably 2-3 times larger as showed in Figure 18.

For RALP cells establishment, H460 cells was transfected with Bcl-2 containing plasmid, which all the process was done by Varisa Pongrakhananon (Pharmaceutical Technology program, Faculty of Pharmaceutical Sciences, Chulalongkorn University, Thailand). RALP cells were then selected for homogenously stable and different Bcl-2 protein expression level. The clones no. 1 and 6 of RALP cells were chosen and named RALP1 and RALP6 cells, respectively. As shown in Figure 19, RALP1 and RALP6 cells expressed Bcl-2 protein at the level of 1.5 and 2.7 times more than their progenitor H460 cells, respectively. In addition, H460/cis cells were also quantitated for the level of Bcl-2 protein expression. It found that H460/cis cells showed 1.9 times higher of Bcl-2 protein expression than that in H460 cells (Figure 19). In contrast to H460/cis cells, RALP1 and RALP6 cells showed the identical shape, size and morphology with their parental H460 cells (Figure 18).

As seen in Figure 19 A, the Bcl-2 protein bands showed the blur bands with multiple bands at the same molecular-weight site. This indicated that the posttranslational modification of Bcl-2 protein affects the protein bands presented in Western blotting analysis. The most prevalent posttranslational modification found in most proteins is phosphorylation which also affects Bcl-2 protein as well [Gross, McDonnell and Korsmeyer, 1999; Pratesi, Perego and Zunino, 2001; Brutus *et al.*, 2009]. Bcl-2 proteins have multiple target site of phosphorylation. Since the phosphorylation of Bcl-2 protein slightly increased the molecular weight of Bcl-2 protein and the antibody against Bcl-2 protein used in this experiment was polyclonal antibody, the Bcl-2 detected bands showed the blur bands with multiple streaks.

H460

H460/cis
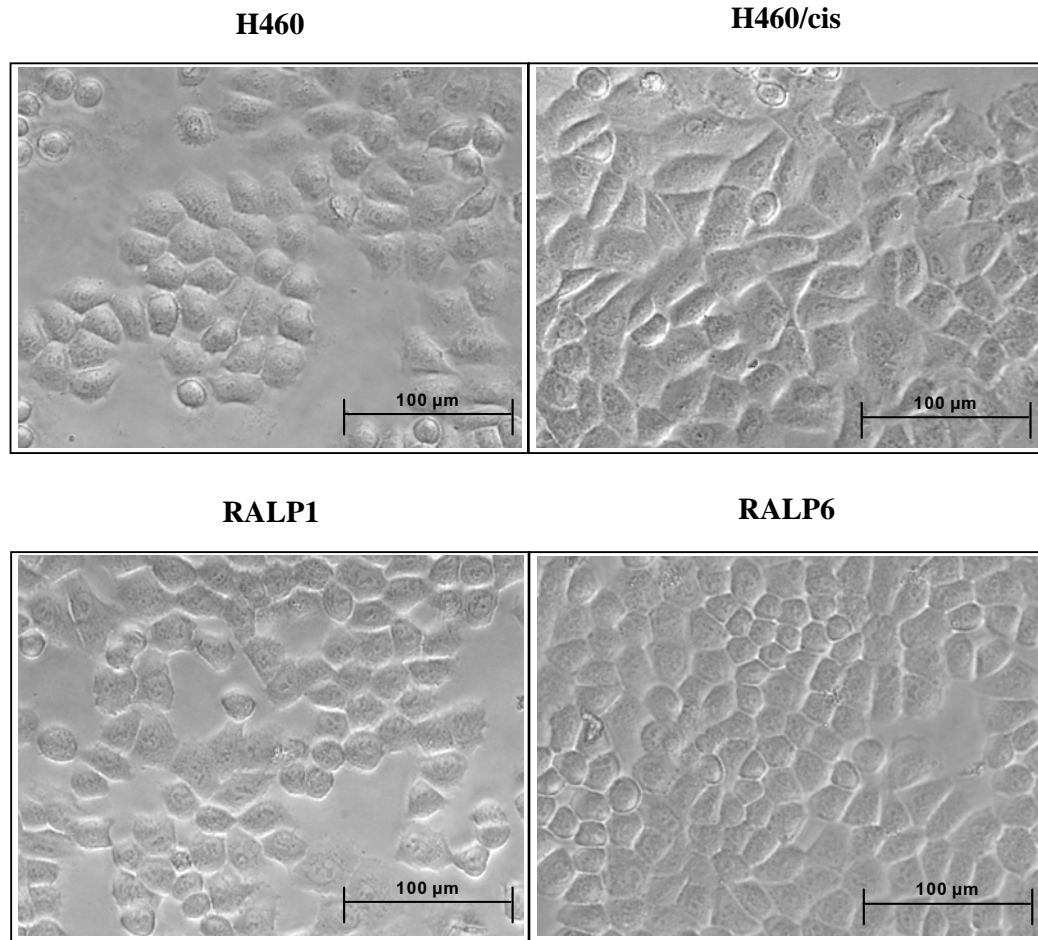
RALP1

RALP6

Figure 18 The phase-contrast images show cell morphology of H460, H460/cis, RALP1 and RALP6 cells. Scale bar is 100 µm.

(A)

(B)
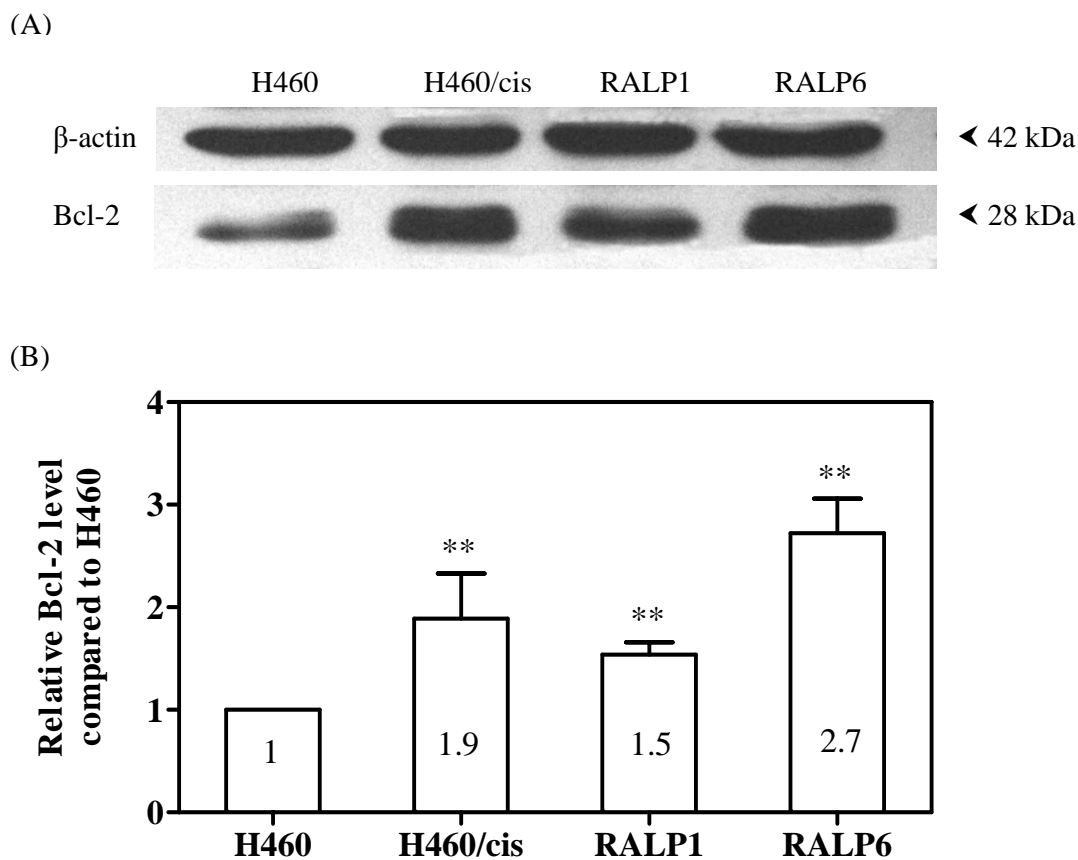
Figure 19   Bcl-2 protein expression levels in H460, H460/cis, RALP1 and RALP6 cells. (A) Western blotting analysis showed the relative level of Bcl-2 expression in all cells. The bands were the represents of one experiment from five experiments. (B) The relative ratio of Bcl-2 expression level compared to H460 cells. Each point represents the mean ± SEM of three independent experiments, **, $p<0.01$ compared to H460 cells.

2. The cytotoxic effects of cisplatin

To determine whether H460/cis, RALP1 and RALP6 cells exhibited the cisplatin-resistant properties, the cytotoxic effect of cisplatin was evaluated and the inhibitory concentration of fifty percentage (IC_{50}) of cisplatin in each cell was compared. In cell viability assay or MTT assay, cells were incubated with cisplatin at various concentrations ranges from 0.1 to 1,000 µM for 24 h. The cell viability of H460, H460/cis, RALP1 and RALP6 cells was decreased in dose-dependent manner (Figure 20 A). In addition, the IC_{50} values of cisplatin in H460/cis, RALP1 and RALP6 cells were significantly different from that in H460 cells. The IC_{50} values of cisplatin in H460, H460/cis, RALP1 and RALP6 cells were 40.64 ± 0.50 µM, 85.61 ± 3.11 µM, 54.53 ± 6.21 µM and 80.82 ± 2.33 µM, respectively. When compared with H460 cells, the IC_{50} value of cisplatin in H460/cis, RALP1 and RALP6 were approximately 2.1, 1.3 and 2.0 times higher, respectively ($p<0.01$) (Figure 20 B).

In order to evaluate the effect of trifluoperazine on cisplatin-induced cytotoxicity, cisplatin at the concentrations between 20-50 µM, which were the concentration around the IC_{50} value of cisplatin in H460 cells were chosen.

(A)

(B)
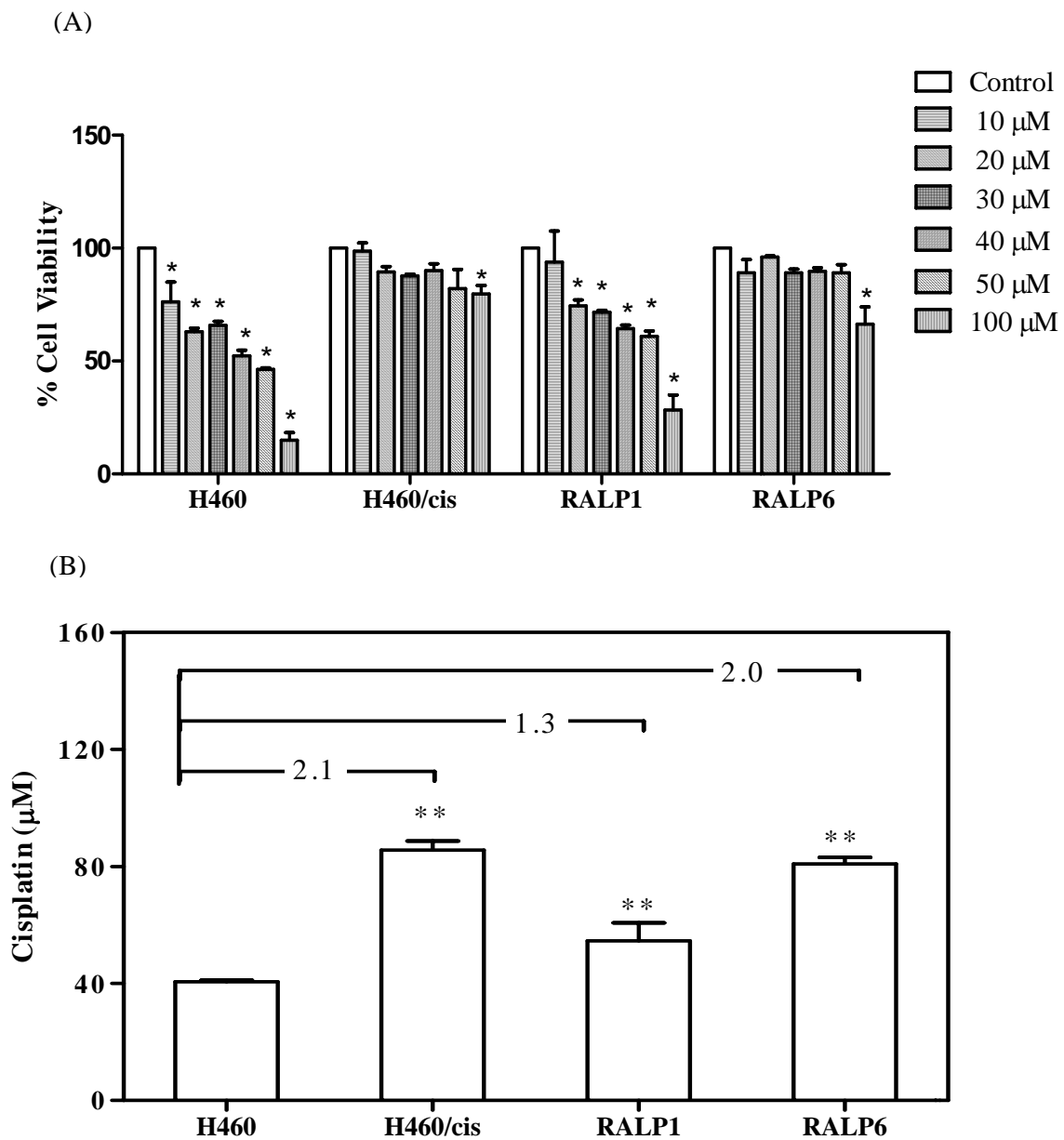
Figure 20   Cytotoxic effect of cisplatin in H460, H460/cis, RALP1 and RALP6 cells. (A) Concentration-response curve of cisplatin-induced cytotoxicity in the cells incubated for 24 h. Data were expressed as % cell viability comparing with control cells measured by MTT assay. (B) The IC_{50} values of cisplatin in all cells. Each point represents the mean ± SEM of four independent experiments, each performed in five wells. *, $p<0.05$ compared to each control cell. **, $p<0.001$ compared to H460 cells.

3. Evaluation the effects of trifluoperazine

Trifluorperazine (TFP), a known autophagy inducer, is a FDA-approved antipsychotic drug. There was evidence supported its autophagic induction effect [Zhang *et al.*, 2007; Ravikumar, Floto and Rubinsztein, 2009]. To choose the proper concentration of TFP in further experiment, the cytotoxic effect of TFP in all cells was checked. TFP concentration caused less than twenty percents of cell viability reduction is recognized as a sub-toxic concentration. In MTT assay, TFP at various concentrations range from 0.625 to 10 µM were incubated with cells for 24 h. As shown in Figure 21, TFP at concentration less than 5 µM was considered as sub-toxic concentration in all cells.

In addition, the autophagic inductive effect of TFP at the concentrations of 1 and 5 µM was also evaluated using acridine orange (AO) staining. AO dye, a specific autophagosome indicator, can freely cross biological membranes and accumulates in acidic compartment, where it is seen as fluorescence bright red.

After all cells were treated with 1 and 5 µM of TFP, they were harvested and stained with 1 µM of AO for 17 min. As shown in Figure 21, the TFP at the concentration of 1 and 5 µM could induce autophagy in all cells; H460, H460/cis, RALP1 and RALP6 cells, observed under fluorescence microscopy. Interestingly, the autophagy observed in H460/cis, RALP1 and RALP6 cells were dramatically decreased in red fluorescence intensity and number of intracellular red spots, rather than that in their parental cells. In order to quantify the accumulation of the acidific component, FACS analysis was confirmed. The results were consistently with those observed in fluorescence inverted microscope, the degree of autophagy in resistant cells were noticeably diminished than that in H460 cells, especially in H460/cis ($p<0.05$) (Figure 22 and 23). The AO intensity and the % relative intensity in untreated H460, H460/cis, RALP1 and RALP6 cells compared to that in H460 cells, which showed in parentheses, were approximately 31.0 (100) %, 18.4 (51.8) %, 25.5 (74.7) % and 21.8 (64.4) %, respectively (Figure 23 A and B).

All cells treated with 1 or 5 µM of TFP indicated the induction of autophagosome detected by flow cytometer. However, only the autophagy induction induced with 5 µM of TFP exhibited the significance ($p<0.05$). The autophagosome formation in response to TFP in all cells was compared with each control cell. It showed the similar ratio in dose-dependent manner as shown in Figure 24. TFP at the

concentration of 1 µM increased the autophagosome formation in all cells approximately 9-15 % and at the concentration of 5 µM, degree of autophagy was increased approximately 20-34 %.
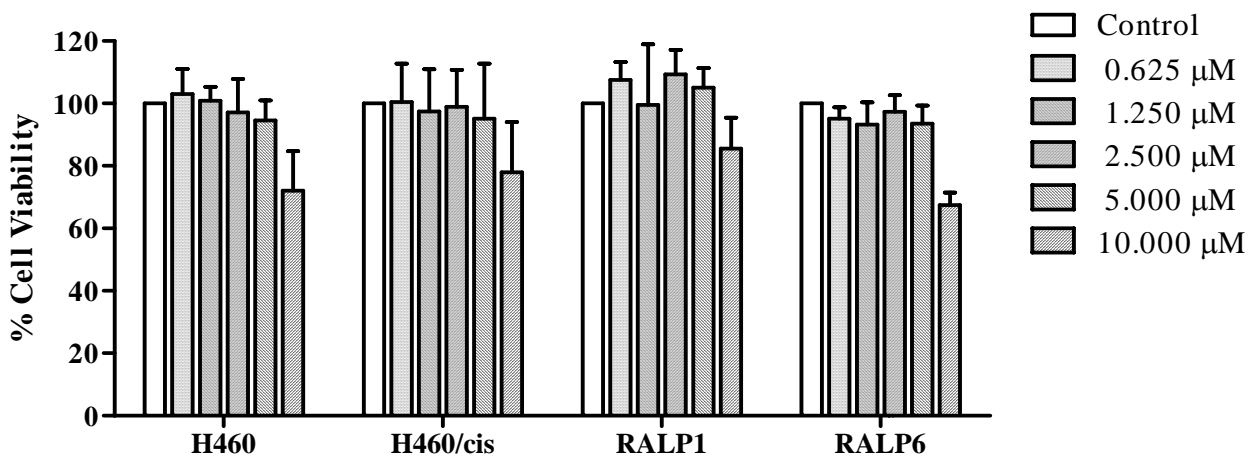
Figure 21   Cytotoxic effect of TFP in H460, H460/cis, RALP1 and RALP6 cells. Cells were incubated with various concentrations of TFP for 24 h. Data were expressed as % cell viability comparing with control cells measured by MTT assay. Each point represents the mean ± SEM of four independent experiments, each performed in five wells.
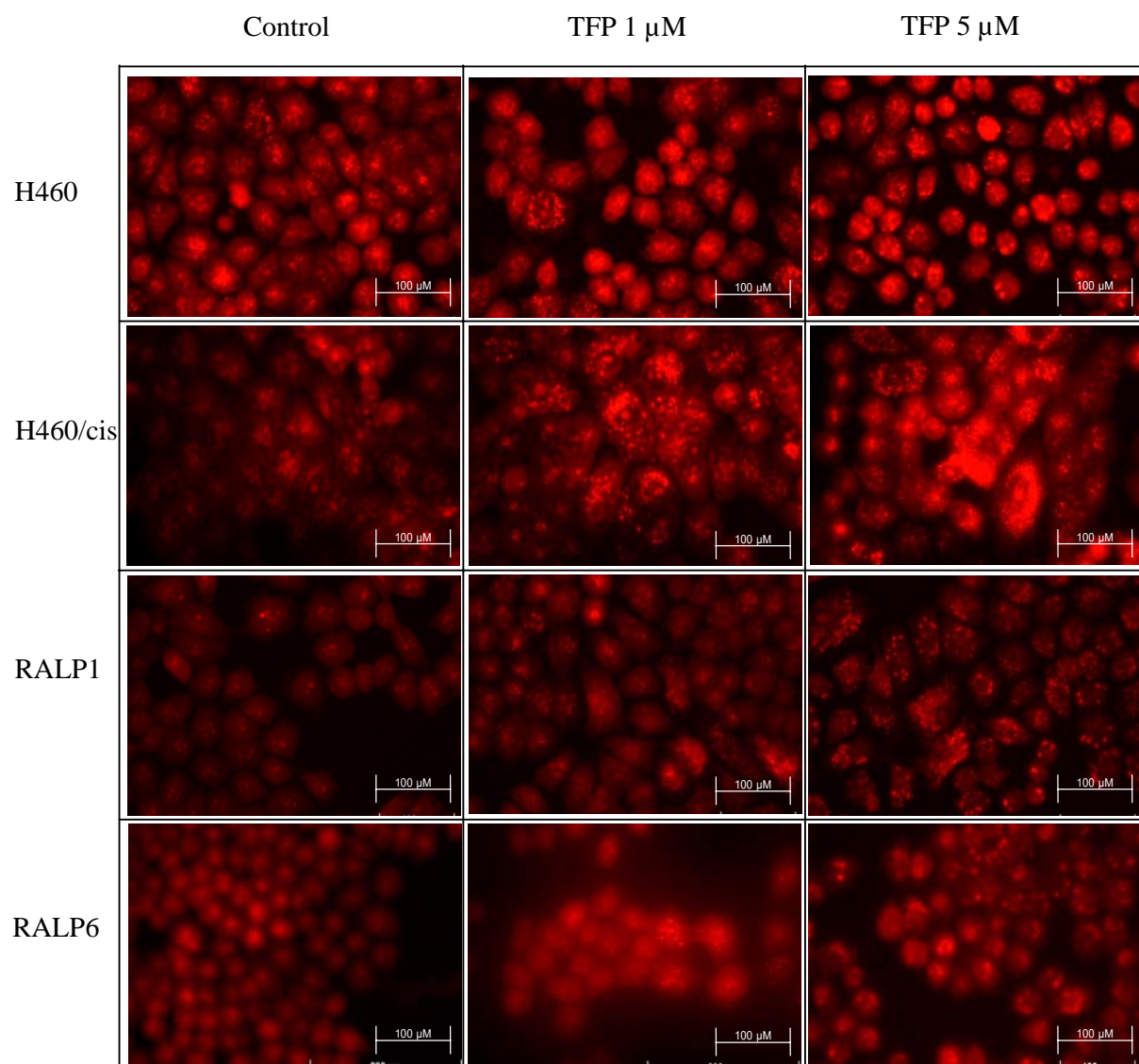
Figure 22 Autophagy induction in response to TFP at the concentration of 1 and 5 µM. The autophagy process detected under fluorescence microscope after staining with AO for 17 min. The red spots represented the number of autophagosome formation. The more red intensity indicated the higher autophagy induction.

(A)

(B)
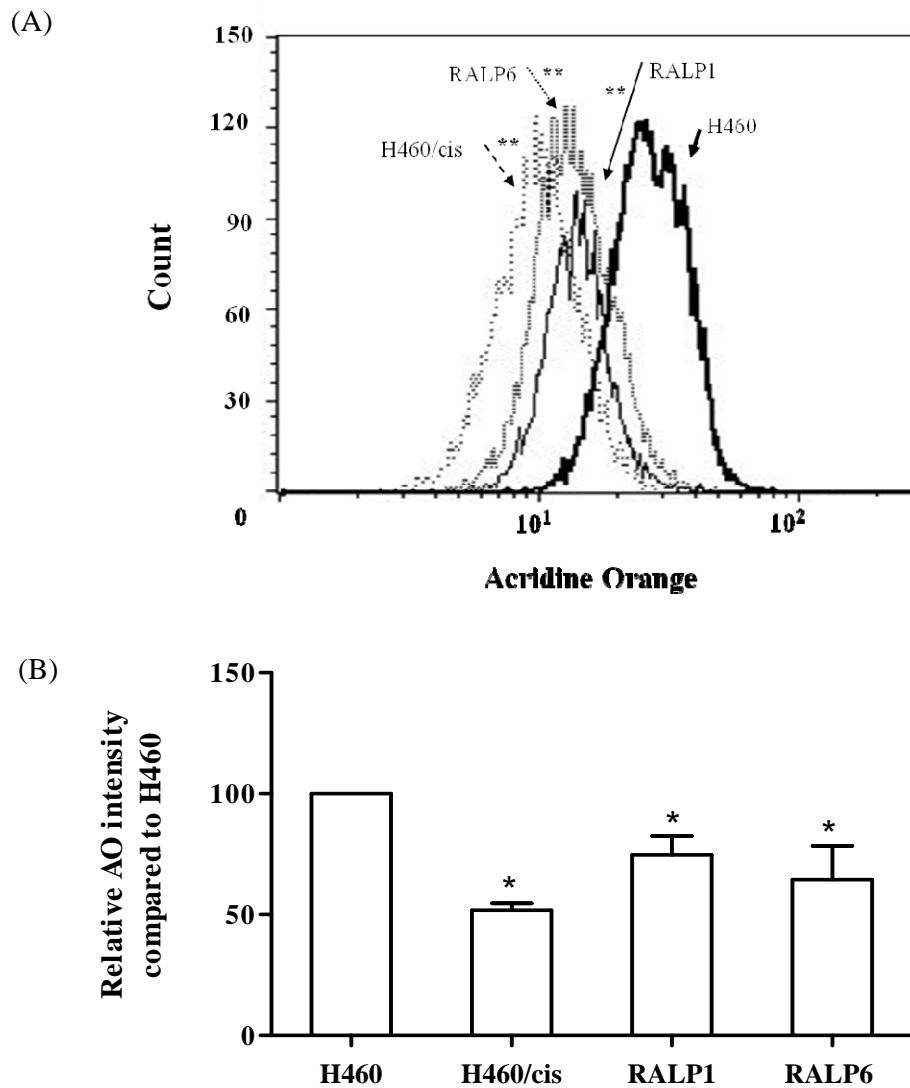
Figure 23   The degree of autophagosome formation in untreated H460, H460/cis, RALP1 and RALP6 cells. (A) Flow cytometric results showing the AO fluorescence intensity in all cells measured by flow cytometer. The overlay is the represent of one experiment which 10,000 cells were analyzed for each experiment. **, $p<0.001$ analyzed by Kolmogorov-Smimov statistic versus H460 control cells. (B) Relative AO intensity compared to H460 untreated cells. Each point represents the mean ± SEM of three independent experiments. *, $p<0.05$ comparing to untreated H460 cells
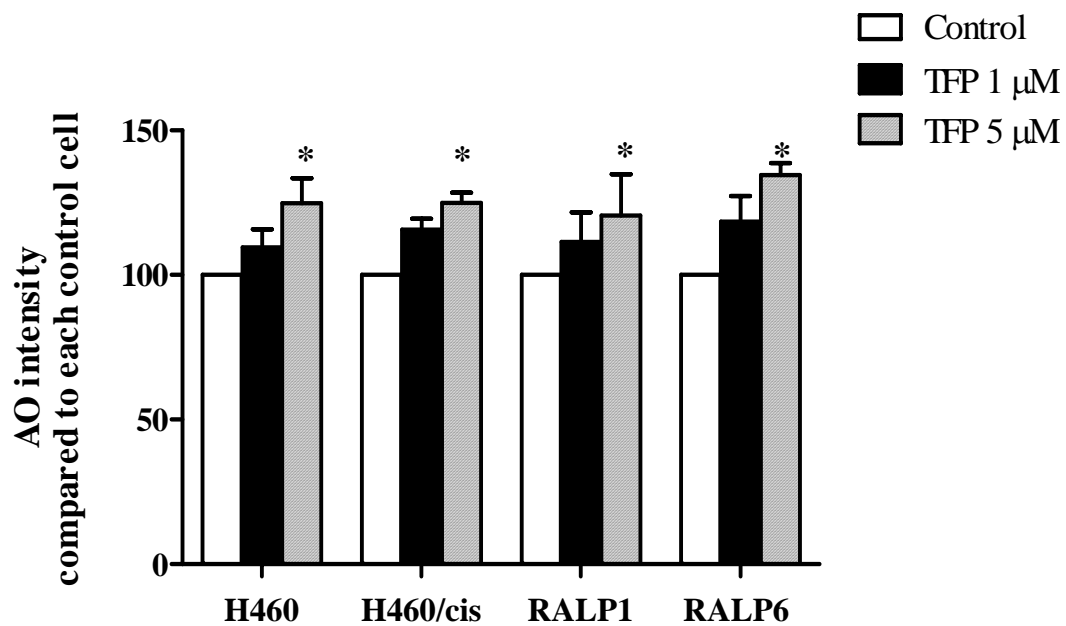
Figure 24　The AO fluorescence intensity in response to TFP at the concentrations of 1 and 5 µM in H460, H460/cis, RALP1 and RALP6 cells measured by FACS analysis. Each point represents the mean ± SEM of three independent experiments. *, $p<0.05$ comparing to each control cells.

4. Evaluation of the effects of trifluoperazine on types of cisplatin-induced cell death

From cytotoxicity testing of cisplatin and TFP, the concentrations for further used of cisplatin were 20 – 50 µM, which were the concentrations around the IC_{50} value of cisplatin in H460 cells, in combination with 1-5 µM of TFP, which were sub-toxic concentrations. For easily understanding, the results will be presented and compared both effects of cisplatin treatment and the combination of cisplatin and TFP.

4.1 Determination of apoptotic and necrotic cell death

To determine whether cisplatin caused apoptotic or necrotic cell death, cell viability assay, cell staining with Hoechst 33342/propidium iodide (PI) and comet assay were performed. In addition, the effects of TFP on cisplatin-induced cell apoptosis were also tested.

4.1.1 Cell viability assay (MTT assay)

In MTT assay, the results indicated that cisplatin could reduce the percentage of cell viability in dose-dependent manner in all cells. As seen in Figure 25, H460 cells exhibited the most susceptibility to cisplatin than that in resistant H460/cis, RALP1 and RALP6 in all concentrations of cisplatin (20 - 50 µM) ($p<0.05$).

In the combination of cisplatin at all concentrations and TFP at the concentration of 5 µM in all resistant H460/cis, RALP1 and RALP6 cells indicated the significantly decrease in the percentage of cell viability compared to that in cisplatin-treated group ($p<0.05$). In addition, RALP1 cells in the combination of all concentrations of cisplatin and TFP at the concentration of 1 µM also showed the significant reduction of the percentage of cell viability ($p<0.05$). In contrast to resistant cells, H460 cells showed no augmentative reduction in the percentage of cell viability in response to the combination of cisplatin and TFP.

These indicated that TFP could potentiate the effect of cisplatin-induced cytotoxicity in resistant cells in dose-response manner. Due to the distinguished results in resistance reversal, the combination of cisplatin at the concentration of 40 µM and TFP at the concentration of 5 µM was further used in cell staining with Hoechst 33342/PI and comet assay.
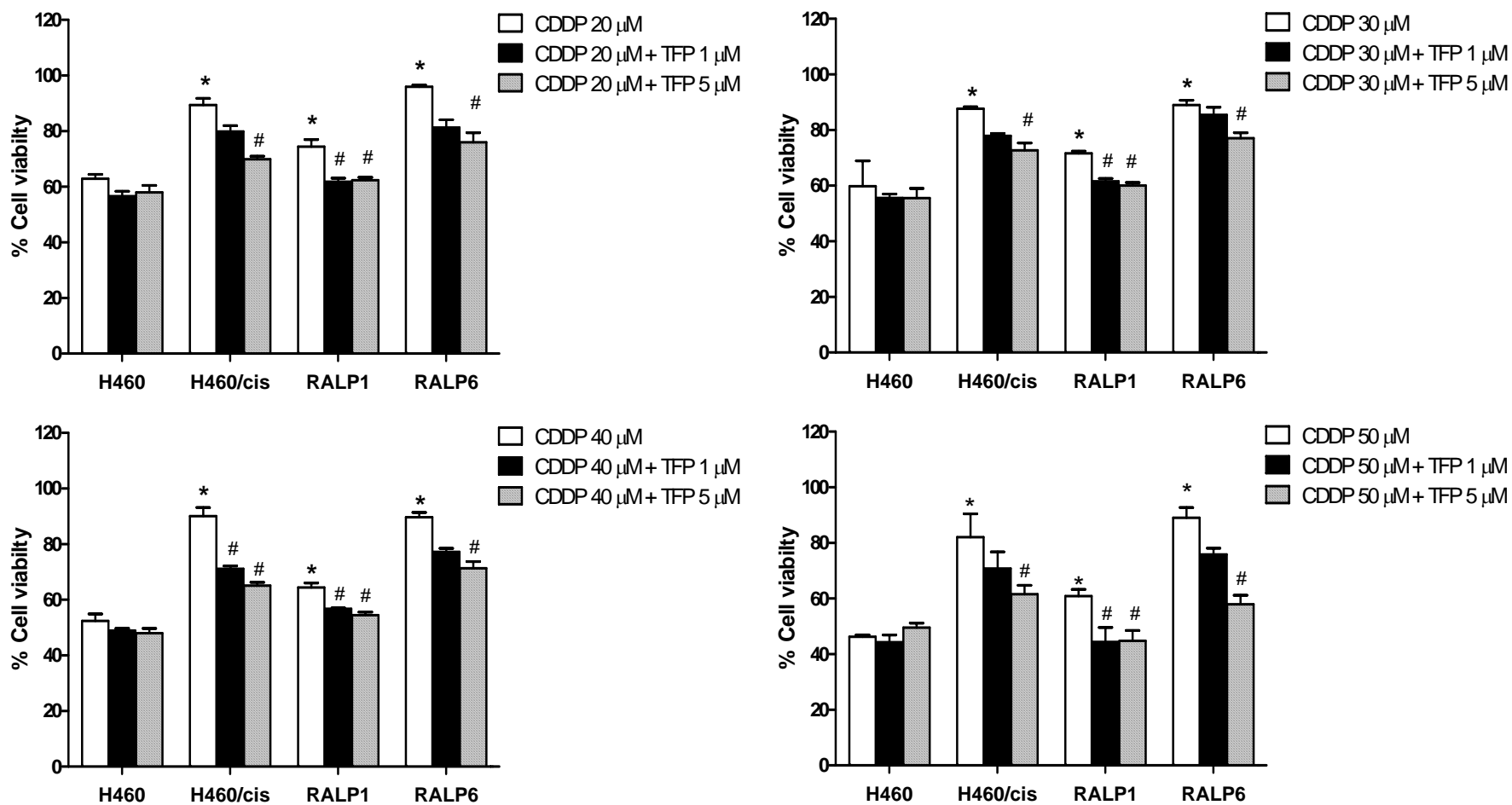
Figure 25 Cytotoxic effect of cisplatin and TFP co-treatment in H460, H460/cis, RALP1 and RALP6 cells. Cells were co-treated with 20-50 µM of cisplatin and 1-5 µM of TFP. Cell viability after 24 h was detected by MTT assay. Each point represented the mean ± SEM of five independent experiments, each performed in five wells. *, $p<0.05$ compared to H460 control cells. #, $p<0.05$ compared to their control cells.

4.1.2 Cell staining with Hoechst 33342 and propidium iodide

In cell staining assay, all cells were treated with cisplatin alone and the combination of cisplatin at the concentration of 40 µM and TFP at the concentration of 5 µM. Cells were then washed and stained with 10 µM of Hoechst 33342 and 1 µM of propidium iodide (PI). In the viable cells, the nuclei showed intermediate blue fluorescence intensity of Hoechst with negative red fluorescence of PI. If cells underwent apoptosis, the increasing of blue fluorescence with condenses or fragmented nuclei were observed. The nuclei of apoptotic cells were partially stained with PI with condense or fragmented nuclei. In contrast to apoptosis, cells underwent necrosis showed the positive red fluorescence with normal size of nuclei. As shown in Figure 26 that modes of cell death caused by cisplatin at 40 µM in H460 cells were mostly from apoptosis and a few from necrosis. To show the characteristics of apoptotic and necrosis cell death, the apoptotic and necrotic cell death was demonstrated in Figure 26. Apoptotic cells showed some condense and fragment nuclei in red arrows and necrotic cells were observed in round red spots in white arrows.

In contrast to H460 cells, the apoptotic and necrosis cell deaths were less observed in resistant H460/cis, RALP1 and RALP6 cells, as shown in Figure 27-29. The percentage of cells underwent apoptosis and necrosis, which was presented in parentheses, in H460, H460/cis, RALP1 and RALP6 were 40.3 (3.6) %, 5.3 (3.0) %, 31.6 (1.3) % and 8.2 (1.76) %, respectively. However, the combination of cisplatin and TFP did not significantly alter apoptotic and necrosis cell death. The percentage of cells underwent apoptosis and necrosis, which was presented in parentheses, in the combination of cisplatin and TFP in H460, H460/cis, RALP1 and RALP6 were 33.2 (3.3) %, 6.3 (0.7) %, 20.0 (1.2) % and 9.6 (1.3) %, respectively.

(A)

Hoechst 33342 | Propidium iodide

Cisplatin 40 µM

Cisplatin 40 µM
TFP 5 µM

100 µm / 200 µm / 200 µm / 200 µm

(B)

% Cell death

40.28

33.15

3.57

3.34

Apoptotic
Necrotic

Cisplatin   Cisplatin+TFP
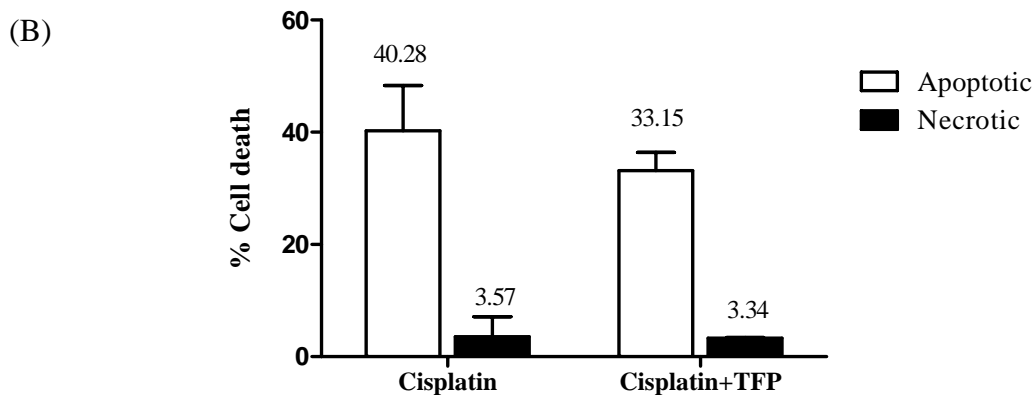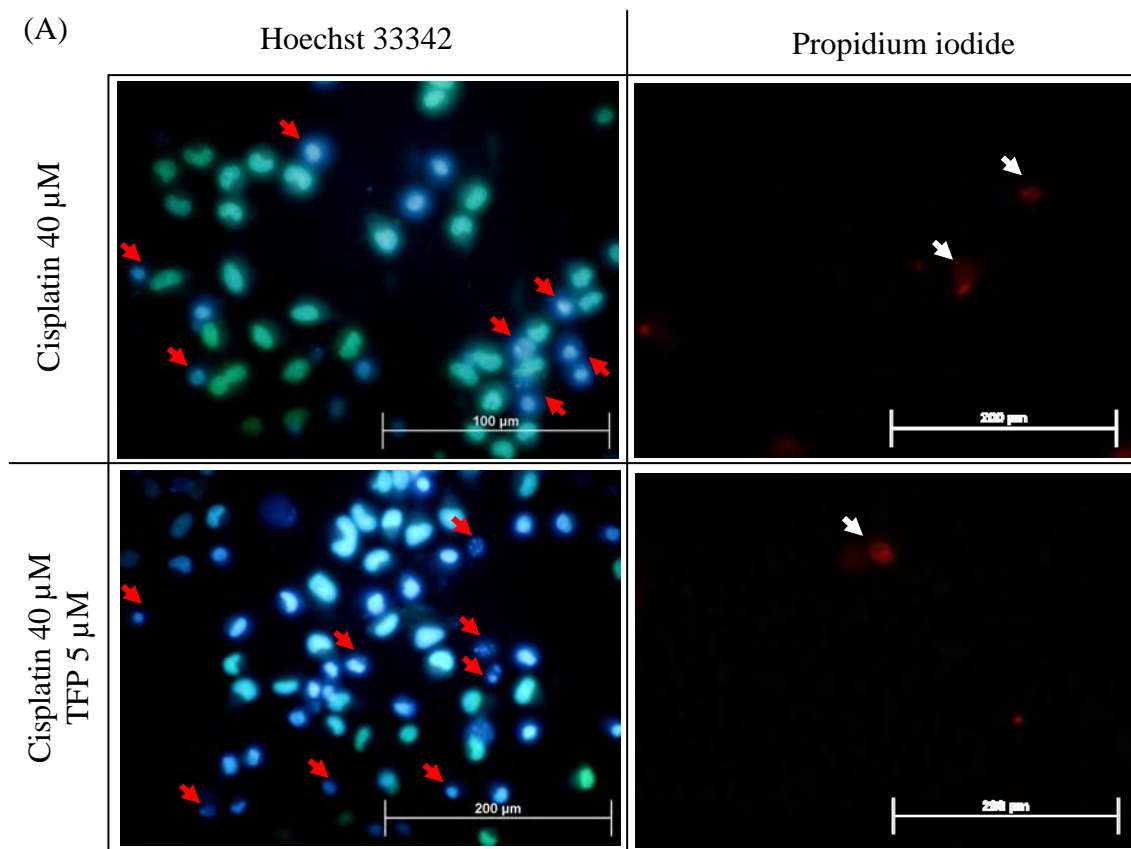
Figure 26   H460 cells in the presence of cisplatin 40 µM with/without TFP 5 µM stained with Hoechst 33342 and propidium iodide. H460 cells were co-treated with cisplatin 40 µM and TFP 5 µM for 24 h. (A) Cell staining detected under inverted-fluorescence microscope. (B) The percentage of apoptotic and necrotic cell death. Each point represents the mean ± SEM of five fields. Cells at least 50 cells were counted in each field.
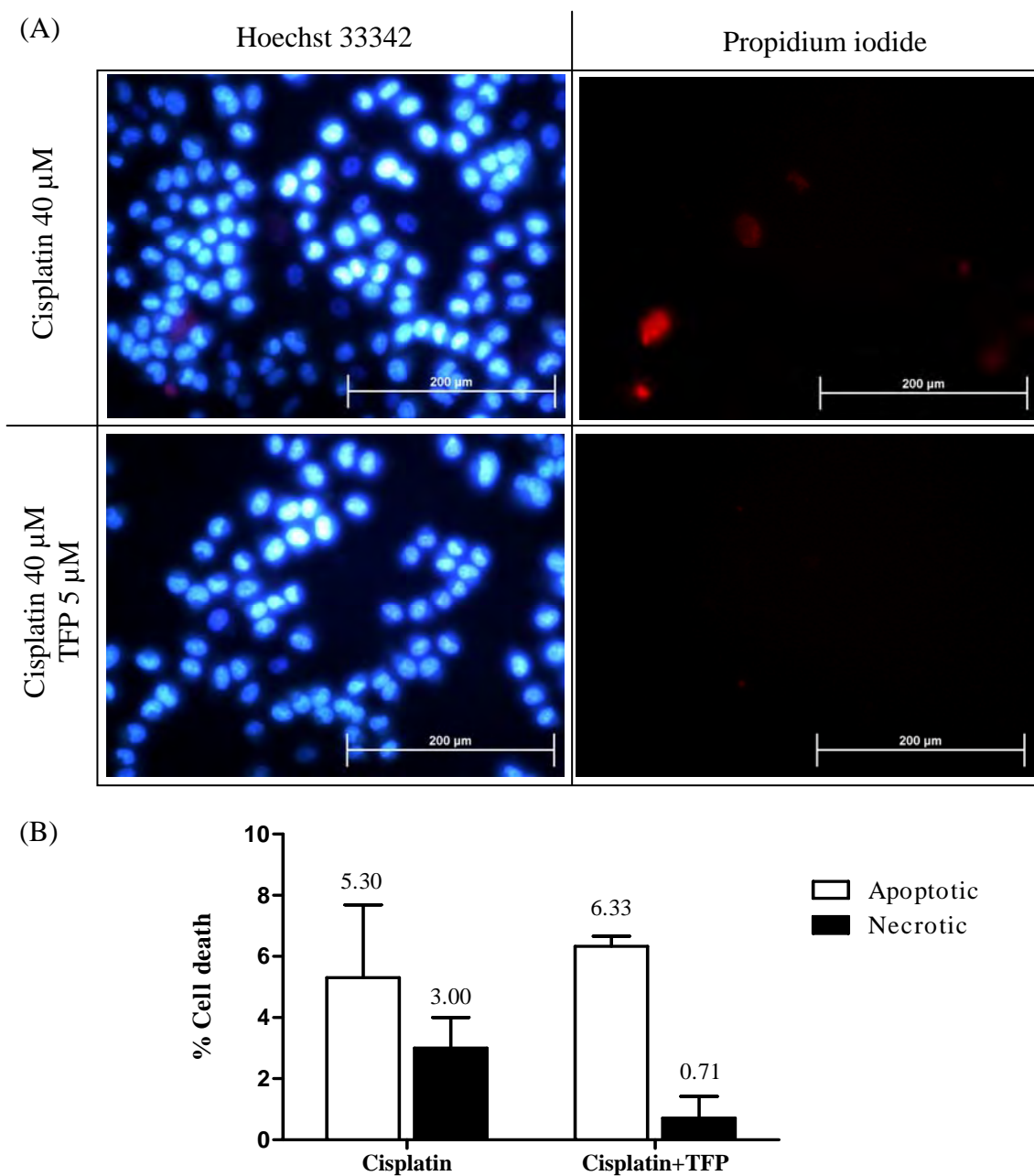
Figure 27 H460/cis cells in the presence of cisplatin 40 µM with/without TFP 5 µM stained with Hoechst 33342 and propidium iodide. H460/cis cells were co-treated with cisplatin 40 µM and TFP 5 µM for 24 h. (A) Cell staining detected under inverted-fluorescence microscope. (B) The percentage of apoptotic and necrotic cell death. Each point represents the mean ± SEM of five fields. Cells at least 50 cells were counted in each field.
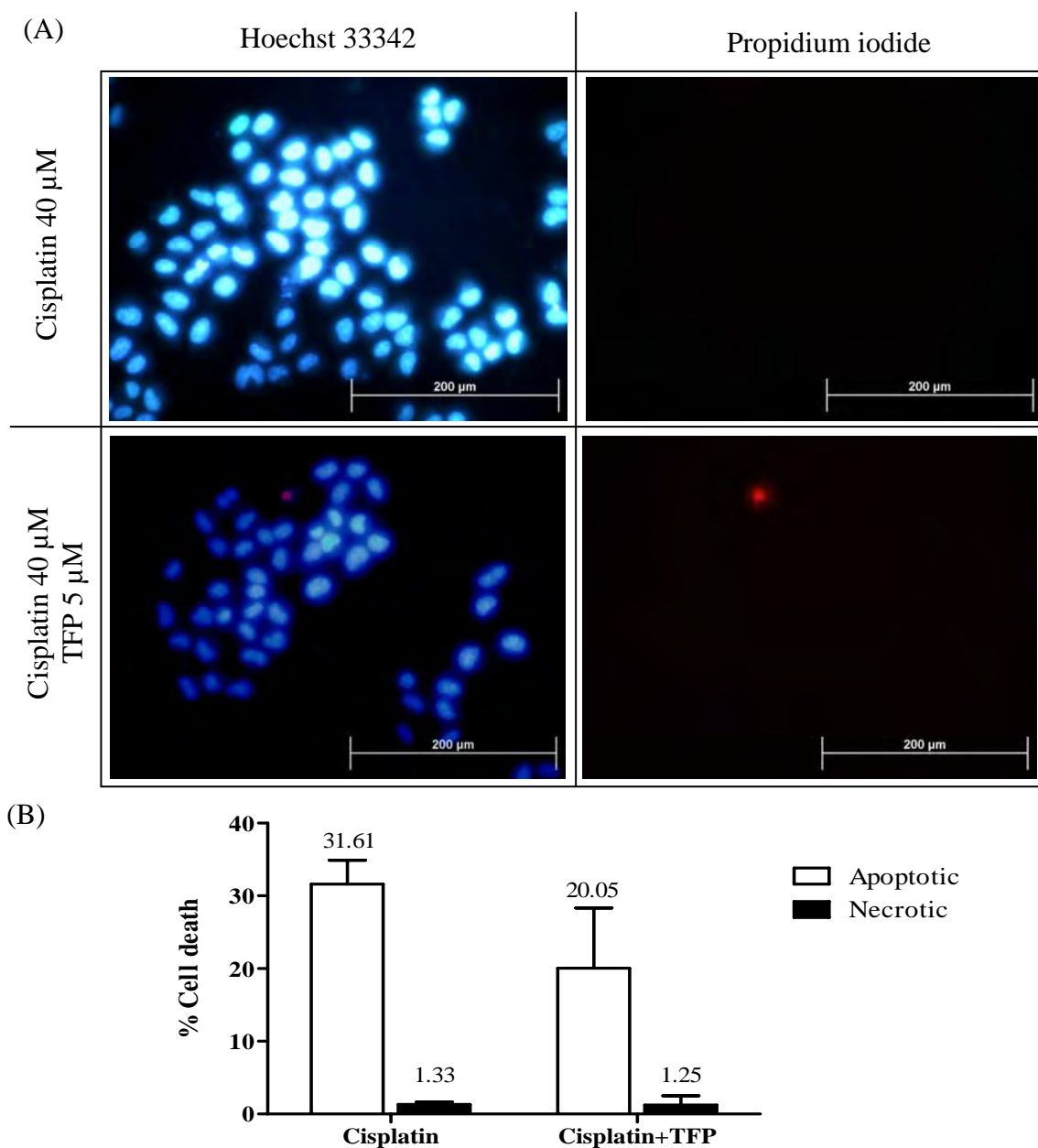
Figure 28 RALP1 cells in the presence of cisplatin 40 µM with/without TFP 5 µM stained with Hoechst 33342 and propidium iodide. RALP1 cells were co-treated with cisplatin 40 µM and TFP 5 µM for 24 h. (A) Cell staining detected under inverted-fluorescence microscope. (B) The percentage of apoptotic and necrotic cell death. Each point represents the mean ± SEM of five fields. Cells at least 50 cells were counted in each field.

(A) Hoechst 33342 | Propidium iodide

Cisplatin 40 µM

Cisplatin 40 µM TFP 5 µM

(B)
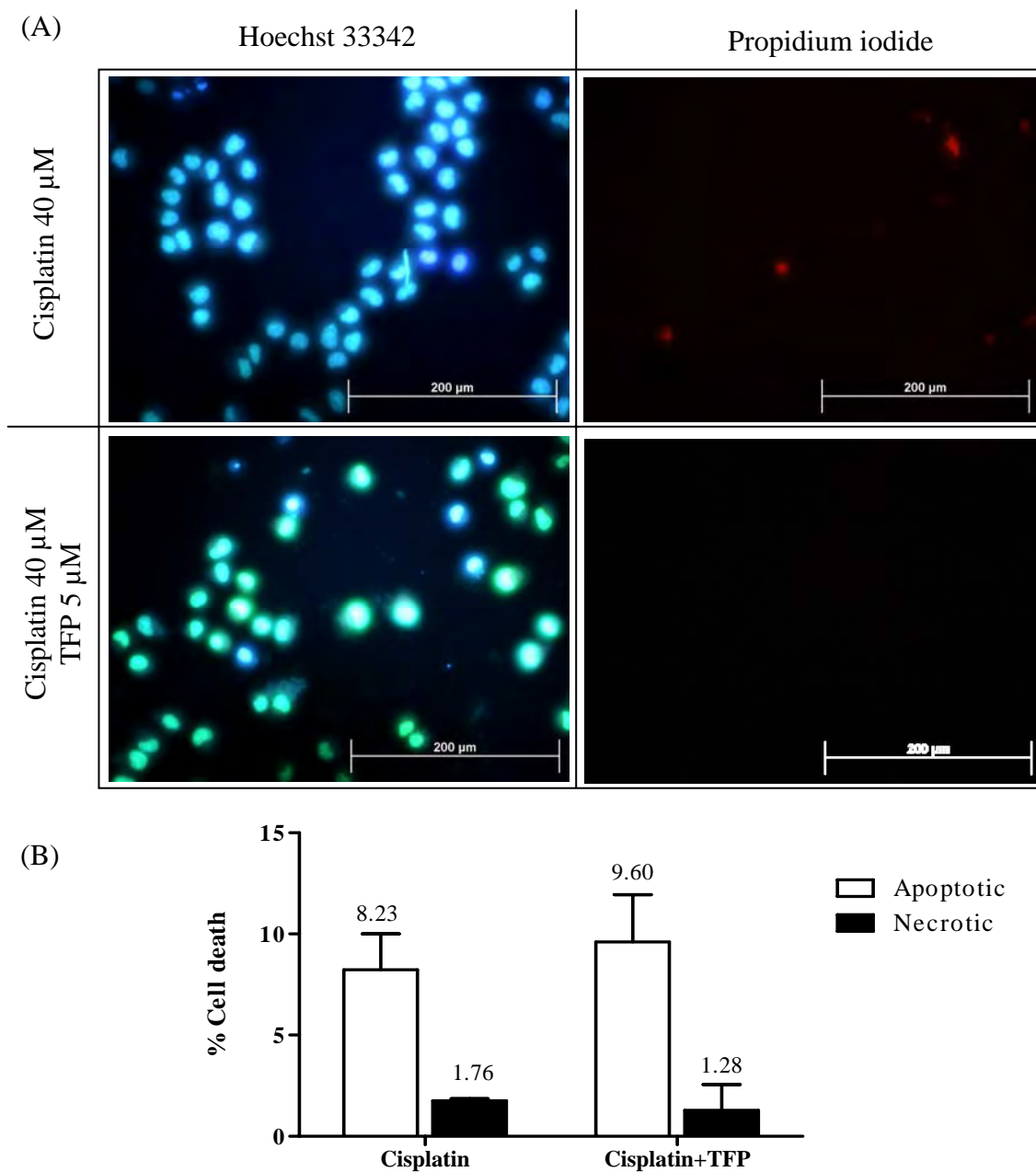
Figure 29 RALP6 cells in the presence of cisplatin 40 µM with/without TFP 5 µM stained with Hoechst 33342 and propidium iodide. RALP6 cells were co-treated with cisplatin 40 µM and TFP 5 µM for 24 h. (A) Cell staining detected under inverted-fluorescence microscope. (B) The percentage of apoptotic and necrotic cell death. Each point represents the mean ± SEM of five fields. Cells at least 50 cells were counted in each field.

4.1.3 Single-Cell Microgel Electrophoresis (Comet Assay)

In order to differentiate types of cell death between apoptosis and autophagic cell death, comet assay was used to quantitate the amount of DNA fragment, which is the unique characteristic of apoptotic process. On the other hands, autophagic cell death does not show DNA laddering but increases in number of autophagic vesicles.

The nuclear morphology detected by comet assay was shown in Figure 30. The control untreated cell showed round nucleus with no DNA fragment. In contrast to untreated control cell, cell treated with cisplatin at concentration of 500 µM showed DNA fragment as the tail of DNA migrated from center.
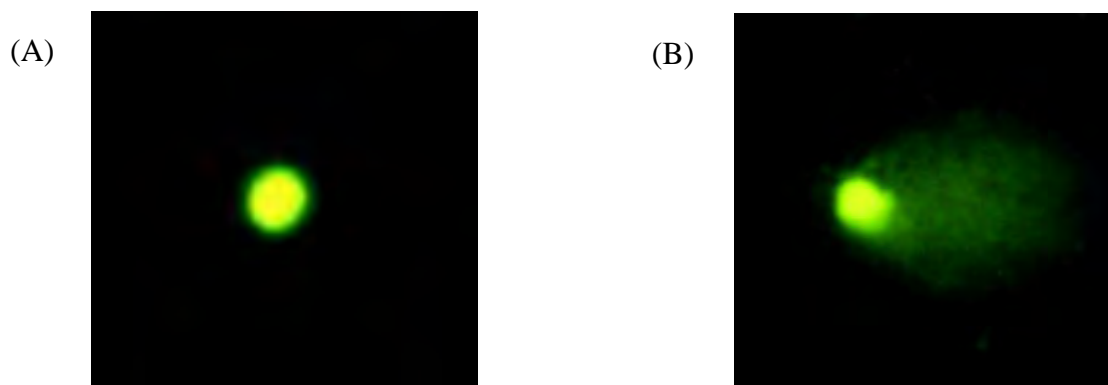
Figure 30   Nuclear morphology detected by comet assay. (A) Nuclear morphology of untreated control cell. (B) Nuclear morphology of cisplatin-induced apoptosis cell.

After all cells were treated with cisplatin at the concentration of 40 µM or the combination of cisplatin at the concentration of 40 µM and TFP at the concentration of 5 µM for 24 h. Cells were embedded in slides and then lysed in alkaline buffer. The fragments of DNA migrating in electrophoresis were stained with SYBRgreen and determined for the parameters of tail length, % DNA in tail, tail moment and olive moment. These parameters represented the relative amount compared to their own

untreated control cells. The ascending of each parameter represented the increasing of DNA fragment referring to apoptotic cell death.

As seen in Figure 31, TFP itself did not increase DNA fragment in all parameters in all cells, but the cisplatin-treated group could significantly increase the amount of DNA fragment in H460 cells ($p<0.05$) as shown the increasing of DNA fragment in all parameters.

In the combination of cisplatin and TFP, the dramatically risen of DNA fragment in all parameters was also observed in H460 cells ($p<0.05$), but only the tail length, tail moment and olive moment parameters showed the higher values than that in cisplatin-treated group. Nevertheless, this elevation of DNA laddering was not significantly different from those of cisplatin-treated group.

Neither cisplatin treatment nor the combination of cisplatin and TFP exhibited the increasing of DNA laddering in resistant H460/cis, RALP1 and RALP6 cells in all parameters. These indicated that the reduction of cell viability in response to the combination of cisplatin and TFP was not the results of apoptotic cell death.
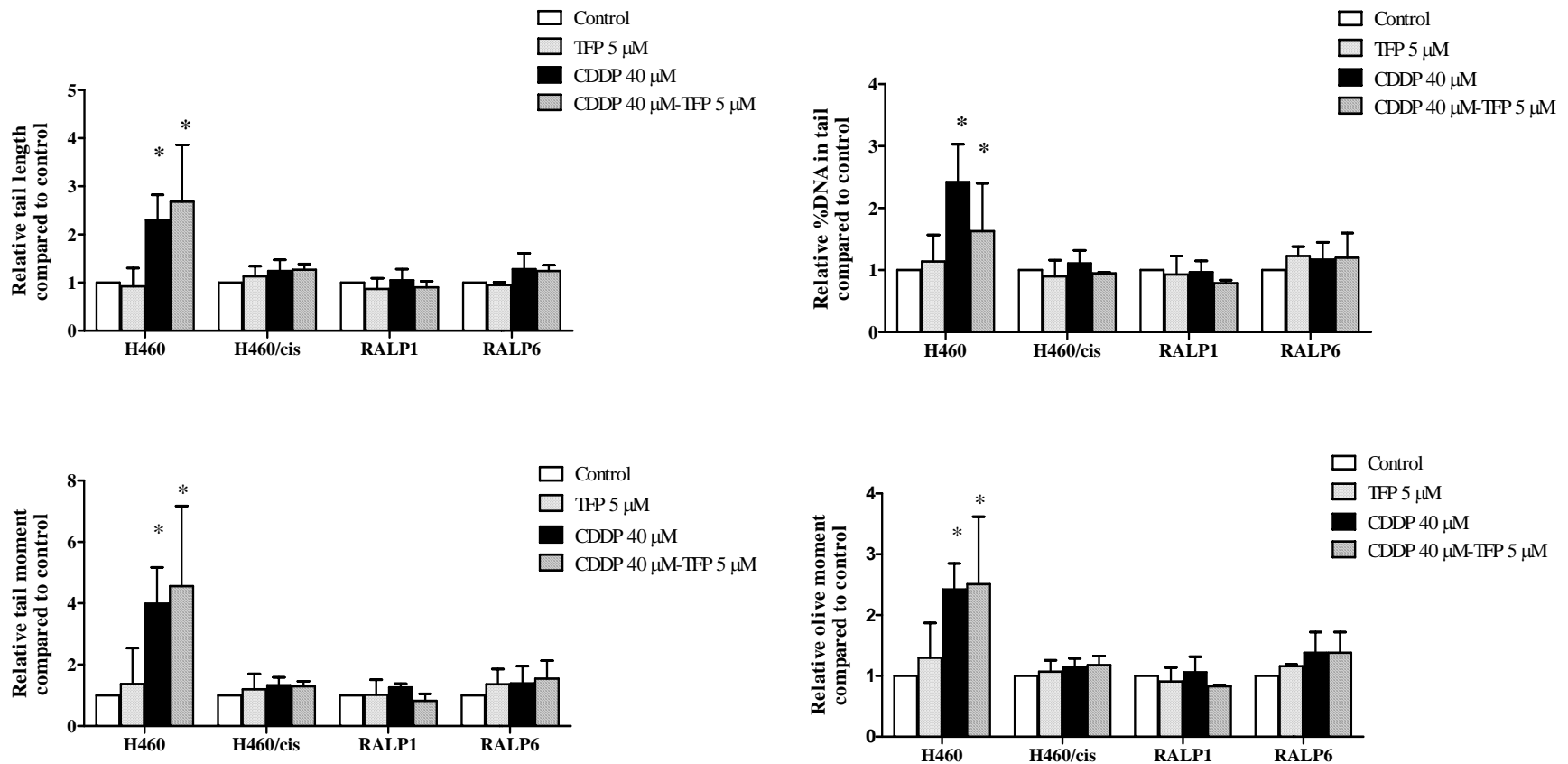
Figure 31   The relative parameters in tail length, % DNA in tail, tail moment and olive moment of cells treated with cisplatin or the combination of cisplatin and TFP detected by comet assay in H460, H460/cis, RALP1 and RALP6 cells. Each point represents the mean ± SEM of three independent experiments. *, $p<0.05$ compared to control.

4.2 Determination of autophagic cell death

To determine autophagic cell death, the degree of autophagic induction was accessed by cell staining with AO detected by fluorescence microscope and flow cytometer. For easily understanding, the results were presented and compared both effects of cisplatin treatment and the combination of cisplatin and TFP.

4.2.1 Cell staining with acridine orange

After treating with either cisplatin at 40 µM or the combination of cisplatin at 40 µM and TFP at 5 µM, cells were stained with 1 µM of AO. The fluorescence AO was detected under flow cytometer and fluorescence microscope for quantitative and qualitative results, respectively. The red AO fluorescence intensity detected from flow cytometer indicated that the autophagosome formation was significantly increased in response to TFP and cisplatin-treated group in all cells ($p<0.05$) as shown in Figure 32. However, the addition of TFP could further induce autophagy as the relative AO intensity was dramatically increased compared to cisplatin-treated cells ($p<0.05$). It could say that TFP and cisplatin could significantly induce autophagy, meanwhile, the combination of cisplatin and TFP could also induce autophagy in much higher degree of induction compared to control cells, TFP or cisplatin treated.

The results detected under fluorescence microscope showed the bright blue nuclei with some condense or fragment chromatin with the intensive red autophagosomes in response to cisplatin treatment and the combination of cisplatin and TFP in all cells, especially in H460 cells as seen in Figure 33-36. Interestingly, when compared in the same field of picture staining with Hoechst 33342 and AO, it found that cells underwent apoptosis showed intense blue fluorescence and condense chromatin but did not show the red fluorescence of AO. Some notices were demonstrated in H460 cells in red arrows (Figure 33). In the same way, the cells shown intense AO red did not show condense chromatin as well. This is the proof that AO could differentiate types of cell death, by which the increasing of AO intensity directly related to the increasing of autophagic cell death.
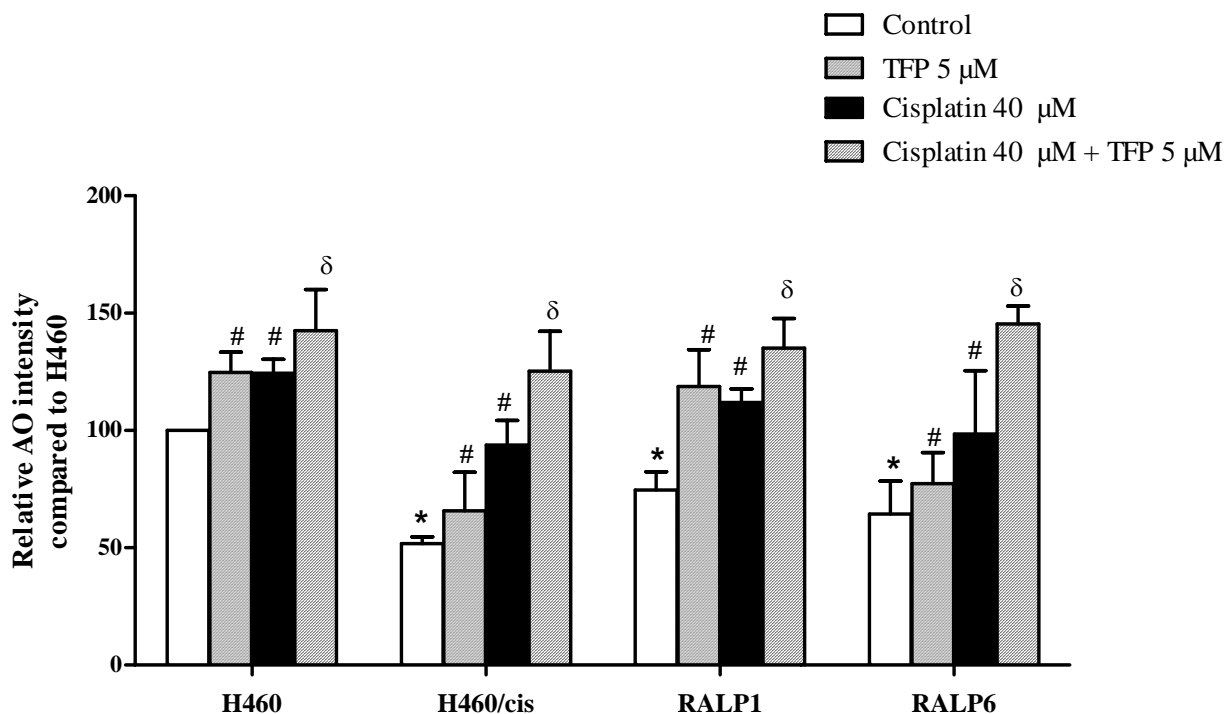
Figure 32 The degree of autophagy induction in response to cisplatin treatment and cisplatin and TFP combination. The relative AO fluorescence intensity was detected by flow cytometer. Each point represents the mean ± SEM of at least three independent experiments. *, $p<0.05$ compared to H460 control cells. #, $p<0.05$ compared to each control cell. δ, $p<0.05$ compared to each cisplatin-treated cell.

	Hoechst 33342	Acridine orange
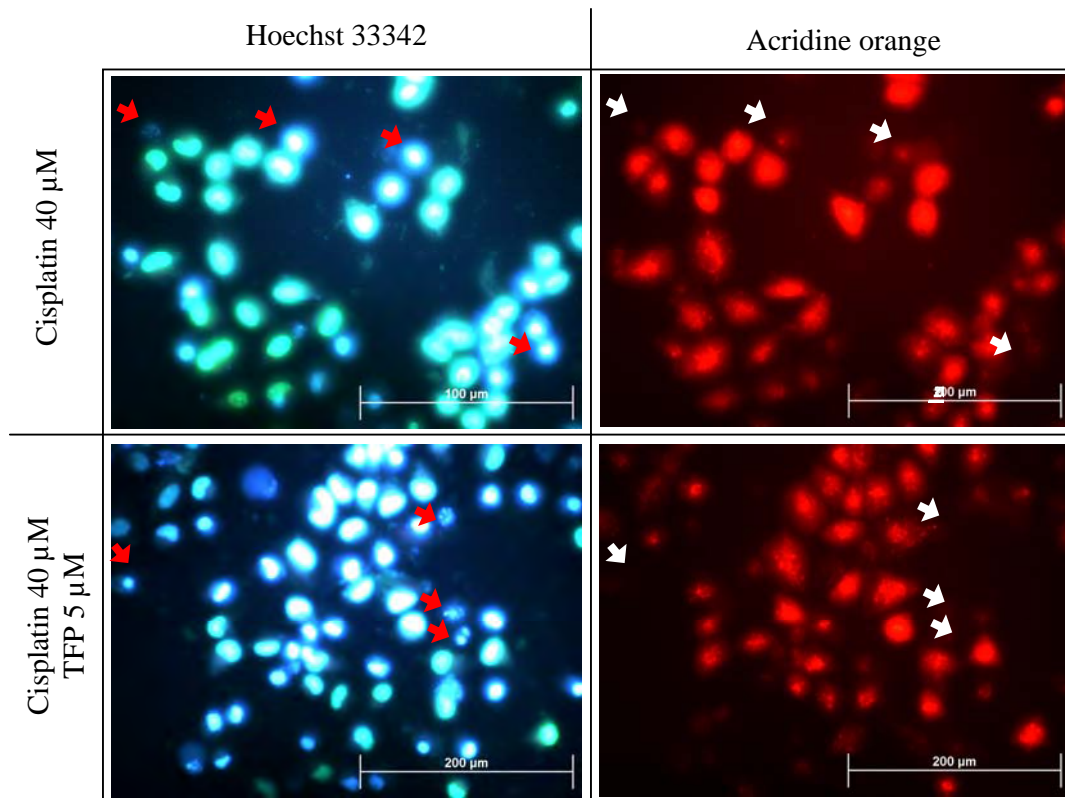
Figure 33   H460 cells stained with Hoechst 33342 and AO. H460 cells were co-treated with cisplatin 40 µM and TFP 5 µM for 24 h. Cell staining was detected under inverted-fluorescence microscope. Red and white arrows represented apoptotic cell death.
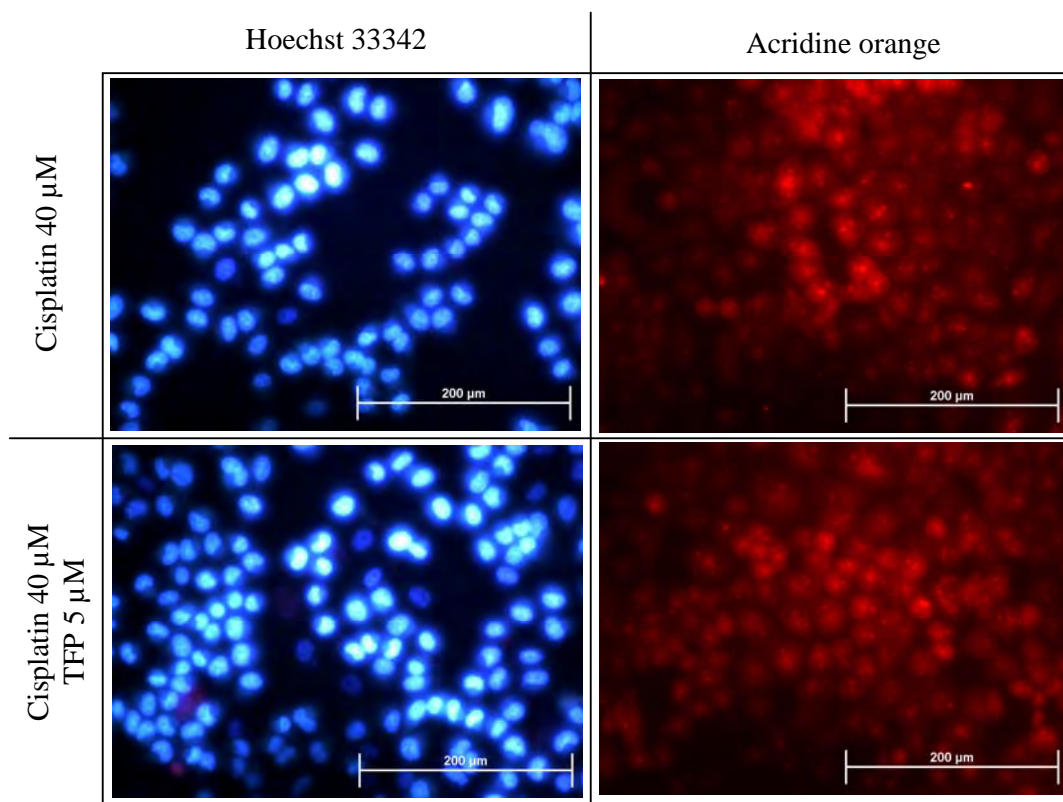
Figure 34   H460/cis cells stained with Hoechst 33342 and AO. H460/cis cells were co-treated with cisplatin 40 μM and TFP 5 μM for 24 h. Cell staining was detected under inverted-fluorescence microscope.
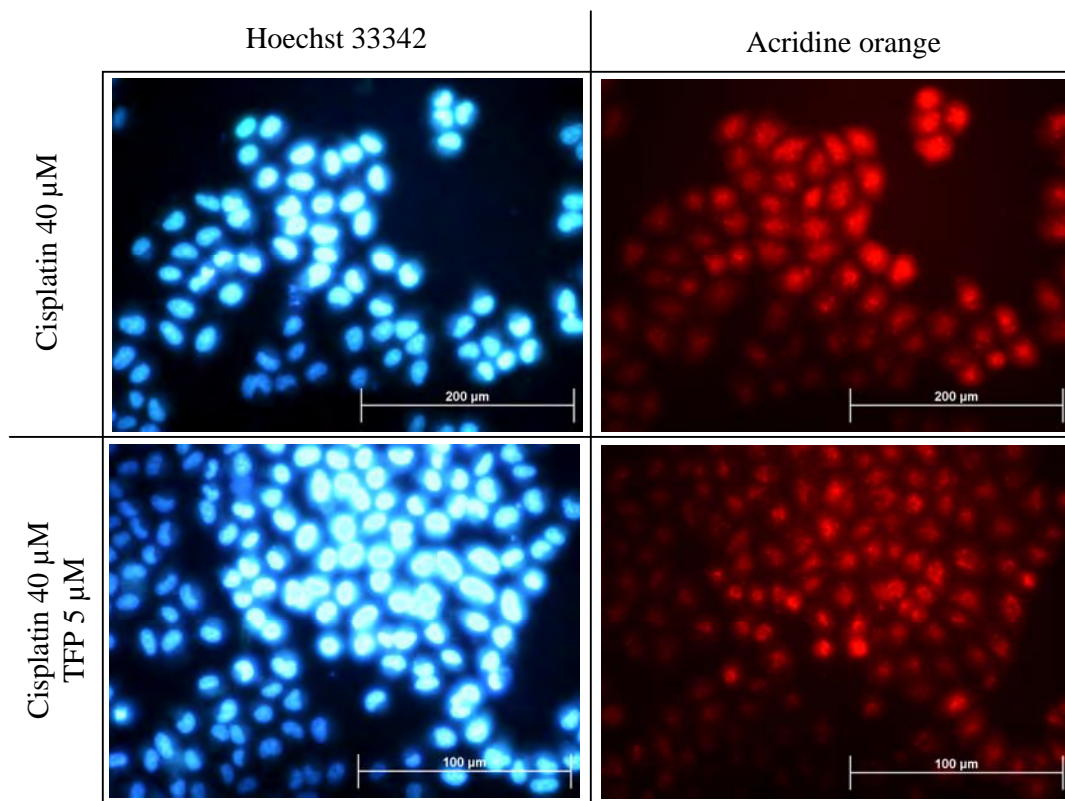
Figure 35   RALP1 cells stained with Hoechst 33342 and AO. RALP cells were co-treated with cisplatin 40 µM and TFP 5 µM for 24 h. Cell staining was detected under inverted-fluorescence microscope.

	Hoechst 33342	Acridine orange
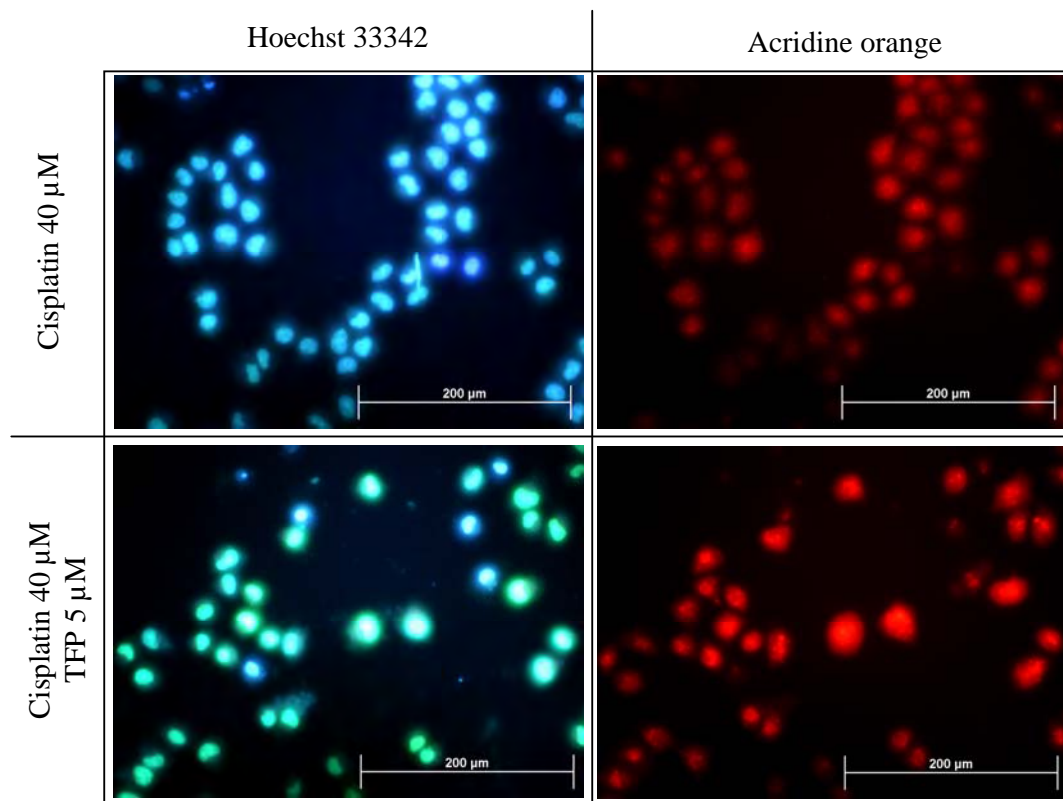
Figure 36   RALP6 cells stained with Hoechst 33342 and AO. RALP6 cells were co-treated with cisplatin 40 µM and TFP 5 µM for 24 h. Cell staining was detected under inverted-fluorescence microscope.

5. Evaluation of the effects of trifluoperazine on types of cisplatin-induced cell death

5.1 Determination of autophagic cell death

Since, there are no reliable methods to detect autophagic cell death available, the cell death excluding from apoptosis and necrosis with the incidence of autophagy induction was assumed as the autophagic cell death. Due to that concept, the amount of autophagic cell death in response to the treatment was recalculated from the results of MTT assay and Hoechst/PI staining. As shown in Figure 37, modes of cell death caused by cisplatin at 40 µM in all cells were apoptotic, necrotic and autophagic cell death, but different in proportion. Apoptosis was the main mode of cell death with small amount of necrosis and autophagic cell death in consequence of cisplatin treatment in all cells. In addition, H460 cells showed the highest portion of apoptotic cell death compared to resistant cells.

After treating with the combination of cisplatin at the concentration of 40 µM and TFP at the concentration of 5 µM, modes of cell death in each cell were changed. Although TFP containing electron-donating groups in structure is likely to interact and detoxify cytotoxic effect of cisplatin, the combination of cisplatin and TFP could significantly reduced % cell viability in resistant cells compared to cisplatin-treated alone. This result indicated that there was no direct interaction between cisplatin and TFP. However, apoptotic cell death was still the main cell-death mode in H460 cells with similar amount of necrosis and the distinguished induction of autophagic cell death compared to cisplatin treatment. In contrast to H460 cells, resistant H460/cis, RALP1 and RALP6 cells showed obviously changes in modes of cell death. In resistant cells, autophagic cell death became the main mode of cell death with similar amount of apoptosis and necrosis, as the percentage of cell death in each mode presented in Table 4. For more understanding, all types of cell death were represented in Figure 37. In cisplatin and TFP combination, the autophagic cell death was increased in ratio of approximately 4.0, 17.0, 9.0 and 16.8 compared to cisplatin-treated group in H460, H460/cis, RALP1 and RALP6 cells, respectively.

Table 4   The types of cell death caused by cisplatin 40 µM and the combination of cisplatin 40 µM and TFP 5 µM in H460, H460/cis, RALP1 and RALP6 cells.

Cell	Treatment	The percentage of cell death				Ratio of Autophagy induction
		Total (100 - % cell viability: MTT)	Apoptotic	Necrotic	Autophagic (Total –apoptosis-necrosis)	
H460	cisplatin	47.64 ± 2.48	40.28 ± 8.06	3.57 ± 2.07	3.79	4.1
	cisplatin +TFP	$51.96 \pm 1.68*$	33.15 ± 3.28	3.34 ± 0.11	15.48	
H460/cis	cisplatin	9.94 ± 3.05	5.30 ± 2.39	3.00 ± 1.00	1.64	17.0
	cisplatin +TFP	$34.86 \pm 1.17*$	6.33 ± 0.33	0.71 ± 0.82	27.81	
RALP1	cisplatin	35.65 ± 1.61	31.61 ± 3.28	1.33 ± 0.58	2.70	9.0
	cisplatin +TFP	$45.56 \pm 1.19*$	20.05 ± 8.28	1.25 ± 0.27	24.26	
RALP6	cisplatin	10.28 ± 1.65	8.23 ± 1.77	1.76 ± 0.09	1.01	16.8
	cisplatin +TFP	$28.73 \pm 2.43*$	9.60 ± 2.34	1.28 ± 1.05	17.85	

Each value of total, apoptotic and necrotic cell death was represented in mean $\pm$ SEM of three independent experiments. The value of autophagic cell death was the sum of the mean of apoptotic and necrotic cell death subtracted from the mean of total cell death. *, $p<0.05$ compared to cisplatin-treated group in each cell.
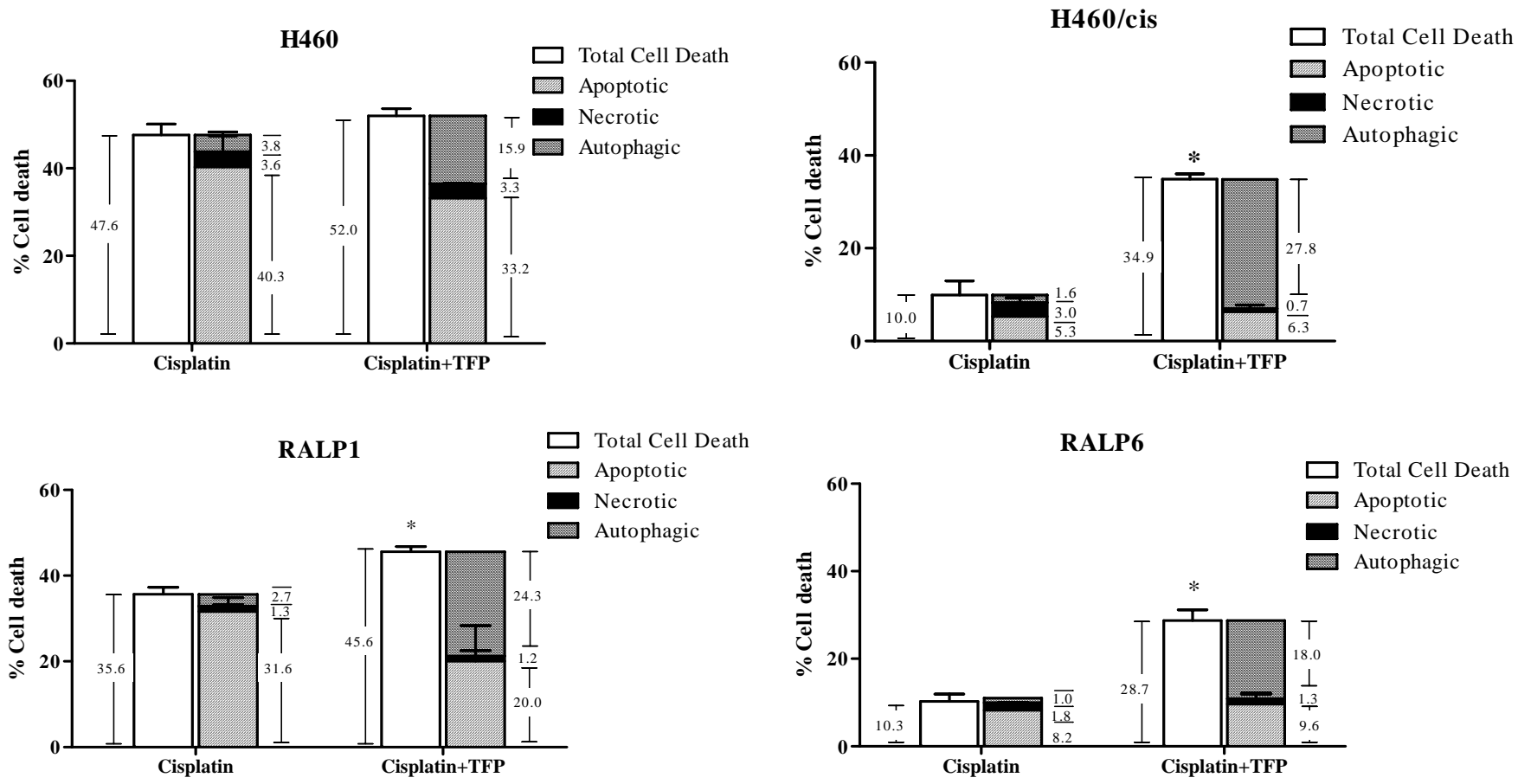
Figure 37 The types of cell death caused by cisplatin 40 µM and the combination of cisplatin 40 µM and TFP 5 µM in H460, H460/cis, RALP1 and RALP6 cells. The percentage of apoptosis and necrosis is presented as mean of three independent experiments. The percentage of autophagic cell death is obtained by calculation as described in 5.1 in Materials and Methods.

5.2 Determination of cytotoxic effect of 3-methyladenine

As we focused on autophagic cell death, the specific inhibitor of class III PI3K-Beclin1 signaling pathway, 3-methyladenine (3-MA), was used. 3-MA specifically inhibits the formation of autophagosomes via the inhibition of class III PI3K-Beclin1 signaling pathway [Seglen and Gordon, 1982; Stroikin *et al.*, 2004] which is one of the pathways regulating autophagy. To prevent misinterpreting the effect of the combination of cisplatin, TFP and 3-MA in H460, H460/cis, RALP1 and RALP6 cells, the cytotoxic effect of 3-MA was evaluated. After treating all cells with various concentrations of 3-MA range from 0.1 µM to 1,000 µM for 24 h, the results from MTT assay indicated that 3-MA at concentration less than 1,000 µM was not toxic as shown in Figure 38. According to the literature reviews, the effective concentration of 3-MA in autophagic inhibition was in the range of 10 µM to 500 µM [Seglen *et al.*, 1982; Takatsuka *et al.*, 2004; Liu *et al.*, 2009]. Therefore, the concentrations of 3-MA at 200 µM was used.
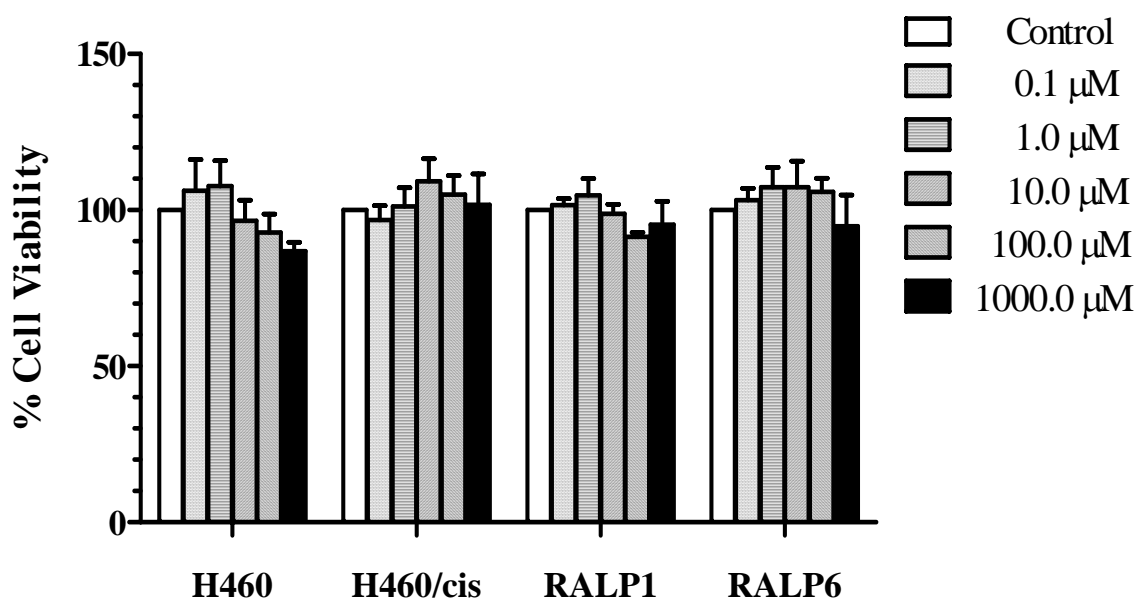
Figure 38   Cytotoxic effect of 3-MA in H460, H460/cis, RALP1 and RALP6 cells. Cells were treated with 3-MA at various concentrations for 24 h and % cell viability was determined by MTT assay. Results were mean ± SEM of three independent experiments.

5.3 Evaluation of the effects of cisplatin, trifluoperazine and 3-methyladenine combination

5.3.1 Cell viability assay (MTT assay)

3-MA at concentration of 200 µM could reverse the cytotoxic effect of cisplatin-TFP co-treatment in all cell types in both time- and concentration-dependent manner as seen in Figure 39. The % cell viability of the combination of cisplatin and TFP in all cells was less than that in cisplatin-treated group since 8 h of incubation. The addition of 3-MA in cisplatin and TFP co-treatment, the reversal effect was also observed since 8 h of incubation. The longer period of incubation showed the more reduction in the percentage of cell viability in the combination of cisplatin and TFP, but in the combination of cisplatin, TFP and 3-MA showed reversal increasing of the percentage of cell viability. However, the increasing of cell viability in all cells treated with the combination cisplatin, TFP and 3-MA was not above that in cisplatin-treated group. At 24 h of incubation, the cell viability in the combination of cisplatin and TFP in resistant cells was significantly decreased ($p<0.05$). In contrast, the cell viability of the combination of cisplatin, TFP and 3 MA in resistant cells was significantly increase as close to that of cisplatin-treated group ($p<0.05$). These results confirmed that the augmentative effect of TFP in cisplatin-induced cell death was due to autophagy induction.
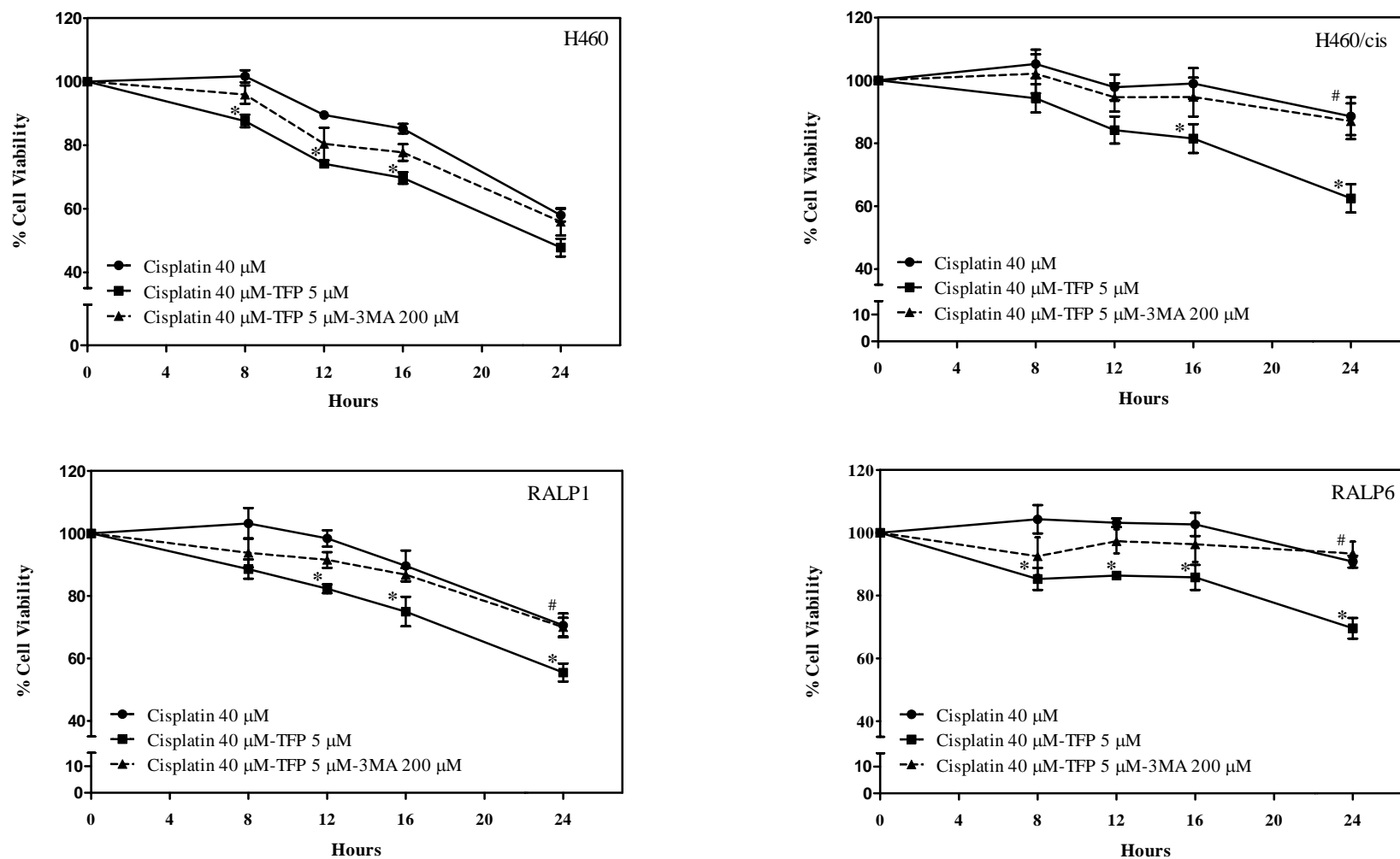
Figure 39   Cytotoxic effect of the combination of 40 μM cisplatin, 5 μM TFP and 200 μM 3-MA in time dependency. Results were mean ± SEM of six independent repeats. *, $p<0.05$ compared to cisplatin-treated group in each cell. #, $p<0.05$ compared to cisplatin-TFP treated group in each cell.

5.3.2 Single-Cell Microgel Electrophoresis (Comet Assay)

To check whether autophagy inhibition by 3-MA could alter apoptotic cell death in response to cisplatin and TFP co-treatment, comet assay was conducted. After all cells were treated with cisplatin, TFP and 3-MA combination for 24 h, cells were embedded in slides and then lysed in alkaline buffer. The fragments of DNA migrating in electrophoresis were stained with SYBRgreen and determined for the parameters of tail length, % DNA in tail, tail moment and olive moment. These parameters presented in the relative amount compared to their own untreated control cells. The ascending of each parameter presented the increasing of DNA fragment, referring to apoptotic cell death.

As seen in Figure 40, the treatments either TFP or 3-MA did not increase DNA fragment in all parameters in all cells. However, the significant increasing of DNA laddering was observed in cisplatin treatment, cisplatin and TFP co-treatment and the combination of cisplatin-TFP and 3-MA in H460 cells compared to control group ($p<0.05$). Those rising in tail length, % DNA in tail, tail moment and olive moment parameters in those 3 different treatments showed similar value compared within these three treatments. For resistant H460/cis, RALP1 and RALP6 cells, no changes in any parameters were observed among those three treatments. The results indicated that apoptotic cell death did not increase in response to the additional 3-MA in cisplatin and TFP co-treatment in all cells.
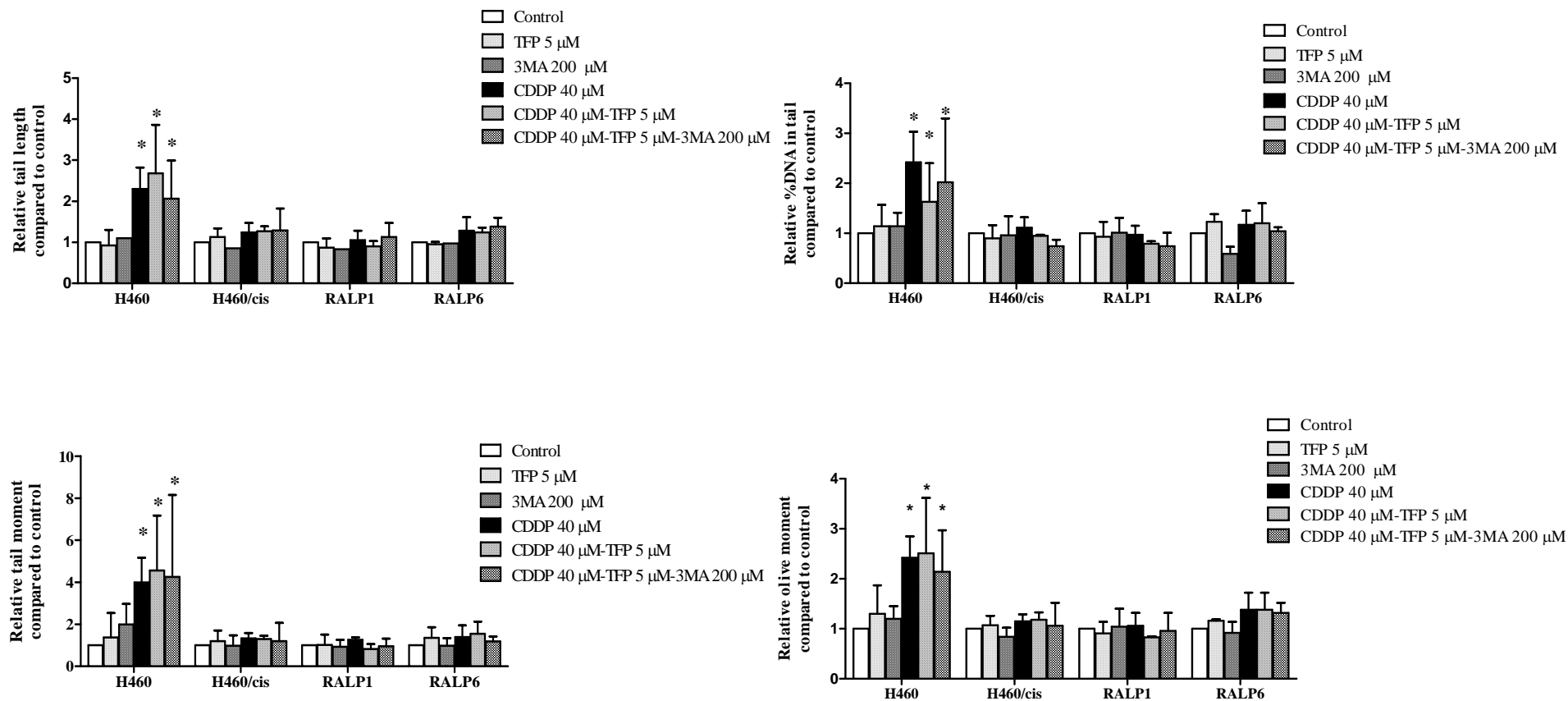
Figure 40   The relative parameters in tail length, % DNA in tail, tail moment and olive moment of cells treated with cisplatin, the combination of cisplatin and TFP or the combination of cisplatin, TFP-3-methyladenine detected by comet assay in H460, H460/cis, RALP1 and RALP6 cells. Each point represents the mean ± SEM of three independent experiments. *, $p<0.05$ compared to control.

5.3.3 Level of LC3 protein expression

As seen in Figure 41, the changes in the cell viability in both combinations (cisplatin-TFP and cisplatin-TFP-3-MA) were observed starting from 8 h and the viable cells were sufficient to detect for the alteration of intracellular proteins without interfering of other protein-degradation pathways. Therefore, the Western blot determining the conversion of microtubule-associated protein 1 light chain 3 (MAP1-LC3) or LC3 from type I to II was conducted at 8 h. As the conversion of LC-3 type I to II is a reliable marker for autophagy activity [Kabeya *et al.*, 2000; Yang *et al.*, 2005; Klionsky, 2007; Mizushima, 2007; Mizushima, Yoshimori and Levine, 2010], the relative ratio of the conversion of LC3 was calculated and compared with untreated control cells. Only H460/cis and RALP6 cells, which showed the highest degree of resistance in different mechanisms, were chosen to quantitate the level of LC3 protein expression compared to that in H460 cells.

In Figure 41, the ratio of LC3 conversion was slightly increased in response to TFP treatment and dramatically decreased in response to 3-MA treatment in H460 cells. However, the conversion was in similar level in cisplatin, cisplatin-TFP and cisplatin-TFP-3-MA treatment. The ratio of LC3-II conversion was 1.1, 0.8, 0.9, 1.3 and 0.8 in TFP, 3-MA, cisplatin, cisplatin-TFP and cisplatin-TFP-3-MA, respectively, compared with untreated control H460 cells. For H460/cis cells, the conversion of LC3-II was distinguishedly induced in TFP, cisplatin and cisplatin-TFP treatment. In contrast, the conversion was decrease in response to the addition of 3-MA in cisplatin-TFP co-treatment. The ratio of LC3-II conversion was 3.0, 1.0, 1.3, 3.0 and 1.8 in TFP, 3-MA, cisplatin, cisplatin-TFP and cisplatin-TFP-3-MA-treated group, respectively, compared with untreated control H460/cis cells (Figure 41). The ratio of LC3 conversion in RALP6 cells was increased in TFP, cisplatin and cisplatin-TFP combination and slightly decreased in 3-MA and the combination of cisplatin-TFP-3-MA treatment as seen in Figure 41. The ratios of LC3 conversion in TFP, 3-MA, cisplatin, cisplatin-TFP and cisplatin-TFP-3-MA-treated group were 2.6, 1.1, 1.2, 2.0 and 1.3, respectively, compared with untreated control RALP6 cells

The results indicated that the conversion of LC3 from type I to II could be induced in response to TFP and the combination of cisplatin-TFP treatments in all cells.

Since the degree of autophagy in sensitive H460 cells was much higher than that in resistant cells, the induction of LC3 conversion was not clearly observed in H460 cells, but the reduction of LC3 conversion was distinguishedly noticed. On the other hand, the resistant H460/cis and RALP6 cells showed much lower degree of autophagy. Therefore, the effects of TFP in autophagy induction were much obviously shown and the treatment of 3-MA alone did not affect much in H460/cis and RALP6 cells (Figure 41).

(A) β-actin

LC3-I

LC3-II

LC3-II ratio	1.00	1.14	0.78	0.91	1.29	0.80

(B) β-actin

LC3-I

LC3-II

LC3-II ratio	1.00	2.96	1.04	1.32	3.03	1.85

β-actin

(C)

LC3-I

LC3-II

LC3-II ratio	1.00	2.57	1.08	1.15	2.02	1.27

cisplatin	-	-	-	40 µM	40 µM	40 µM
TFP	-	5 µM	-	-	5 µM	5 µM
3MA	-	-	200 µM	-	-	200 µM
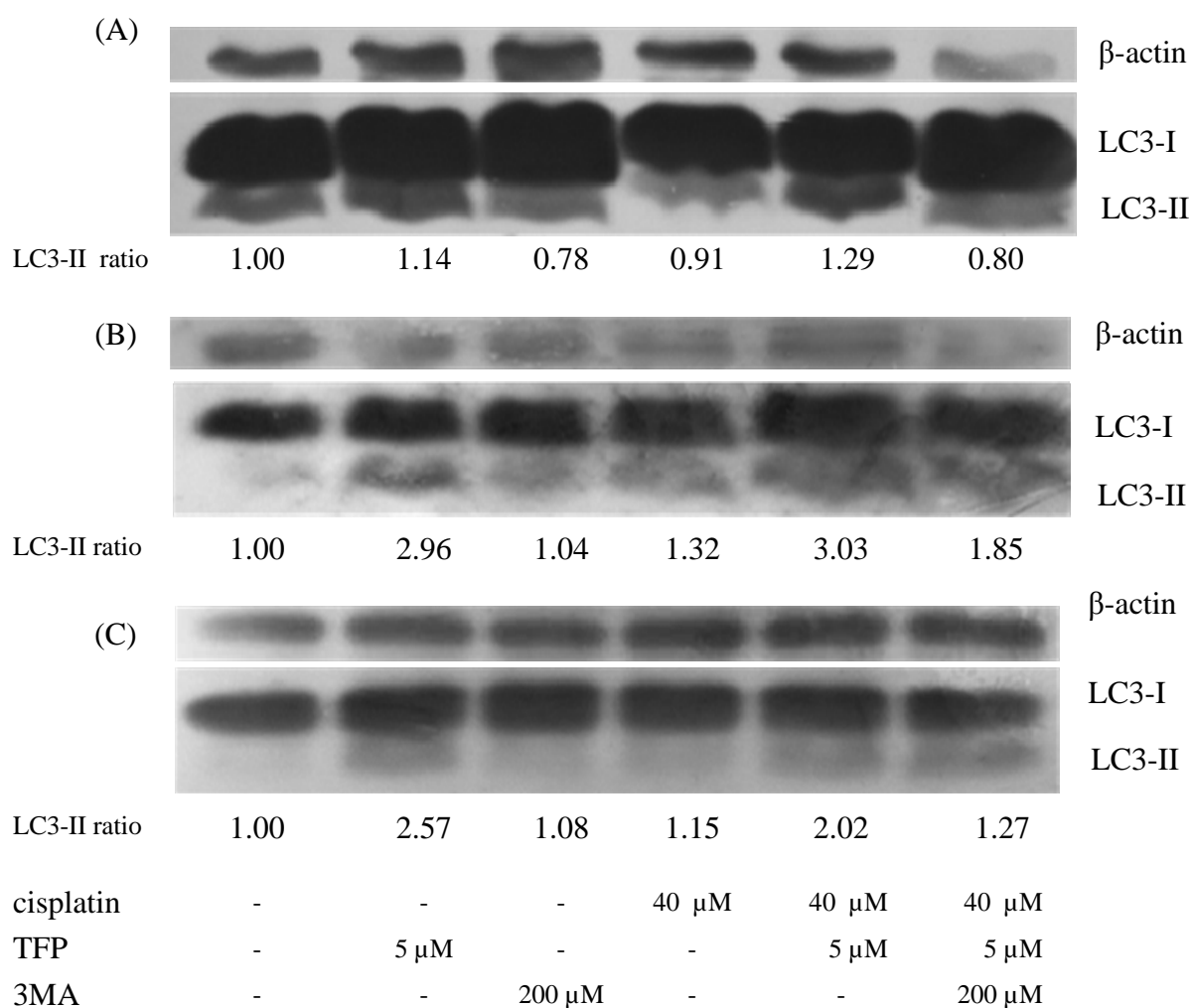
Figure 41   The ratio of LC3 conversion in H460 cells (A), H460/cis cells (B) and RALP6 cells (C) in response to the combination of cisplatin, TFP and 3-MA at 8 h. Relative ratio of LC3-II conversion represented one experiment from three independent experiments.

5.3.3 Level of Bcl-2 protein

Due to RALP6 cells expressed the highest level of Bcl-2 protein, it was chosen to quantitate the level of Bcl-2 protein in this experiment. As RALP6 cells was Bcl-2-mediated cisplatin resistance and the combination of TFP could sensitize cells to cisplatin-induced cytotoxicity, the level of Bcl-2 change in response to the treatment was investigated. To avoid the protein degradation from other pathways that would lead to misinterpret the results, Western blot analysis was conducted at 8 h which the changes could be observed.

The Bcl-2 protein level in response to the combination of cisplatin and TFP trended to decrease when compared to untreated control cells (The relative Bcl-2 ratio was 0.84) which could be reversed by autophagy inhibitor (The relative Bcl-2 ratio was 1.40) as shown in Figure 42. Since the Bcl-2 expression in RALP6 cells were stable exogenous Bcl-2-forced expression, the level of Bcl-2 proteins in cells was stable expressed in the numerous amount and the change in protein level could not be obviously observed.

Bcl-2 ratio	1.00	0.84	1.44	1.45	0.79	1.40
cisplatin	-	-	-	40 µM	40 µM	40 µM
TFP	-	5 µM	-	-	5 µM	5 µM
3MA	-	-	200 µM	-	-	200 µM
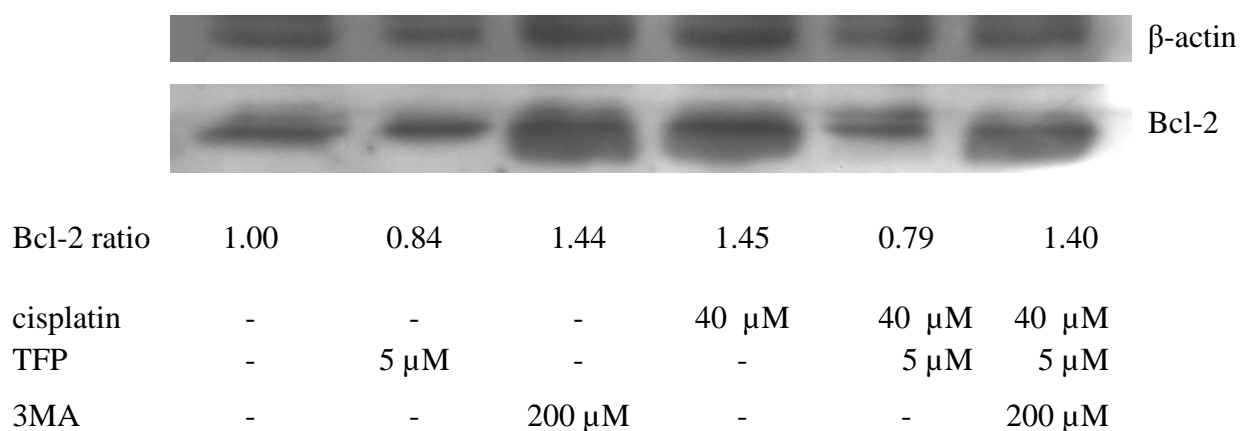
Figure 42　Bcl-2 protein levels in RALP6 cells in response to the combination of cisplatin, TFP and 3-MA at 8 h. Relative ratio of Bcl-2 protein to untreated cells represented one experiment from three independent experiments.

CHAPTER V

DISCUSSION AND CONCLUSION

Since most non-small cell lung cancers (NSCLC) patients are in an advance stage of disease at the time of first detection, intensive treatments in a long duration are required. Long term exposure to cisplatin-based treatment, the first-line therapy, has been reported to increase an incidence of acquired chemotherapeutic resistance [Chang, 2011]. In order to evaluate the potential sensitizing effects of trifluoperazine (TFP) on cisplatin-induced NSCLC cell death, H460/cis, a resistant clone generated by long-term exposure of the H460 cells to cisplatin, were used as an acquired-resistant cell model. Since overexpression or up-regulation of anti-apoptotic Bcl-2 protein has been accepted to be a vital mechanism of cancer cells in acquiring resistance to cisplatin, RALP cells were generated by transfection of H460 cells with Bcl-2 enforced-expression plasmids. Therefore, RALP cells were used as a cell model for Bcl-2 mediated cisplatin resistance in the present study. H460/cis, RALP1 and RALP6 cells significantly resisted to cisplatin-induced cytotoxicity compared to parental H460 cells. H460/cis cells exhibited the highest degree of resistance following by RALP6 and RALP1, sequentially as seen in Figure 20. The cisplatin resistance between RALP1 and RALP6 relied on the level of Bcl-2 protein. RALP6 cells had higher Bcl-2 level compared to that of H460/cis cells as shown in Figure 19, however, they showed lower degree of cisplatin resistance. These results suggested there are other paths of resistance in H460/cis cells. The major mechanism of cisplatin resistance in cancer cells was accepted to due to the defection of apoptotic machinery, such as increasing of anti-apoptotic proteins, like Bcl-2 protein upregulation, several studies have proposed the additional possible mechanisms, for example, reduction of drug accumulation, activation of detoxifying systems, increment of DNA repair machinery and deficiency of apoptosis induction [Mese *et al.*, 1998; Yoon *et al.*, 2001; Sartorius and Krammer, 2002; Siddik, 2003; Hövelmann, Beckers and Schmidt, 2004; Martínez-Lacaci *et al.*, 2007; Rabik and Dolan, 2007; Stewart, 2007; de Bruin and Medema, 2008; Chang, 2011]. Furthermore, H460/cis cells showed the

enlargement of cell size and irregular shape, obviously different from its parental H460 cells (Figure 18).

Autophagy showed the connections between carcinogenesis and the response to cancer treatment [Gozuacik and Kimchi, 2004; Shintani and Klionsky, 2004 ; Levine, 2007; Rosenfeldt and Ryan, 2009]. Downregulation of autophagic process could result in growth promotion of mutant cells, which later became cancers [Edinger and Thompson, 2003; Degenhardt *et al.*, 2006; Chen and Debnath, 2010; Tschan and Simon, 2010]. For the response to cancer treatments, there were evidence indicated that autophagy was the complement of apoptosis causing cell-death in radiotherapy or chemotherapy [Lamparska-Przybysz, Gajkowska and Motyl, 2004; Furuya *et al.*, 2005; Kessel and Reiners Jr, 2007]. On the other hand, autophagic cell death was claimed to be the only mode of cell death in response to particular agents [Opipari *et al.*, 2004; Ito *et al.*, 2006; Chai *et al.*, 2007; Li *et al.*, 2008]. The information garnered from this study suggested that downregulation of autophagy also contributed to cisplatin resistance. As seen in H460/cis, with unknown resistance mechanism developing after long-term cisplatin exposure, the degree of autophagy was dramatically decreased (Figure 22-23). We also found the dramatically low degree of autophagy in Bcl-2 overexpressed RALP1 and RALP6 cells as shown in Figure 22-23. This supports the previous reports regarding the suppressing activity of Bcl-2 protein on autophagy process [Waggoner *et al.*, 1998; Saeki *et al.*, 2000; Shimizu *et al.*, 2004; Pattingre *et al.*, 2005; Pattingre and Levine, 2006; Kessel *et al.*, 2007]. Moreover, Beclin 1, a key protein regulation in autophagic process, is mutated in a number of cancer lines [Liang *et al.*, 1999; Qu *et al.*, 2003; Rubinsztein *et al.*, 2007]. Perhaps, this mutation may play a role in the reduction in autophagy level in cisplatin-induced resistance H460/cis cells. Therefore, restoration or maintaining autophagic basal level in chemotherapeutic-resistant cells might be the promising approach for cancer treatment.

Although autophagy is an inducible process, it gives variable results depending on specific cell types and particular inducing agents [Kondo *et al.*, 2005]. Among autophagic inducers, trifluoperazine (TFP) [Zhang *et al.*, 2007] exhibited the most interesting properties, since it was a FDA-approved anti-psychotic drug. Moreover, previous evidences strongly supported its chemosensitizing attributes which sub-toxic

concentrations of TFP was able to retard cancer cell growth [Shin *et al.*, 2004], to inhibit DNA repair and sensitize cancer cells to cell death [Gangopadhyay *et al.*, 2007; Polischouk *et al.*, 2007] and to suppress P-glycoprotein expression in adriamycin-resistant leukemia [Shina *et al.*, 2006].

In this study, we provided evidence indicating sensitizing effects of TFP on cisplatin-induced cell death in resistant H460/cis, RALP1 and RALP6 cells. At sub-toxic concentrations, TFP alone could increase a number of autophagosome formation (Figure 22 and 24). Addition of TFP in the cisplatin-treated cells, significantly decreased the percentage of cell viability compared to cisplatin-treated control in dose- and time-dependent manners (Figure 25 and 39). The types of cell death in response to the additive effects of TFP in cisplatin-induced cytotoxicity were determined. Since there are no reliable methods to elucidate autophagic cell death yet, it was indirectly recalculated and considered together with the incidence of autophagosome formation.

In cisplatin treatment, it indicated the combination of three types of cell death, apoptosis, necrosis and autophagic cell death. In sensitive H460 cells, cisplatin treatment exerted a great number of apoptotic cell death with small amount of autophagic and necrotic cell death as summarized in Table 4 and Figure 37. Even though, resistant H460/cis, RALP1 and RALP6 cells could initiate cell death, they showed much smaller proportion in all types of cell death compared to H460 cells. All cells showed the induction of autophagy in response to cisplatin as indicated by the increasing of acridine orange intensity as shown in Figure 32. This supported the existing evidence that cisplatin could induce autophagy [Periyasamy-Thandavan *et al.*, 2008].

The sensitizing effect of TFP in cisplatin treatment did not change amount of apoptosis and necrosis, as no increasing in DNA fragment or PI-stained cells were detected. Thus, the increasing of cell viability reduction was considered as autophagic cell death as the combination exerted a great amount of autophagosome production (Figure 32) and increasing of LC3 conversion (Figure 41). Moreover, the induction of autophagy was also correlated with the reduction of cell viability as shown in Table 4 and Figure 37.

There are two pathways of autophagy formation, which are via class I and Class III of phosphatidylinositol 3-kinases (PI3K) family. Class I PI3K regulates autophagy

through Akt/PKB-mTOR pathway [Kroemer and Jäättelä, 2005; Maiuri *et al.*, 2007]. In normal physiology with sufficient nutrients and energy, this pathway is activated and results in inhibition of autophagy. The inhibition of mTOR, in turn, activates and enhances autophagy. This pathway relates to cell survival and proliferation [Kroemer *et al.*, 2005; Rosenfeldt *et al.*, 2009]. There was evidence claimed that cisplatin could dephosphorylate mTOR, resulting in inhibiting its function, in turn, activating autophagy [Castedo, Ferri and Kroemer, 2002]. In contrast, class III PI3K-Beclin 1 pathway stimulates autophagy. Most pharmacologic autophagy inducers activate autophagy through this class of PI3K [Morselli *et al.*, 2009; Mizushima, Yoshimori and Levine, 2010].

As there were evidence claimed that the autophagy inductive effect of TFP was mTOR-independent pathway [Zhang *et al.*, 2007; Ravikumar, Floto and Rubinsztein, 2009] and its effects in modulating cisplatin-induced cell death was blocked with 3-MA, a potent inhibitor of class III PI3K [Seglen and Gordon, 1982; Stroikin *et al.*, 2004]. The percentage of cell viability significantly increased after treating with 200 µM of 3-MA together with the combination of cisplatin-TFP in resistance H460/cis, RALP1 and RALP6 cells (Figure 39). The cytotoxic effect of cisplatin-TFP combination was inhibited by 3-MA in time-dependent manner. It could be stated that the mechanism of TFP in activating autophagy may in part occur via class III PI3K. Though autophagy was inhibited by 3-MA, this could not shift mode of cell death back to apoptosis that might be because of the ascending level of Bcl-2 expression in resistance cells.

As the level of Bcl-2 protein might be altered during cisplatin-TFP combination therapy, the level of Bcl-2 in RALP6 cells was evaluated. It found that the level of Bcl-2 protein was dramatically decreased in response to cisplatin-TFP treatment and was reversed to approximately to the same level in control RALP6 cells as shown in Figure 42. Our results also provided the evidence supporting that downregulation of Bcl-2 protein can induce autophagic cell death [Saeki *et al.*, 2000]. Therefore, the downregulation of Bcl-2 level may be another mechanism of TFP in modulating cisplatin-induced cell death. However, this reduction of Bcl-2 level could not result in apoptosis induction as detected no change in DNA fragmentation in response to combination of cisplatin-TFP.

Even though, there are the connection between apoptosis and autophagy, two processes are polarized which the dominant way has to be determined [Maiuri *et al.*, 2007; Maiuri, Criollo and Kroemer, 2010]. Autophagy and apoptosis could initiate in response to the mutual stimuli, but the sensitivity thresholds are different [Maiuri *et al.*, 2010]. Moreover, the different localization of Bcl-2 protein affects its functions. Bcl-2 protein localized in outer mitochondrial membrane regulating mitochondrial membrane permeability was responsible for apoptosis induction [Maiuri *et al.*, 2007; de Bruin *et al.*, 2008], whereas, Bcl-2 protein localized in ER membrane interacted with Beclin 1 was believed to regulated autophagy [Reed, 2006]. Although, the results showed that the downregulation of Bcl-2 in response to TFP combination could not activate apoptosis in cisplatin treatment. This might be due to this Bcl-2 downregulation was generally throughout the cells, both mitochondria and ER, but the reduction was just enough to trigger autophagy, not yet beyond the threshold to trigger apoptotic induction. Thus, no change of DNA condensation and fragmentation was observed.

As summarized in Figure 43, cisplatin treatment activated various cell death signaling, such as BH3-only proteins (Bak or Bax) and then initiated mitochondrial outer membrane permeabilization (MOMP) [Siddik, 2003]. The release of mitochondrial cytochrome c (Cyt c) from MOMP resulted in assembling of a caspase-activating complex between caspase-9 and Apaf1. Finally, apoptosis was ultimately initiated. Besides Cyt c release, other molecules such as ROS (reactive oxygen species), AIF (apoptosis-inducing factor) or EndoG were also released and then induced necrosis. Cisplatin also inhibited mTOR, which in turn activated small amount of autophagy [Castedo *et al.*, 2002]. In cisplatin and trifluoperazine combination, trifluoperazine could activate phosphatidylinositol-3 kinase (PI3K) class III-Beclin1 pathway and initiate autophagy as shown in thick lines. Moreover, trifluoperazine could down-regulate Bcl-2 protein and augment autophagy induction and MOMP.

In conclusion, this study reported herein that the long-term exposure of H460 cells to cisplatin could precede resistance in non small-cell lung cancer H460 cells by at least two mechanisms which were upregulation of Bcl-2 level and attenuation of autophagy. We also firstly provided the evidence that TFP co-treated with cisplatin could sensitize the resistance non-small cell lung cancer H460/cis, RALP1 and RALP6 cells to

cisplatin-induced cell death through activation of autophagic cell death partially via class III PI3K-Beclin 1 pathway and Bcl-2 downregulation. Therefore, upregulation of autophagy with TFP may be gained a benefit as an adjuvant approach for cancer treatment to prevent and overcome resistance in NSCLC therapy.
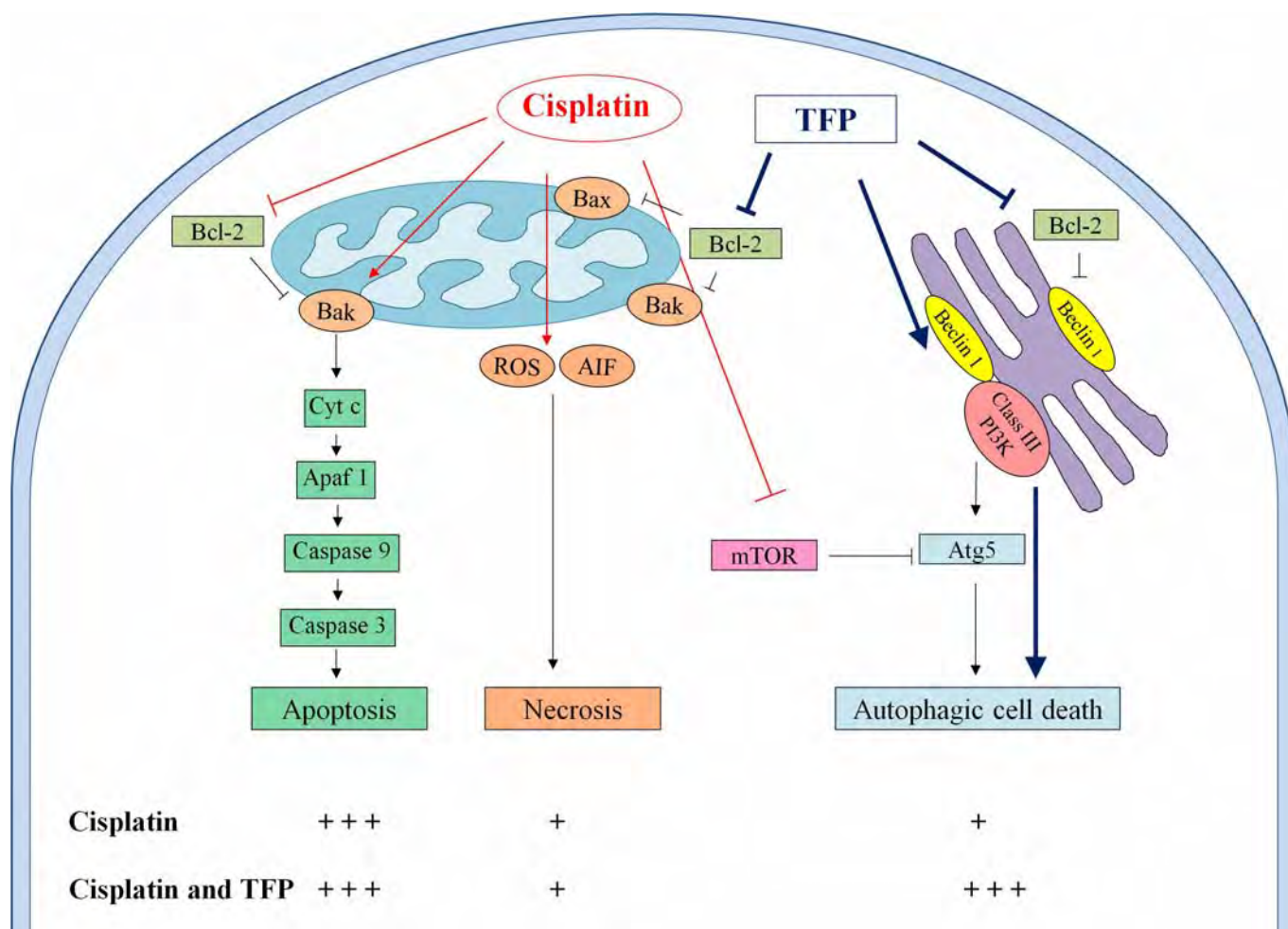
Figure 43   The possible mechanisms of trifluoperazine in potentiating cisplatin - induced cell death. The novel findings of this study are presented in thick line.

REFERENCES

Arthur, C. R., Gupton, J. T., Kellogg, G. E., Yeudall, W. A., Cabot, M. C., Newsham, I. F., *et al.* 2007. Autophagic cell death, polyploidy and senescence induced in breast tumor cells by the substituted pyrrole JG-03-14, a novel microtubule poison. <u>Biochemical Pharmacology</u> 74: 981-991.

Azmi, A. S. and Mohammad, R. M. 2009. Non-peptidic small molecule inhibitors against Bcl-2 for cancer therapy. <u>Journal of Cellular Physiology</u> 218: 13-21.

Azzoli, C. G., Giaccone, G. and Temin, S. 2010. American Society of clinical oncology clinical practice guideline update on chemotherapy for stage IV non-small-cell lung cancer. <u>Journal of Oncology Practice</u> 6: 39-43.

Boya, P., González-Polo, R. A., Casares, N., Perfettini, J. L., Dessen, P., Larochette, N., *et al.* 2005. Inhibition of macroautophagy triggers apoptosis. <u>Molecular and Cellular Biology</u> 25: 1025-1040.

Brown, W. J., DeWald, D. B., Emr, S. D., Plutner, H. and Balch, W. E. 1995. Role for phosphatidylinositol 3-kinase in the sorting and transport of newly synthesized lysosomal enzymes in mammalian cells. <u>Journal of Cell Biology</u> 130: 781-796.

Brutus, N. A., Hanley, S., Ashraf, Q. M., Mishra, O. P. and Delivoria-Papadopoulos, M. 2009. Effect of hyperoxia on serine phosphorylation of apoptotic proteins in mitochondrial membranes of the cerebral cortex of newborn piglets. <u>Neurochemical Research</u> 34: 1219-1225.

Carmichael, J., DeGraff, W. G. and Gazdar, A. F. 1987. Evaluation of a tetrazolium-based semiautomated colorimetric assay: Assessment of chemosensitivity testing. <u>Cancer Research</u> 47: 936-942.

Castedo, M., Ferri, K. F. and Kroemer, G. 2002. Mammalian target of rapamycin (mTOR): Pro- and anti-apoptotic. <u>Cell Death and Differentiation</u> 9: 99-100.

Chai, C. Y., Huang, Y. C., Hung, W. C., Kang, W. Y. and Chen, W. T. 2007. Arsenic salts induced autophagic cell death and hypermethylation of DAPK promoter in SV-40 immortalized human uroepithelial cells. <u>Toxicology Letters</u> 173: 48-56.

Chakraborty, S., Kundu, T., Dey, S., Bhattacharya, R. K., Siddiqi, M. and Roy, M. 2006. Tea-induced apoptosis in human leukemia K562 cells as assessed by

comet formation. <u>Asian Pacific journal of cancer prevention : APJCP.</u> 7: 201-207.

Chang, A. 2011. Chemotherapy, chemoresistance and the changing treatment landscape for NSCLC. <u>Lung Cancer</u> 71: 3-10.

Chen, N. and Debnath, J. 2010. Autophagy and tumorigenesis. <u>FEBS Letters</u> 584: 1427-1435.

Cho, H. J., Kim, J. K., Kim, K. D., Yoon, H. K., Cho, M. Y., Park, Y. P.*, et al.* 2006. Upregulation of Bcl-2 is associated with cisplatin-resistance via inhibition of Bax translocation in human bladder cancer cells. <u>Cancer Letters</u> 237: 56-66.

Coates, J. M., Virudachalam, S., Muilenburg, D. J. and Bold, R. J. 2009. Bcl-2 overexpression confers resistance to autophagy in pancreatic cancer cells. <u>Journal of Surgical Research</u> 151: 253-253.

Daido, S., Yamamoto, A., Fujiwara, K., Sawaya, R., Kondo, S. and Kondo, Y. 2005. Inhibition of the dna-dependent protein kinase catalytic subunit radiosensitizes malignant glioma cells by inducing autophagy. <u>Cancer Research</u> 65: 4368-4375.

de Bruin, E. C. and Medema, J. P. 2008. Apoptosis and non-apoptotic deaths in cancer development and treatment response. <u>Cancer Treatment Reviews</u> 34: 737-749.

Deesomchok, A., Dechayonbancha, N. and Thongprasert, S. 2005. Lung cancer in Maharaj Nakorn Chiang Mai Hospital: Comparison of the clinical manifestations between the young and old age groups. <u>Journal of the Medical Association of Thailand</u> 88: 1236-1241.

Degenhardt, K., Mathew, R., Beaudoin, B., Bray, K., Anderson, D., Chen, G.*, et al.* 2006. Autophagy promotes tumor cell survival and restricts necrosis, inflammation, and tumorigenesis. <u>Cancer Cell</u> 10: 51-64.

Douarre, C., Gomez, D., Morjani, H., Zahm, J. M., O'Donohue, M. F., Eddabra, L.*, et al.* 2005. Overexpression of Bcl-2 is associated with apoptotic resistance to the G-quadruplex ligand 12459 but is not sufficient to confer resistance to long-term senescence. <u>Nucleic Acids Research</u> 33: 2192-2203.

Edinger, A. L. and Thompson, C. B. 2003. Defective autophagy leads to cancer. <u>Cancer Cell</u> 4: 422-424.

Eisenberg-Lerner, A., Bialik, S., Simon, H. U. and Kimchi, A. 2009. Life and death partners: Apoptosis, autophagy and the cross-talk between them. Cell Death and Differentiation 16: 966-975.

Fisher, D. E. 1994. Apoptosis in cancer therapy: Crossing the threshold. Cell 78: 539-542.

Furuya, D., Tsuji, N., Yagihashi, A. and Watanabe, N. 2005. Beclin 1 augmented *cis*-diamminedichloroplatinum induced apoptosis via enhancing caspase-9 activity. Experimental Cell Research 307: 26- 40.

Gangopadhyay, S., Karmakar, P., Dasgupta, U. and Chakraborty, A. 2007. Trifluoperazine stimulates ionizing radiation induced cell killing through inhibition of DNA repair. Mutation Research/Genetic Toxicology and Environmental Mutagenesis 633: 117-125.

Gozuacik, D. and Kimchi, A. 2004. Autophagy as a cell death and tumor suppressor mechanism. Oncogene 23: 2891-2906.

Gross, A., McDonnell, J. M. and Korsmeyer, S. J. 1999. BCL-2 family members and the mitochondria in apoptosis. Genes and Development 13: 1899-1911.

Hövelmann, S., Beckers, T. and Schmidt, M. 2004. Molecular alterations in apoptotic pathways after PKB/Aktmediated chemoresistance in NCI H460 cells. British Journal of Cancer 90: 2370 - 2377.

Inbal, B., Bialik, S., Sabanay, I., Shani, G. and Kimchi, A. 2002. DAP kinase and DRP-1 mediate membrane blebbing and the formation of autophagic vesicles during programmed cell death. Journal of Cellular Biology 157: 455-468.

Ito, H., Aoki, H., Kühnel, F., Kondo, Y., Kubicka, S., Wirth, T.*, et al.* 2006. Autophagic cell death of malignant glioma cells induced by a conditionally replicating adenovirus. Journal of the National Cancer Institute 98: 625-636.

Kabeya, Y., Mizushima, N., Ueno, T., Yamamoto, A., Kirisako, T., Noda, T.*, et al.* 2000. LC3, a mammalian homologue of yeast Apg8p, is localized in autophagosome membranes after processing. EMBO Journal 19: 5720-5728.

Kang, M. H. and Reynolds, C. P. 2009. BcI-2 Inhibitors: Targeting mitochondrial apoptotic pathways in cancer therapy. Clinical Cancer Research 15: 1126-1132.

Kanzawa, T., Kondo, Y., Ito, H., Kondo, S. and Germano, I. 2003. Induction of autophagic cell death in malignant glioma cells by arsenic trioxide. Cancer Research 63: 2103-2108.

Karpathiou, G., Sivridis, E., Koukourakis, M., Mikroulis, D., Bouros, D., Froudarakis, M., *et al.* 2010. LC3A autophagic acivity and prognostic significance in non-small cell lung carcinomas. Chest [Epub ahead of print].

Katayama, M., Kawaguchi, T., Berger, M. and Pieper, R. 2007. DNA damaging agent-induced autophagy produces a cytoprotective adenosine triphosphate surge in malignant glioma cells. Cell Death and Differentiation 14: 548-558.

Kelland, L. 2007. The resurgence of platinum-based cancer chemotherapy. Nature 7: 573-584.

Kessel, D. and Reiners Jr, J. J. 2007. Initiation of apoptosis and autophagy by the Bcl-2 antagonist HA14-1. Cancer Letters 249 294-299.

Kihara, A., Kabeya, Y., Ohsumi, Y. and Yashimori, T. 2001. Beclin-phoshatidylinosital 3-kinase complex function at the *trans*-golgi network. EMBO reports 2: 330-335.

Kim, K. W., Hwang, M., Moretti, L., Jaboin, J. J., Cha, Y. I. and Lu, B. 2008. Autophagy upregulation by inhibitors of caspase-3 and mTOR enhances radiotherapy in a mouse model of lung cancer. Autophagy 4: 659 - 668.

Klionsky, D. J. 2007. Autophagy: from phenomenology to molecular understanding in less than a decade. Nature Reviews Molecular Cell Biology 8: 931-937.

Klionsky, D. J., Abeliovich, H., Agostinis, P., Agrawal, D. K., Aliev, G., Askew, D. S., *et al.* 2008. Guidelines for the use and interpretation of assays for monitoring autophagy in higher eukaryotes. Autophagy 4: 151-175.

Kondo, S., Yokoyama, T., Shinojima, N., Shingu, T., Bogler, O. and Kondo, Y. 2008. Role of autophagy in cancer resistance. European Journal of Cancer Supplements 79.

Kondo, Y., Kanzawa, T., Sawaya, R. and Kondo, S. 2005. The role of autophagy in cancer development and response to therapy. Nature Reviews Cancer 5: 726-734.

Kondo, Y. and Kondo, S. 2006. Spotlight on cancer autophagy and cancer therapy. Autophagy 2: 85-90.

Kroemer, G. and Jäättelä, M. 2005. Lysosomes and autophagy in cell death control. Nature Reviews Cancer 5: 886-897.

Kroemer, G. 2008. Oncogenes and tumor suppressor genes control autophagy. European Journal of Cancer Supplements 79.

Kuwana, T. and Newmeyer, D. D. 2003. Bcl-2-family proteins and the role of mitochondria in apoptosis. Current Opinion in Cell Biology 15: 691-699.

Lamparska-Przybysz, M., Gajkowska, B. and Motyl, T. 2004. Autophagy as a complementary to apoptosis from of cell death in camptothecin treated brest cancer MCF-7 cells. Proceedings of the 12th Euroconference on Apoptosis, Chania, Greece, 96.

Le Chevalier, T., Brisgand, D., Soria, J. C., Douillard, J. Y., Pujol, J. L., Ruffie, P., *et al.* 2001. Long term analysis of survival in the european randomized trial comparing vinorelbine/cisplatin to vindesine/cisplatin and vinorelbine alone in advanced non-small cell lung cancer. Oncologist 6: 8-11.

Lefranc, F., Facchini, V. and Kiss, R. 2007. Proautophagic drugs: A novel means to combat apoptosis-resistant cancers, with a special emphasis on glioblastomas. Oncologist 12: 1395-1403.

Levine, B. and Klionsky, D. J. 2004. Development by self-digestion: molecular mechanisms and biological functions of autophagy. Developmental Cell 6: 463-477.

Levine, B. 2007. Autophagy and cancer. Nature 446: 745-747.

Levine, B., Sinha, S. and Kroemer, G. 2008. Autophagy in higher eukaryotes-A matter of survival or death bcl-2 family members dual regulators of apoptosis and autophagy. Autophagy 4: 600-606.

Li, H. B., Yi, X., Gao, J. M., Ying, X. X., Guan, H. Q. and Li, J. C. 2007. Magnolol-induced H460 cells death via autophagy but not apoptosis. Archives of Pharmacal Research 30: 1566-1574.

Liang, X. H., Jackson, S., Seaman, M., Brown, K., Kempkes, B., Hibshoosh, H., *et al.* 1999. Induction of autophagy and inhibition of tumorigenesis by beclin 1. Nature 402: 672-676.

Liu, D., Yang, Y., Liu, Q. and Wang, J. 2009. Inhibition of autophagy by 3-MA potentiates cisplatin-induced apoptosis in esophageal squamous cell carcinoma cells. Medical Oncology 1-7.

Liu, Q., Wang, J. J., Pan, Y. C., Meng, L. F., Zhan, X. and Zheng, Q. F. 2008. Expression of autophagy-related genes Beclin1 and MAPLC3 in non-small cell lung cancer. Chinese journal of cancer 27: 25-29.

Lu, B. 2008. Targeting apoptosis-resistant cancer cells through autophagic cell death. European Journal of Cancer Supplements 79.

Maiuri, M. C., Zalckvar, E., Kimchi, A. and Kroemer, G. 2007. Self-eating and self-killing: crosstalk between autophagy and apoptosis. Nature Reviews Molecular Cell Biology 8: 741-752.

Maiuri, M. C., Criollo, A. and Kroemer, G. 2010. Crosstalk between apoptosis and autophagy within the Beclin 1 interactome. EMBO J 29: 515-516.

Martinet, W., Agostinis, P., Vanhoecke, B., Dewaele, M. and De Meyer, G. R. Y. 2009. Autophagy in disease: A double-edged sword with therapeutic potential. Clinical Science 116: 697-712.

Martínez-Lacaci, I., GarcÍa Morales, P., Soto, J. L. and Saceda, M. 2007. Tumour cells resistance in cancer therapy. Clinical and Translational Oncology 9: 13-20.

McCoy, F., Hurwitz, J., McTavish, N., Paul, I., Barnes, C., O'Hagan, B., *et al.* 2010. Obatoclax induces Atg7-dependent autophagy independent of beclin-1 and BAX/BAK. Cell Death and Disease 1 [publish online].

Mese, H., Sasaki, A., Alcalde, R. E., Nakayama, S. and Matsumura, T. 1998. Establishment and characterization of cisplatin-resistant human epidermoid carcinoma cell line, A431 cell. Chemotherapy 44: 414-420.

Mizushima, N. 2007. Autophagy: Process and function. Genes and Development 21: 2861-2873.

Mizushima, N., Yoshimori, T. and Levine, B. 2010. Methods in mammalian autophagy research. Cell 140: 313-326.

Moretti, L., Yang, E. S., Kim, K. W. and Lu, B. 2007. Autophagy signaling in cancer and its potential as novel target to improve anticancer therapy. Drug Resistance Updates 10: 135-143.

Moretti, M., Villarini, M., Scassellati-Sforzolini, G., Monarca, S., Salucci, A. and Rodriguez, A. V. 1999. Application of the single-cell gel-electrophoresis ('comet') assay to the detection of primary DNA damage in workers of the rubber industry: Comparison of manual and computerized analysis. Toxicological and Environmental Chemistry 72: 13-24.

Morselli, E., Galluzzi, L., Kepp, O., Vicencio, J. M., Criollo, A., Maiuri, M. C., *et al.* 2009. Anti- and pro-tumor functions of autophagy. Biochimica et Biophysica Acta - Molecular Cell Research 1793: 1524-1532.

Mosmann, T. 1983. Rapid colorimetric assay for cellular growth and survival: Application to proliferation and cytotoxicity assays. Journal of Immunological Methods 65: 55-63.

Ogier-Denis, E., Pattingre, S., Benna, J. E. and Codogno, P. 2000. Erk1/2-dependent phosphorylation of Ga-interacting protein stimulates its GTPase accelerating activity and autophagy in human colon cancer cells. Journal of Biological Chemistry 275: 39090-39095.

Okada, H. and Mak, T. W. 2004. Pathways of apoptotic and non-apoptotic death in tumour cells. Nature Reviews Cancer 4: 592-603.

Olive, P. L., Durand, R. E., Banáth, J. P. and Johnston, P. J. 2001. Analysis of dna damage in individual cells. Methods in Cell Biology. 234-249.

Opipari, A. W., Tan, L., Boitano, A. E., Sorenson, D. R., Aurora, A. and Liu, J. R. 2004. Resveratrol-induced autophagocytosis in ovarian cancer cells. Cancer Research 64: 696-703.

Paglin, S., Hollister, T., Delohery, T., Hackett, N., McMahill, M., Sphicas, E., *et al.* 2001. A novel response of cancer cells to radiation involves autophagy and formation of acidic vesicles. Cancer Research 61: 439-444.

Paik, P., Rudin, C., Brown, A., Rizvi, N., Takebe, N., Travis, W., *et al.* 2010. A phase I study of obatoclax mesylate, a Bcl-2 antagonist, plus topotecan in solid tumor malignancies. Cancer Chemotherapy and Pharmacology 66: 1079-1085.

Patel, M. R., Masood, A., Patel, P. S. and Chanan-Khan, A. A. 2009. Targeting the Bcl-2. Current Opinion in Oncology 21: 516-523.

Pattingre, S., Tassa, A., Qu, X., Garuti, R., Liang, X. H., Mizushima, N., *et al.* 2005. Bcl-2 antiapoptotic proteins inhibit Beclin 1-dependent autophagy. Cell Death and Differentiation 122: 927-939.

Pattingre, S. and Levine, B. 2006. Bcl-2 inhibition of autophagy: A new route to cancer? Cancer Research 66: 2885-2888.

Periyasamy-Thandavan, S., Jiang, M., Wei, Q., Smith, R., Yin, X.-M. and Dong, Z. 2008. Autophagy is cytoprotective during cisplatin injury of renal proximal tubular cells. Kidney International 74: 631-640.

Pisters, K. M. W., Evans, W. K., Azzoli, C. G., Kris, M. G., Smith, C. A., Desch, C. E., *et al.* 2007. Cancer Care Ontario and American Society of clinical oncology adjuvant chemotherapy and adjuvant radiation therapy for stages I-

IIIA resectable non-small-cell lung cancer guideline. Journal of Clinical Oncology 25: 5506-5518.

Polischouk, A. G., Holgersson, Å., Zong, D., Stenerlöw, B., Karlsson, H. L., ller, L. M*., et al.* 2007. The antipsychotic drug trifluoperazine inhibits DNA repair and sensitizes non–small cell lung carcinoma cells to DNA double-strand break–induced cell death. Molecular Cancer Therapy 6: 2303.

Pongrakhananon, V., Nimmannit, U., Luanpitpong, S., Rojanasakul, Y. and Chanvorachote, P. 2010. Curcumin sensitizes non-small cell lung cancer cell anoikis through reactive oxygen species-mediated Bcl-2 downregulation. Apoptosis 15: 574-585.

Pratesi, G., Perego, P. and Zunino, F. 2001. Role of Bcl-2 and its post-transcriptional modification in response to antitumor therapy. Biochemical Pharmacology 61: 381-386.

Qu, X., Yu, J., Bhagat, G., Furuya, N., Hibshoosh, H., Troxel, A*., et al.* 2003. Promotion of tumorigenesis by heterozygous disruption of the beclin 1 autophagy gene. Journal of Clinical Investigation 112: 1809-1820.

Rabik, C. A. and Dolan, M. E. 2007. Molecular mechanisms of resistance and toxicity associated with platinating agents. Cancer Treatment Reviews 33: 9- 23.

Ravikumar, B., Futter, M., Jahreiss, L., Korolchuk, V. I., Lichtenberg, M., Luo, S*., et al.* 2009a. Mammalian macroautophagy at a glance. Journal of Cell Science 122: 1707-1711.

Ravikumar, S. B., Floto, R. A. and Rubinsztein, D. C. 2009b. Rapamycin and mTOR-independent autophagy inducers ameliorate toxicity of polyglutamine expanded huntingtin and related proteinopathies. Cell Death and Differentiation 16: 46-56.

Reed, J. C. 2006. Drug Insight: Cancer therapy strategies based on restoration of endogenous cell death mechanisms. Nature Clinical Practice Oncology 3: 388-398.

Rosenfeldt, M. T. and Ryan, K. M. 2009. The role of autophagy in tumour development and cancer therapy. Expert reviews in molecular medicine 11 [Publish online].

Rubinsztein, D. C., Gestwicki, J. E., Murphy, L. O. and Klionsky, D. J. 2007. Potential therapeutic applications of autophagy. Nature Reviews Drug Discovery 6: 304-312.

Saeki, K., Yuo, A., Okuma, E., Yazaki, Y., Susin, S., Kroemer, G.*, et al.* 2000. Bcl-2 down-regulation causes autophagy in a caspase-independent manner in human leukemic HL60 cells. Cell Death and Differentiation 7: 1263-1269.

Sartorius, U. A. and Krammer, P. H. 2002. Upregulation of Bcl-2 is involved in the mediation of chemotherapy resistance in human small cell lung cancer cell lines. International Journal of Cancer 97: 584-592.

Scarlatti, F., Bauvy, C., Ventruti, A., Sala, G., Cluzeaud, F., Vandewalle, A.*, et al.* 2004. Ceramide-mediated macroautophagy involves inhibition of protein kinase b and up-regulation of Beclin 1. Journal of Biological Chemistry 279: 18384-18391.

Seglen, P. O. and Gordon, P. B. 1982. 3-Methyladenine: Specific inhibitor of autophagic/lysosomal protein degradation in isolated rat hepatocytes. Proceedings of the National Academy of Sciences of the United States of America 79: 1889-1892.

Shimizu, S., Kanaseki, T., Mizushima, N., Mizuta, T., Arakawa-Kobayashi, S., Thompson, C. B.*, et al.* 2004. Role of Bcl-2 family proteins in a non-apoptotic programmed cell death dependent on autophagy genes. Nature Cell Biology 6: 1221-1228.

Shin, S. Y., Kim, C. G., Hong, D. D., Kim, J.-H. and Lee, Y. H. 2004. Implication of Egr-1 in trifluoperazine-induced growth inhibition in human U87MG glioma cells. Experimental and Molecular Medicine 36: 380-386.

Shina, S. Y., Choia, B. H., Kimb, J.-R., Kimb, J.-H. and Leea, Y. H. 2006. Suppression of P-glycoprotein expression by antipsychotics trifluoperazine in adriamycin-resistant L1210 mouse leukemia cells. European Journal of Pharmaceutical Sciences 28: 300-306.

Shintani, T. and Klionsky, D. J. 2004 Autophagy in health and disease: A double-edged sword. Science 306 990-995.

Siddik, Z. H. 2003. Cisplatin: mode of cytotoxic action and molecular basis of resistance. Oncogene 22: 7265-7279.

Singh, N. P., McCoy, M. T., Tice, R. R. and Schneider, E. L. 1988. A simple technique for quantitation of low levels of DNA damage in individual cells. Experimental Cell Research 175: 184-191.

Singh, N. P. 2000. A simple method for accurate estimation of apoptotic cells. Experimental Cell Research 256: 328-337.

Stewart, D. J. 2007. Mechanisms of resistance to cisplatin and carboplatin. <u>Critical Reviews in Oncology/Hematology</u> 63: 12-31.

Stoppler, M. C. 2005. <u>Lung Cancer Signs and Symptoms</u> [Web Page]. from <u>http://www.webmd.com/lung-cancer/guide/lung-cancer-types</u> [March 10 2009].

Stroikin, Y., Dalen, H., Lööf, S. and Terman, A. 2004. Inhibition of autophagy with 3-methyladenine results in impaired turnover of lysosomes and accumulation of lipofuscin-like material. <u>European Journal of Cell Biology</u> 83: 583-590.

Swerdlow, S., McColl, K., Rong, Y., Lam, M., Gupta, A. and Distelhorst, C. W. 2008. Apoptosis inhibition by Bcl-2 gives way to autophagy in glucocorticoidtreated lymphocytes. <u>Autophagy</u> 4: 612-620.

Takatsuka, C., Inoue, Y., Matsuoka, K. and Moriyasu, Y. 2004. 3-Methyladenine Inhibits Autophagy in Tobacco Culture Cells under Sucrose Starvation Conditions. <u>Plant and Cell Physiology</u> 45: 265-274.

Thorburn, A. 2008. Apoptosis and Autophagy: regulatory connections between two supposedly different processes. <u>Apoptosis</u> 13: 1-9.

Tschan, M. P. and Simon, H. U. 2010. The role of autophagy in anticancer therapy: promises and uncertainties. <u>Journal of Internal Medicine</u> 268: 410-418.

Waggoner, S. E., Baunoch, D. A., Anderson, S. A., Leigh, F. and Zagaja, V. G. 1998. Bcl-2 protein expression associated with resistance to apoptosis in clear cell adenocarcinomas of the vagina and cervix expressing wild-type p53. <u>Annals of Surgical Ontology</u> 5: 544-547.

Wang, C. W. and Klionsky, D. J. 2003. The molecular mechanism of autophagy. <u>Molecular Medicine</u> 9: 65-76.

Wang, D. and Lippard, S. J. 2005. Cellular processing of platinum anticancer drugs. <u>Nature Reviews Drug Discovery</u> 4: 307-320.

Wang, S. H., Shih, Y. L., Kuo, T. C., Ko, W. C. and Shin, C. M. 2009. Cadmium toxicity toward autophagy through ROS-activated GSK-3b in mesangial cells. <u>Toxicological Sciences</u> 108: 124-131.

Wang, Z. h., Xu, L., Duan, Z. l., Zeng, L. q., Yan, N. h. and Peng, Z. l. 2007. Beclin 1-mediated macroautophagy involves regulation of caspase-9 expression in cervical cancer HeLa cells. <u>Gynecologic Oncology</u> 107: 107-113.

Wesarg, E., Hoffarth, S., Wiewrodt, R., Kröll, M., Biesterfeld, S., Huber, C.*, et al.* 2007. Targeting BCL-2 family proteins to overcome drug resistance in non-small cell lung cancer. International Journal of Cancer 121: 2387-2394

Yang, Y. P., Liang, Z. Q., Gu, Z. L. and Qin, Z. H. 2005. Molecular mechanism and regulation of autophagy. Acta Pharmacologica Sinica 26: 1421-1434.

Yoon, S. S., Ahn, K. S., Kim, S. H., Shim, Y. M. and Kim, J. 2001. In vitro establishment of cis-diammine-dichloroplatinum(II) resistant lung cancer cell line and modulation of apoptotic gene expression as a mechanism of resistant phenotype. Lung Cancer 33: 221-228.

Yu, L., Alva, A., Su, H., Dutt, P., Freundt, E., Welsh, S.*, et al.* 2004. Regulation of an ATG7–beclin1 program of autophagic cell death by caspase-8. Science 304: 1500-1502.

Zhang, L., Yu, J., Pan, H., Hu, P., Hao, Y., Cai, W.*, et al.* 2007. Small molecule regulators of autophagy identified by an image-based high-throughput screen. Proceedings of the National Academy of Sciences of the United States of America 104: 19023-19028.

Zhang, Y., Wub, Y., Tashiro, S. I., Onodera, S. and Ikejima, T. 2009. Involvement of PKC signal pathways in oridonin-induced autophagy in HeLa cells: A protective mechanism against apoptosis. Biochemical and Biophysical Research Communications 378: 273-278.

Zhu, J. H., Horbinski, C., Guo, F., Watkins, S., Uchiyama, Y. and Chu, C. T. 2007. Regulation of autophagy by extracellular signal-regulated protein kinases during 1-Methyl-4-Phenylpyridinium-induced cell death. American Journal of Pathology 170: 75-86.

APPENDICES

APPENDIX A
PREPARATION OF REAGENTS

Growth medium of H460, H460/cis and RALP cells

   RPMI1640 powder (1 package) was dissolved with ultrapure water and the 2.0 g of sodium bicarbonate was added. The medium was mixed well and adjusted pH to 7.2-7.4 with HCl. The medium was then adjust volume to 1,000 ml and further sterilized by filtration with 0.2 µM Bottle-Top Vacuum Filters. Before using, the medium was supplement with 10% FBS, and 1% penicillin and streptomycin.

Phosphate buffer saline (PBS)

   To make 1 L of PBS, the ingredients including 8.00 g of NaCl, 0.20 g of KCl, 1.15 g of Na_2HPO_4, and 0.20 g of KH_2PO_4 were dissolved in 800 ml of Ultrapure water and adjusted the pH to 7.2-7.4 with HCl. The solution was then adjusted volume to 1,000 ml and sterilized by autoclave for 20 min at 15 lb/sq and then store at room temperature.

Acrylamide gel

   50 % Acrylamide

     To make 100 ml of 50% Acrylamide, 49.2 g of Acrylamide and 0.8 g of N,N'-Methylene bisacrylamide were dissolved in 50 ml of ultrapure water. The solution was stirred until completely solubilized, then adjusted volume to 100 ml and stored in dark bottles at room temperature.

   Caution: Acrylamide is a neurotoxin. Use extreme care when handling solids and solutions containing acrylamide and bisacrylamide. Wear a mask and gloves when weighing out solid acrylamide.

   4X separating buffer (100 ml)

     1.5 M Tris-HCl (pH 8.8)

     0.4% SDS

     Adjust volume with ultrapure water to 100 ml

4X stacking buffer (100 ml)

> 0.5 M Tris-HCl (pH 6.8)
>
> 0.4% SDS
>
> Adjust volume with ultrapure water to 100 ml

10 % Ammonium persulfate (APS)

APS 100 mg were dissolved in 1 ml of ultrapure water. The solution was mixed and stored in dark at -20 $^{\circ}$C.

1. **Preparation of separating gel (main gel)**

   To make two plates of 12 % acrylamide gel, the ingredients of separating gel were

Ultrapure water	5.1	ml
4X separating buffer	2.5	ml
50 % Acrylamide	2.4	ml
10% APS	50	µl
TEMED	10	µl

   All the ingredients were thoroughly mixed and immediately pour between the glass plates. Before gel polymerization was complete, DDW was layered on the top of the separating gel (4-5 mm thick). The gels were leaved for approximately 20-30 min.

2. **Preparation of stacking gel (top gel)**

   Once the separating gel has completely polymerized, DDW was removed from the top of the polymerized gel. To make stacking gel, the ingredients were

Ultrapure water	2.6	ml
4X stacking buffer	1.0	ml
50% Acrylamide	0.4	ml
10% APS	30	µl
TEMED	5	µl

   All the ingredients were thoroughly mixed and immediately pour gel between the glass plates. The combs were inserted between the two glass plates of two sets of gel apparatus. The gels were leaved for approximately 30-40 min to polymerize.

3. Application of samples

Once the stacking gel has completely polymerized, the combs were gently removed. The wells were flushed out thoroughly with electrophoresis buffer. The clips and sealing tapes were removed and set up the gel chamber. Electrophoresis buffer was filled out both inner and outer chamber. Before loading samples and protein marker, the air bubbles between layers were removed by gently rolling the chamber.

10X Electrophoresis and transfer buffer for Western blot analysis

To make 1 L of 10X of Electrophoresis and Transfer Buffer (2.5 M Tris pH 8.3, 19.2 M glycine) for stock solution, the ingredients were

Tris-base   30.3 g

Glycine   144.2 g

All ingredients were dissolved in ultrapure water with continuously stirring. The solution was adjusted volume to 1,000 ml.

1X Electrophoresis buffer for Western blot analysis

To make 1 L of 1X Electrophoresis Buffer (250 mM Tris, 1.92 M glycine and 0.5% SDS), the ingredients were

10X Electrophoresis and Transfer Buffer   100 ml

Ultrapure water   890 ml

10% SDS   10 ml

1X Transfer buffer for Western blot analysis

To make 1 L of 1X Transfer Buffer (160 mM Tris, 0.25 M glycine and 20% methanol), the ingredients were

10X Electrophoresis and Transfer Buffer   80 ml

Ultrapure water   720 ml

Methanol   200 ml

Tris-buffered saline, 0.05% Tween 20 (TBST)

To make 1 L of 10X TBST (100 mM Tris, pH 7.5, 1 M NaCl) for stock solution, 50 ml of 2 M Tris and 87.6 g of NaCl were dissolved in ultrapure and adjusted volume to 1,000 ml. Before using, the solution was diluted to 1X TBST (10 mM Tris and 100 mM NaCl) with ultrapure and 0.05 % of tween was added.

Sample buffer for Western blot analysis

To make 5X sample buffer, for stock solution, the ingredients were

60 mM Tris HCl

25% glycerol

2% SDS

14.4 mM 2-mercaptoethanol

0.1% Bromphenol blue

All ingredients, except 2-mercaptoethanol, were dissolved in ultrapure water with continuously stirring. The solution was adjusted volume to 50 ml and then filtered with filter paper no. 93. 14.4 mM 2-mercaptoethanol was later added and 5X sample was aliquoted into 1 ml/tube and stored at -20 ^{o}C.

2X Lysis buffer for Western blot analysis

To make 2X Lysis buffer, the ingredients were

40 mM Tris HCl (pH 7.4)

300 mM NaCl

2% Triton X-100

2 % Sodium deoxycholate

20 mM NaF

2 mM Pefabloc

2 mM Sodium orthovanadate

All ingredients were mixed well in ultrapure water and aliquoted into 1 ml/tube and stored at -20 ^{o}C. Before using, 1 ml of 2X lysis buffer was supplement with 10 ul protease inhibitor cocktail.

Bradford reagent for protein determination

To make 1 L of Bradford reagent, the ingredients were

Coomassie Blue G250 (Brilliant blue G-250)	100	mg
95% MeOH	50	ml
85% Phosphoric acid	100	ml

After all ingredients were mixed well by continuously stirring and adjusted volume with ultrapure water to 1,000 ml, the solution was filtered though Whatman filter paper no.93. The solution was kept in container protect from light at 4 ^{o}C.

Single-cell microgel electrophoresis (Comet assay)

Alkaline lysis solution

To make 200 ml of alkaline lysis solution (2.5M NaCl, 0.1M EDTA, 10 mM Tris pH 10, 1% Triton X-100 and 10% DMSO), the ingredients were

5M NaCl	100	ml
0.5M EDTA	40	ml
1M Tris pH 10	2	ml
Ultrapure	36	ml

All ingredients were mixed well and kept at 4 ^{o}C until use. Before using, 2 ml of Triton X-100 and 20 ml of DMSO were added and the solution was more turbid. Then, the solution was refrigerated for at least 30 min prior to slide addition.

Electrophoresis buffer

To make 2 L of Electrophoresis Buffer (0.3M NaOH, 1 mM EDTA), the ingredients were

10 M NaOH	60	ml
0.5 M EDTA	4	ml

All ingredients were mixed well and adjusted volume with ultrapure water to 2,000 ml. The buffer was freshly prepared and pH was more than 13.

Tris buffer solution pH 7.5

To make 200 ml of Tris buffer solution (0.4 M Tris pH 7.5), 80 ml of 1 M Tris-base pH 10 was diluted with ultrapure water, adjusted pH to 7.5 and adjusted volume to 200 ml.

Slide coating for single-cell microgel electrophoresis (Comet assay)

The microscope glass slides (7.5 cm x 2.5 cm) were coated with 200 µl of 0.8 % normal melting agarose gel in ultrapure. The agarose gel needed heat to complete soluble. Then, the agarose was dropped in the center of slide and spread homogeneously. The coated slides were dry in 60 ^{o}C oven until they were completely dry.

Low melting agarose

To make 1 ml of low melting agarose, 10 mg of low melting agarose was dissolved in 1000 µl of PBS with heat. The agarose was stored in 37 ^{o}C incubator until use.

APPENDIX B

TABLES OF EXPERIMENTAL RESULTS

Table 5 The relative Bcl-2 protein expression quantitated by Western blot analysis.

Cells	Relative ratio
H460	1.00 ± 0.00
H460/cis	1.89 ± 0.44*
RALP1	1.54 ± 0.12*
RALP6	2.72 ± 0.34*

Each value represented the mean $\pm$ SEM of three independent experiments. *, $p< 0.001$ compared to H460 cells.

Table 6   The percentage of cell viability of cisplatin treatment measured by MTT assay in concentration-dependent manner for 24 h.

cells	Control	Cisplatin (µM)								
		0.1	1.0	10.0	20	30	40	50	100.0	1000.0
H460	100	91.6 ± 10.8	84.1 ± 7.81	76.2 ± 8.8*	62.9 ± 1.6*	65.8 ± 1.8*	52.4 ± 2.5*	46.3 ± 0.7*	14.9 ± 3.4*	7.9 ± 1.9*
H460/cis	100	100.5 ± 3.9	95.3 ± 2.32	98.7 ± 3.6	89.4 ± 2.4	87.7 ± 0.7	90.1 ± 3.0	82.1 ± 8.4	79.7 ± 3.8*	6.3 ± 2.7*
RALP1	100	104.4 ± 7.2	105.6 ± 8.92	93.8 ± 13.7	74.4 ± 2.6*	71.6 ± 0.8*	64.4 ± 1.6*	60.9 ± 2.4*	28.3 ± 6.7*	7.0 ± 0.9*
RALP6	100	96.2 ± 5.1	94.5 ± 6.72	89.0 ± 5.9	96.0 ± 0.6	89.0 ± 1.7	89.7 ± 1.6	89.1 ±.5.7	66.3 ± 7.6**	4.0 ± 1.3*

Each value represented the mean ± SEM of four independent experiments, each preformed in five wells. *, $p < 0.001$ compared to H460 cells at each cisplatin concentration.

Table 7   The inhibitory concentration of fifty percent (IC_{50}) of cisplatin in H460, H460/cis, RALP1 and RALP6 cells.

cells	IC_{50} of cisplatin (µM)	Relative ratio
H460	40.64 ± 0.50	1
H460/cis	85.61 ± 3.11 **	2.1
RALP1	54.53 ± 6.21 **	1.4
RALP6	80.82 ± 2.33**	2.0

Each point represents the mean ± SEM of four independent experiments. **, $p<0.001$ compared to H460 cells

Table 8   The percentage of cell viability of TFP treatment measured by MTT assay in concentration-dependent manner for 24 h.

cells	TFP (µM)				
	0.625	1.250	2.500	5.000	10.000
H460	103.05 ± 7.96	100.88 ± 4.52	97.20 ± 10.69	94.57 ± 6.37	72.05 ± 12.69
H460/cis	100.48 ± 12.30	97.43 ± 13.49	98.90 ± 11.82	95.20 ± 17.59	77.97 ± 16.08
RALP1	107.58 ± 5.63	99.57 ± 19.42	109.33 ± 7.85	105.00 ± 6.31	85.50 ± 9.92
RALP6	95.14 ± 3.62	93.21 ± 7.11	97.39 ± 5.29	93.56 ± 5.76	67.47 ± 3.94

Each value represented the mean ± SEM of four independent experiments, each preformed in five wells.

Table 9   The acridine orange fluorescence intensity in response to TFP at 1 and
5 µM measured by flow cytometer compared to H460 cells.

cells	control	TFP (µM)	
		1 µM	5 µM
H460	31.0 ± 2.75	33.46 ± 2.78	37.33 ± 4.76
H460/cis	18.44± 2.37	19.87 ± 0.64	21.54 ± 3.01
RALP1	25.47 ± 5.17	29.76 ± 7.57	33.01 ± 8.24
RALP6	21.78 ± 3.80	25.15 ± 8.38	26.22 ± 6.70

Each point represents the mean ± SEM of three independent experiments.

Table 10   The relative acridine orange fluorescence intensity in response to TFP
at 1 and 5 µM measured by flow cytometer compared to H460 cells

cells	control	TFP (µM)	
		1 µM	5 µM
H460	100 ± 0.00	109.55 ± 6.29	124.79 ± 8.60##
H460/cis	51.84 ± 2.82*	62.71 ± 4.11	65.79 ± 16.33##
RALP1	74.67 ± 7.75*	95.81 ± 10.32	118.76 ± 15.60##
RALP6	64.4 ± 14.00*	72.36 ± 18.94	77.31 ± 13.25##

Each point represents the mean ± SEM of three independent experiments.
*, $p<0.05$ compared to control H460 cells. # #, $p<0.01$ compared to their control
cells.

Table 11   The relative acridine orange fluorescence intensity in response to TFP at 1 and 5 µM measured by flow cytometer compared to each control cells

cells	control	TFP (µM)	
		1 µM	5 µM
H460	100 ± 0.00	109.55 ± 6.29	$124.79 \pm 8.60^{\#\#}$
H460/cis	100 ± 0.00	115.69 ± 3.80	$124.98 \pm 3.48^{\#\#}$
RALP1	100 ± 0.00	111.49 ± 10.15	$120.58 \pm 14.24^{\#\#}$
RALP6	100 ± 0.00	118.44 ± 8.91	$134.61 \pm 4.02^{\#\#}$

Each point represents the mean $\pm$ SEM of three independent experiments. ##, $p < 0.01$ compared to each control cell.

Table 12   The percentage of cell viability of the combination of 20 µM of cisplatin and 1-5 µM of TFP measured by MTT for 24 h.

cells	cisplatin 20 µM		
	control	TFP 1 µM	TFP 5 µM
H460	62.89 ± 5.44	58.48 ± 11.30	59.74 ± 12.35
H460/cis	$81.45 \pm 13.84^*$	78.23 ± 10.83	$73.69 \pm 7.35^{\#}$
RALP1	$83.62 \pm 19.38^*$	$69.00 \pm 8.73^{\#}$	$68.59 \pm 8.59^{\#}$
RALP6	$94.12 \pm 12.69^*$	84.55 ± 12.79	$79.05 \pm 13.01^{\#}$

Each value represented the mean $\pm$ SEM of five independent experiments, each preformed in five wells. *, $p<0.05$ compared to H460 cells. #, $p< 0.05$ compared to their control cells.

Table 13   The percentage of cell viability of the combination of 30 µM of cisplatin and 1-5 µM of TFP measured by MTT for 24 h.

cells	cisplatin 30 µM		
	control	TFP 1 µM	TFP 5 µM
H460	59.77 ± 9.09	59.88 ± 10.21	62.28 ± 11.65
H460/cis	88.17 ± 8.68*	83.60 ± 8.08	82.03 ± 8.69[#]
RALP1	73.68 ± 9.91*	68.63 ± 7.59#	70.74 ± 10.07[#]
RALP6	88.96 ± 9.69*	88.96 ± 9.58	81.13 ± 9.31[#]

Each value represented the mean ± SEM of five independent experiments, each preformed in five wells. *, $p<0.05$ compared to H460 cells. #, $p< 0.05$ compared to their control cells.

Table 14   The percentage of cell viability of the combination of 40 µM of cisplatin and 1-5 µM of TFP measured by MTT for 24 h.

cells	cisplatin 40 µM		
	control	TFP 1 µM	TFP 5 µM
H460	52.36 ± 2.48	48.92 ± 0.79	48.0 ± 41.68
H460/cis	90.06 ± 3.05*	71.24 ± 0.99[#]	65.14 ± 1.17[#]
RALP1	64.35 ± 1.61*	56.77 ± 0.29[#]	54.44 ± 1.19[#]
RALP6	89.72 ± 1.65*	77.21 ± 1.30	71.27 ± 2.43[#]

Each value represented the mean ± SEM of five independent experiments, each preformed in five wells. *, $p<0.05$ compared to H460 cells. #, $p< 0.05$ compared to their control cells.

Table 15   The percentage of cell viability of the combination of 50 µM of cisplatin and 1-5 µM of TFP measured by MTT for 24 h.

cells	cisplatin 50 µM		
	control	TFP 1 µM	TFP 5 µM
H460	46.31 ± 0.66	44.27 ± 2.56	49.45 ± 1.69
H460/cis	82.10 ± 8.45*	70.77 ± 5.96	61.58 ± 3.22$^{\#}$
RALP1	60.89 ± 2.45*	44.39 ± 5.23$^{\#}$	44.83 ± 3.69$^{\#}$
RALP6	89.10 ± 3.57*	75.83 ± 2.27	57.91 ± 3.31$^{\#}$

Each value represented the mean ± SEM of five independent experiments, each preformed in five wells. *, $p<0.05$ compared to H460 cells. #, $p< 0.05$ compared to their control cells.

Table 16   The percentage of apoptotic and necrotic cells in response to 40 µM of cisplatin and 5 µM of TFP co-treatment detected by staining with Hoechst 33342 and propidium iodide.

cells	cisplatin 40 µM		cisplatin 40 µM + TFP 5 µM	
	apoptosis	necrosis	apoptosis	necrosis
H460	40.28 ± 8.06	3.57 ± 3.57	33.15 ± 3.28	3.34 ± 0.11
H460/cis	5.30 ± 2.39	3.00 ± 1.00	6.33 ± 0.33	0.71 ± 0.71
RALP1	31.61 ± 3.28	1.33 ± 0.33	20.05 ± 8.28	1.25 ± 1.25
RALP6	8.23 ± 1.77	1.76 ± 0.09	9.60 ± 2.34	1.28 ±1.28

Each point represents the mean ± SEM of five fields. Cells at least 50 cells were counted in each field.

Table 17 The relative tail length parameter in comet assay in cisplatin and TFP co-treatment compared to control groups.

Cells	Control	TFP 5 µM	3MA 200 µM	cisplatin 40 µM	cisplatin 40 µM TFP 5 µM	cisplatin 40 µM TFP 5 µM 3MA 200 µM
H460	1.00 ± 0.00	0.92 ± 0.38	1.10 ± 0.24	2.30 ± 0.52*	2.68 ± 1.18*	2.06 ± 0.93*
H460/cis	1.00 ± 0.00	1.13 ± 0.21	0.85 ± 0.19	1.24 ± 0.23	1.27 ± 0.12	1.29 ± 0.53
RALP1	1.00 ± 0.00	0.87 ± 0.22	0.83 ± 0.20	1.05 ± 0.23	0.90 ± 0.13	1.13 ± 0.34
RALP6	1.00 ± 0.00	0.95 ± 0.06	0.97 ± 0.26	1.28 ± 0.33	1.24 ± 0.12	1.38 ± 0.22

Each point represents the mean ± SEM of three independent experiments. *, $p < 0.05$ compared to control each cells.

Table 18 The relative % DNA in tail parameter in comet assay in cisplatin and TFP co-treatment compared to control groups.

Cells	Control	TFP 5 µM	3MA 200 µM	cisplatin 40 µM	cisplatin 40 µM TFP 5 µM	cisplatin 40 µM TFP 5 µM 3MA 200 µM
H460	1.00 ± 0.00	1.14 ± 0.43	1.14 ± 0.27	2.42 ± 0.61*	1.63 ± 0.77*	2.02 ± 1.28*
H460/cis	1.00 ± 0.00	0.90 ± 0.26	0.96 ± 0.38	1.11 ± 0.21	0.95 ± 0.02	0.74 ± 0.13
RALP1	1.00 ± 0.00	0.93 ± 0.30	1.01 ± 0.30	0.97 ± 0.18	0.79 ± 0.05	0.74 ± 0.27
RALP6	1.00 ± 0.00	1.23 ± 0.15	0.59 ± 0.14	1.17 ± 0.28	1.20 ± 0.40	1.04 ± 0.08

Each point represents the mean ± SEM of three independent experiments. *, $p < 0.05$ compared to control each cells.

Table 19 The relative tail moment parameter in comet assay in cisplatin and TFP co-treatment compared to control groups.

Cells	Control	TFP 5 µM	3MA 200 µM	cisplatin 40 µM	cisplatin 40 µM TFP 5 µM	cisplatin 40 µM TFP 5 µM 3MA 200 µM
H460	1.00 ± 0.00	1.37 ± 1.17	1.99 ± 0.98	3.99 ± 1.18*	4.56 ± 2.61*	4.25 ± 3.91*
H460/cis	1.00 ± 0.00	1.20 ± 0.50	0.98 ± 0.49	1.33 ± 0.26	1.30 ± 0.16	1.20 ± 0.87
RALP1	1.00 ± 0.00	1.02 ± 0.49	0.93 ± 0.33	1.26 ± 0.12	0.82 ± 0.23	0.95 ± 0.37
RALP6	1.00 ± 0.00	1.36 ± 0.50	0.98 ± 0.36	1.39 ± 0.56	1.55 ± 0.58	1.18 ± 0.24

Each point represents the mean ± SEM of three independent experiments. *, $p < 0.05$ compared to control each cells.

Table 20 The relative olive moment parameter in comet assay in cisplatin and TFP co-treatment compared to control groups.

Cells	Control	TFP 5 µM	3MA 200 µM	cisplatin 40 µM	cisplatin 40 µM TFP 5 µM	cisplatin 40 µM TFP 5 µM 3MA 200 µM
H460	1.00 ± 0.00	1.30 ± 0.57	1.20 ± 0.25	2.42 ± 0.43*	2.51 ± 1.11*	2.14 ± 0.83*
H460/cis	1.00 ± 0.00	1.07 ± 0.19	0.84 ± 0.18	1.15 ± 0.14	1.18 ± 0.15	1.06 ± 0.46
RALP1	1.00 ± 0.00	0.91 ± 0.23	1.04 ± 0.36	1.06 ± 0.26	0.83 ± 0.02	0.96 ± 0.36
RALP6	1.00 ± 0.00	1.16 ± 0.03	0.92 ± 0.22	1.38 ± 0.34	1.38 ± 0.34	1.32 ± 0.20

Each point represents the mean ± SEM of three independent experiments. *, $p < 0.05$ compared to control each cells.

Table 21   The relative acridine orange fluorescence intensity detected by flow cytometer in cisplatin and TFP co-treatment.

cells	control	TFP 5 µM	cisplatin 40 µM	
			control	TFP 5 µM
H460	100.00 ± 0.00	$124.79 \pm 8.60^{\#}$	$124.38 \pm 5.96^{\#}$	$142.59 \pm 17.43^{\delta}$
H460/cis	$51.84 \pm 2.82^*$	$65.79 \pm 16.33^{\#}$	$93.81 \pm 10.48^{\#}$	$125.24 \pm 17.09^{\delta}$
RALP1	$74.67 \pm 7.75^*$	$118.76 \pm 15.60^{\#}$	$111.97 \pm 5.76^{\#}$	$135.11 \pm 12.55^{\delta}$
RALP6	$64.40 \pm 14.00^*$	$77.311 \pm 3.25^{\#}$	$98.44 \pm 27.04^{\#}$	$145.43 \pm 7.64^{\delta}$

Each point represents the mean $\pm$ SEM of at least three independent experiments. *, $p < 0.05$ compared to H460 control cells. #, $p < 0.05$ compared to each control cell. δ, $p < 0.05$ compared to each cisplatin-treated cell.

Table 22   The percentage of cell viability of 3-MA treatment measured by MTT assay in concentration-dependent manner for 24 h.

cells	3-MA (µM)				
	0.1	1.0	10.0	100.0	1000.0
H460	106.17±14.13	107.71±11.54	96.33±9.58	91.89±9.45	86.30±4.76
H460/cis	96.81±6.57	101.25±8.34	109.23±10.21	104.88±8.72	101.68±14.01
RALP1	101.62±2.85	104.70±7.62	98.87±4.16	91.49±1.82	95.31±10.67
RALP6	103.14±5.44	107.27±9.13	107.28±11.83	105.83±6.19	94.82±14.04

Each point represents the mean $\pm$ SEM of three independent experiments.

Table 23 The percentage of cell viability of cisplatin, TFP and 3-MA combination measured by MTT assay in time-dependent manner for 24 h.

Cell	Treatment	Time (h)				
		0	8	12	16	24
H460	cisplatin 40 µM	100.00 ± 0.00	101.74 ± 1.89	89.54 ± 0.81	85.17 ± 1.51	58.01 ± 1.99
	cisplatin 40 µM + TFP 5 µM	100.00 ± 0.00	87.61 ± 1.95*	74.20 ± 0.78*	69.71 ± 1.77*	47.80 ± 2.76
	cisplatin 40 µM + TFP 5 µM + MA 200 µM	100.00 ± 0.00	95.91 ± 2.87	80.44 ± 5.10	77.66 ± 2.58	55.89 ± 4.32
H460/cis	cisplatin 40 µM	100.00 ± 0.00	105.20 ± 4.62	97.82 ± 4.06	99.02 ± 4.86	88.58 ± 6.03
	cisplatin 40 µM + TFP 5 µM	100.00 ± 0.00	94.27 ± 4.48	84.16 ± 4.28	81.47 ± 4.56*	62.48 ± 4.53*
	cisplatin 40 µM + TFP 5 µM + MA 200 µM	100.00 ± 0.00	102.13 ± 6.17	94.59 ± 4.46	94.74 ± 6.17	86.99 ± 5.68$^{\#}$
RALP1	cisplatin 40 µM	100.00 ± 0.00	103.23 ± 4.86	98.44 ± 2.60	89.57 ± 4.89	70.62 ± 3.81
	cisplatin 40 µM + TFP 5 µM	100.00 ± 0.00	88.58 ± 3.06	82.28 ± 1.41*	75.03 ± 4.67*	55.50 ± 2.91*
	cisplatin 40 µM + TFP 5 µM + MA 200 µM	100.00 ± 0.00	93.82 ± 4.58	91.50 ± 2.50	86.79 ± 2.11	70.02 ± 3.02$^{\#}$
RALP6	cisplatin 40 µM	100.00 ± 0.00	104.29 ± 4.52	103.21 ± 1.37	102.69 ± 3.73	90.84 ± 1.86
	cisplatin 40 µM + TFP 5 µM	100.00 ± 0.00	85.26 ± 3.51	86.45 ± 0.79*	85.78 ± 4.01*	69.57 ± 3.28*
	cisplatin 40 µM + TFP 5 µM + MA 200 µM	100.00 ± 0.00	92.48 ± 6.03	97.35 ± 3.80	96.33 ± 5.58	93.42 ± 3.76$^{\#}$

Each value represented the mean ± SEM of at six independent experiments. *, $p < 0.05$ compared to cisplatin-treated group in each cell. #, $p < 0.05$ compared to cisplatin-TFP treated group in each cell.

Table 24   The relative ratio of LC3 type II levels, normalized by β-actin and quantitated by Western blot analysis.

Cells	Control	TFP 5 µM	3MA 200 µM	cisplatin 40 µM		
				control	TFP	TFP 3MA
H460	1.00 ± 0.00	1.40 ± 0.12*	0.82 ± 0.06	1.18 ± 0.15	1.20 ± 0.20	1.17± 0.06
H460/cis	1.00 ± 0.00	1.54 ± 0.89	1.00 ± 0.55	1.48 ± 0.74	1.61 ± 0.59	0.97 ± 0.13
RALP6	1.00 ± 0.00	2.10 ± 0.81	0.73 ± 0.12	1.15 ± 0.52	1.14 ± 0.21	1.35 ± 0.29

Each value represented the mean ± SEM of three independent experiments. *, $p<0.05$ compared to each control cell.

Table 25   The relative ratio of LC3 conversion, normalized by β-actin and quantitated by Western blot analysis.

Cells	Control	TFP 5 µM	3MA 200 µM	cisplatin 40 µM		
				control	TFP	TFP 3MA
H460	1.00 ± 0.00	1.26 ± 0.07*	0.67 ± 0.08*	0.94 ± 0.15	0.94 ± 0.14	0.85 ± 0.11
H460/cis	1.00 ± 0.00	1.63 ± 0.50	1.04 ± 0.36	1.32 ± 0.46	1.73 ± 0.51	0.72 ± 0.11
RALP6	1.00 ± 0.00	1.49 ± 0.38	0.89 ± 0.10	1.30 ± 0.38	1.13 ± 0.29	0.91 ± 0.10

Each value represented the mean ± SEM of three independent experiments. *, $p<0.05$ compared to each control cell.

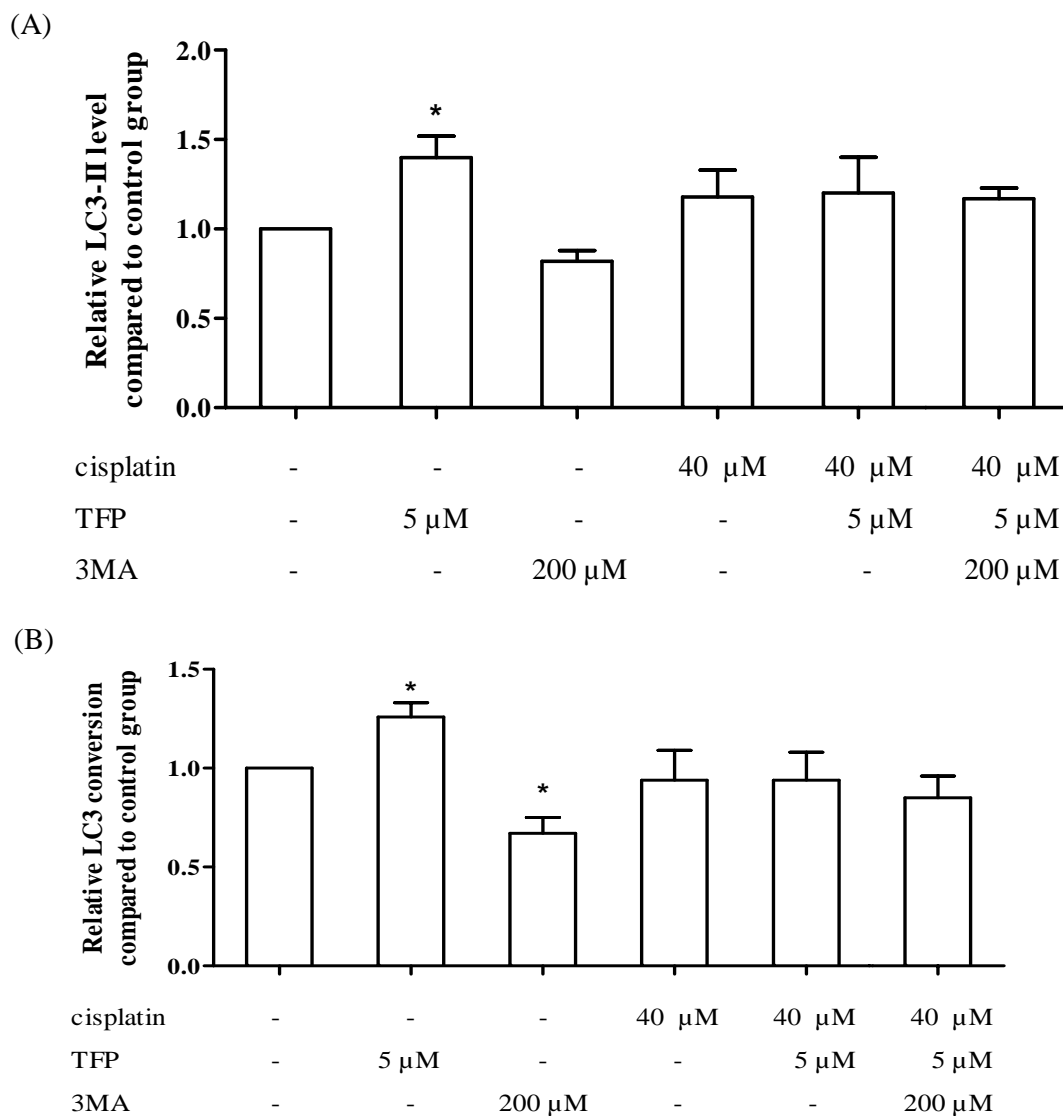**Table 26**   The relative Bcl-2 protein level normalized by β-actin and quantitated by Western blot analysis in RALP6.

			cisplatin 40 µM		
Control	TFP 5 µM	3MA 200 µM	control	TFP 5 µM	TFP 5 µM 3MA 200 µM
1.00	1.06 ± 0.14	1.13 ± 0.15	1.10 ± 0.19	0.75 ± 0.09	0.92 ± 0.15

Each value represented the mean ± SEM of three independent experiments.

(A)

				cisplatin		
cisplatin	-	-	-	40 μM	40 μM	40 μM
TFP	-	5 μM	-	-	5 μM	5 μM
3MA	-	-	200 μM	-	-	200 μM

(B)

cisplatin	-	-	-	40 μM	40 μM	40 μM
TFP	-	5 μM	-	-	5 μM	5 μM
3MA	-	-	200 μM	-	-	200 μM

Figure 44   The autophagic activity in response to the combination of cisplatin, TFP and 3-MA in H460 cells at 8 h. (A) The relative LC3-II level compared to control group. (B) The relative LC3-II conversion compared to control group. The values are presented the mean ± SEM of three independent experiments.

(A)

cisplatin	-	-	-	40 µM	40 µM	40 µM
TFP	-	5 µM	-	-	5 µM	5 µM
3MA	-	-	200 µM	-	-	200 µM

(B)

cisplatin	-	-	-	40 µM	40 µM	40 µM
TFP	-	5 µM	-	-	5 µM	5 µM
3MA	-	-	200 µM	-	-	200 µM
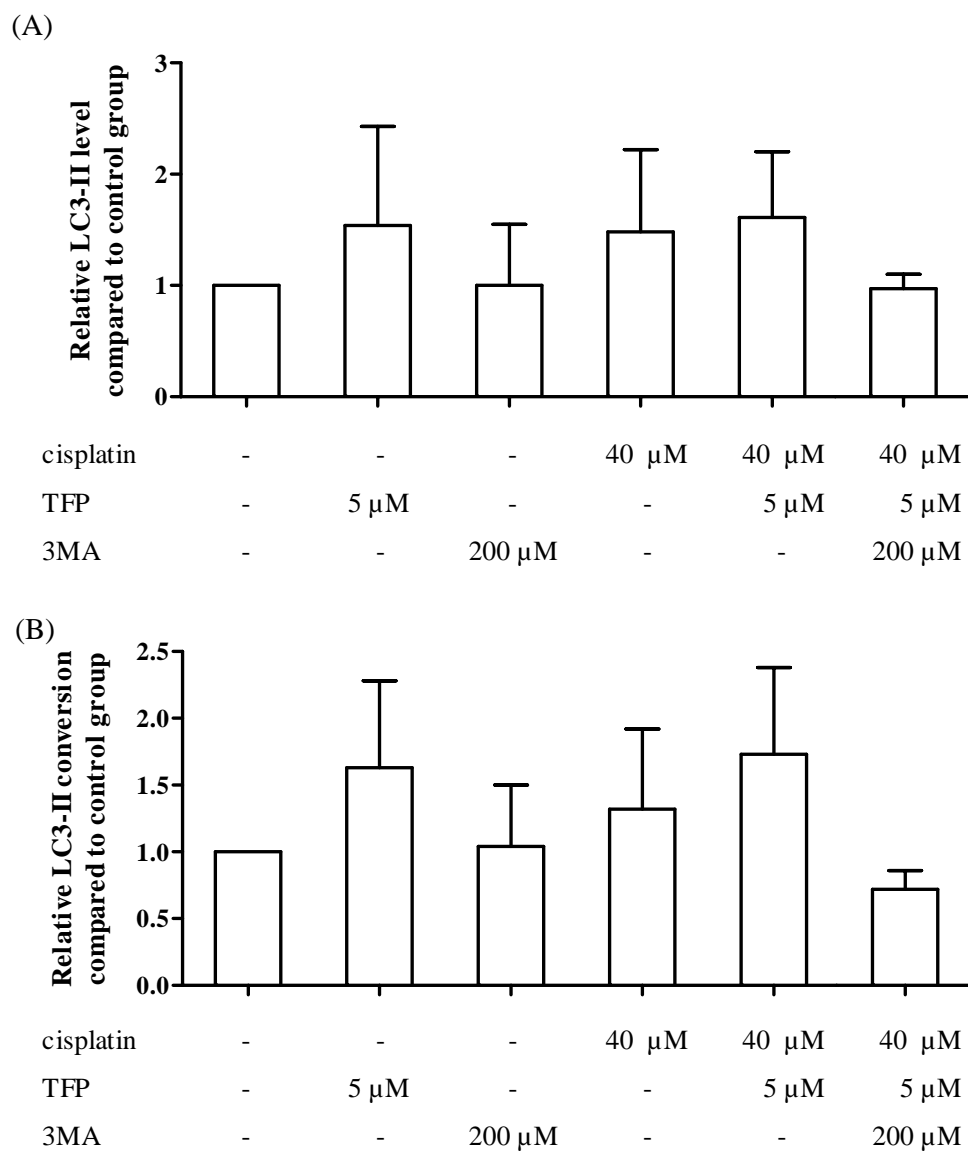
Figure 45 The autophagic activity in response to the combination of cisplatin, TFP and 3-MA in H460/cis cells at 8 h. (A) The relative LC3-II level compared to control group. (B) The relative LC3-II conversion compared to control group. The values are presented the mean ± SEM of three independent experiments.
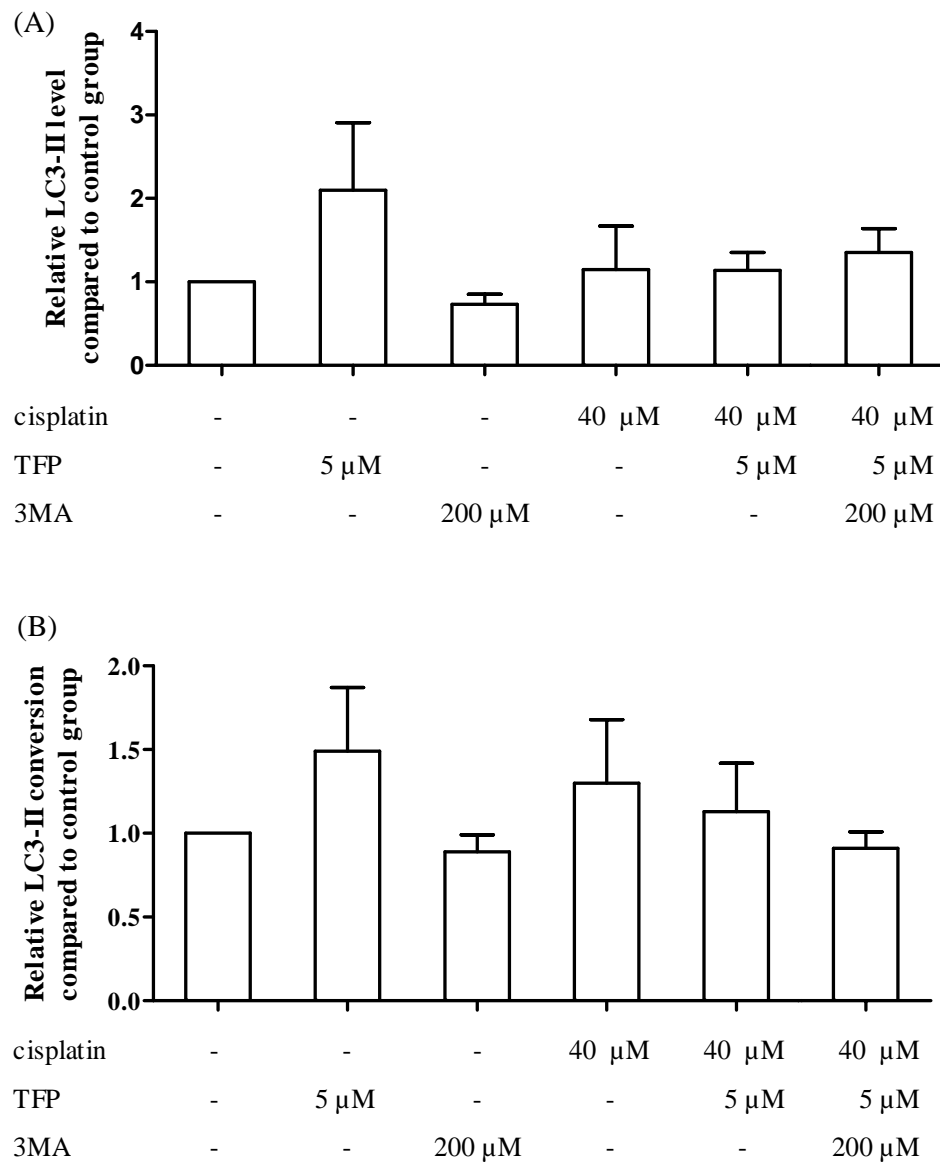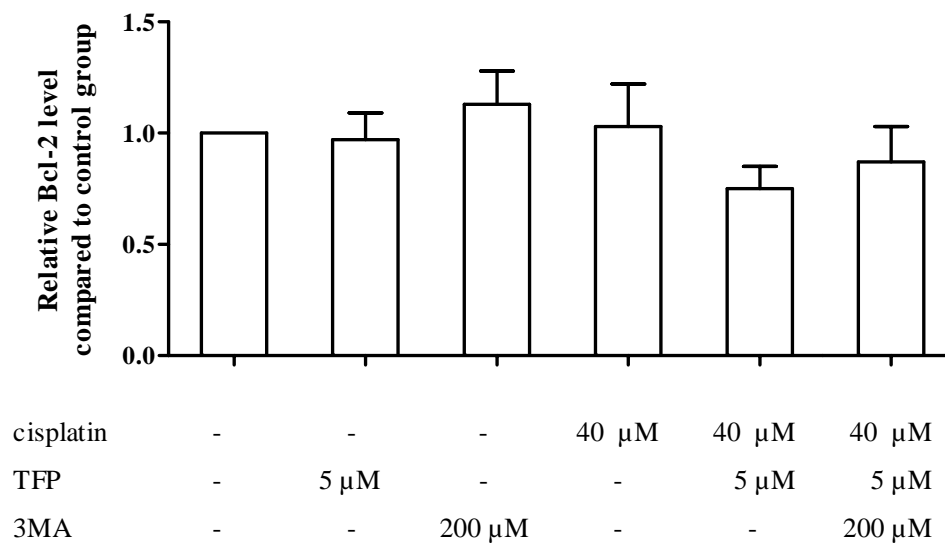
Figure 46 The autophagic activity in response to the combination of cisplatin, TFP and 3-MA in RALP6 cells at 8 h. (A) The relative LC3-II level compared to control group. (B) The relative LC3-II conversion compared to control group. The values are presented the mean ± SEM of three independent experiments.

cisplatin	-	-	-	40 µM	40 µM	40 µM
TFP	-	5 µM	-	-	5 µM	5 µM
3MA	-	-	200 µM	-	-	200 µM

Figure 47 Relative Bcl-2 protein levels in response to the combination of cisplatin, TFP and 3-MA at 8 h in RALP6 cells. The values are presented the mean ± SEM of three independent experiments.

VITA

Miss Buntitabhon Sirichanchuen was born on October 23, 1983 in Chiangmai, Thailand. She received her Bachelor in Pharmacy (Honors) from the Faculty of Pharmacy, Chiang Mai University in 2006. Since graduation, she entered the PhD's degree program in Biopharmaceutical Sciences at the Faculty of Pharmaceutical Sciences, Chulalongkorn University in 2006.